



Nueces Delta Restoration Study
Publication CBBEP – 84
Project Number – 1001
December 2012

Prepared by

Ben R. Hodges, Kenneth H. Dunton, Paul A. Montagna and George H. Ward

Center for Research in Water Resources, University of Texas at Austin
Marine Science Institute, University of Texas at Austin
Harte Research Institute for Gulf of Mexico Studies, Texas A&M University – Corpus Christi

Submitted to:
Coastal Bend Bays & Estuaries Program
1305 N. Shoreline Blvd. Ste 205
Corpus Christi, Texas 78401

Nueces Delta Restoration Study

FINAL REPORT

Principal Investigators

Ben R. Hodes¹ **Kenneth H. Dunton²** **Paul A. Montagna³** **George H. Ward¹**

Collaborators

Andrea J. Ryan¹ **San-Rul Park²** **Joseph Stachelek²** **Alexey L. Sadovski⁴**
Scott King⁵ **Kevin C. Nelson³** **Terry Palmer³**

Submitted to the Coastal Bend Bays and Estuaries Program

December 31, 2012

¹ Center for Research in Water Resources, University of Texas at Austin

² Marine Science Institute, University of Texas at Austin

³ Harte Research Institute for Gulf of Mexico Studies, Texas A&M University – Corpus Christi

⁴ Dept. of Mathematics and Statistics, Texas A&M University – Corpus Christi

⁵ School of Engineering and Computing Sciences, Texas A&M University – Corpus Christi

Suggested Citation:

Hodges, B.R., K.H. Dunton, P.A. Montagna, G.H. Ward, et al. 2012. *Nueces Delta Restoration Study*. Report to the Coastal Bend Bays and Estuaries Program, Project 1001.

Executive Summary

Freshwater flow from the Nueces River through Rincon Bayou into the marshes of the Nueces Delta is ecologically vital for two reasons: 1) it creates *connectivity for aquatic habitat* between the marsh and Nueces Bay that is critical for growth and development of estuarine-dependent animal species, and 2) it promotes *marsh plant maintenance and growth* by maintaining porewater salinity levels within acceptable limits. These two functions are synergistic because healthy marsh vegetation is necessary to maintain the tidal channels and connectivity for aquatic habitat, as well as to prevent collapse of the delta front to wave-induced erosion. Thus every gallon of fresh water entering the marsh provides multiple environmental benefits.

A primary motivation for restoring the Nueces Delta is that it provides critical nursery habitat for both commercial and non-commercial fish, crab, shrimp, and invertebrates that are necessary for a functioning food web in the coastal system. The marsh further provides migratory bird habitat and broader ecosystem services. The danger of the “no action” alternative to restoration is eventual loss of the delta, an outcome that can be understood very succinctly: *Without the delta, one of the major rivers of the Gulf of Mexico will be reduced to a simple outfall without any significant aquatic nursery habitat or migratory bird refuge.* The Nueces Delta is the southernmost marsh on the western Gulf of Mexico that is associated with a major river and, if lost, represents a major economic loss (in millions of dollars annually) to the estuarine fishery of the greater Corpus Christi area.

The long-term prognosis for the Nueces Delta under present conditions is poor and the vulnerability of the system is high. Freshwater inundation over the past 30 years has simply been insufficient in volume and distribution to maintain a healthy marsh, so the delta front is eroding into Nueces Bay, the marsh plants are under stress, and the connectivity of aquatic habitat is threatened. In the present study, we were able to develop a better scientific understanding of why the system is degrading. We provide restoration recommendations (below) and suggest new tools for improved management and restoration.

Our study comprised three major efforts: 1) field studies of the interactions of porewater salinity and plant physiology, 2) modeling of predicted marsh coverage under varying climatic conditions, and 3) hydrodynamic modeling of inundation. Key observations, abstracted here, are:

- Porewater salinity in vegetation zones provides the dominant control on marsh health. Controlling porewater salinity requires overbank inundation in sufficient amounts and frequency to limit salinity increase caused by evaporation and transpiration.
- Strategies for managing long-term marsh health must use multi-year rather than year-by-year analyses. The present state of the marsh combined with climatological conditions of the past several years and possible climatological

conditions over the next several years must play a role in managing fresh water. Thus, management requires predictive models to understand how the sequence of prior and possible future climatological conditions will affect marsh health.

- Effects of freshwater inundation, whether controlled through the Rincon Bayou Pipeline or through episodic floods, are strongly dependent on the timing of the inundation relative to the tidal elevation. When the tidal elevations are higher, freshwater inundation has a broader effect over the marsh.
- The physiography of the delta has been affected by its bisection with a railroad embankment that limits connectivity. Furthermore, old ranch road improvements by previous landowners have also disrupted hydrologic connections in different areas of the marsh.

Some of our recommended strategies to limit the vulnerability of this ecosystem to further degradation include:

- Develop spatially-based models of net production to provide more detailed estimates of the interaction between tidal creek water and sediment pore water with respect to inundation frequency and soil hydraulic conductivity.
- Integrate the hydrodynamics model with the marsh ecology model to examine how different restoration scenarios and historic tidal conditions provide the most optimum use of available freshwater.
- Using hydrodynamic, elevation, and tidal models, provide guidance on maximizing overbanking events from freshwater releases under different environmental forcing conditions, including biannual secular tidal excursions.
- Consider improving hydrologic connectivity through engineering solutions, including creation of channels, installation of culverts and diversions of water to historic drainage areas and tidal creeks in the Nueces marsh.
- Possible restoration alternatives should include the diversion of all the Nueces River main channel flow into the delta, alteration of freshwater pumping schemes, and establishment of breakwaters for shoreline stabilization at the delta front.

Recent changes in local climatology and resulting drought conditions now prevalent across south Texas have increased the vulnerability of this ecosystem to degradation. Consequently, we encourage actions to address the concerns and recommendations summarized in this report before further irreversible environmental losses result in enormous long-term economic consequences for the region.

Acknowledgements

We are grateful to Jace Tunnell for his constructive comments and oversight in administering the grant through the Coastal Bend Bays and Estuaries Program (CBBEP). We would like to thank our U.S. Army Corps of Engineers project manager, Marcia Hackett (Forth Worth District), whose support has been invaluable. Her recognition of the vulnerability of the Nueces Delta within the overall context of the Nueces River Basin has made this project possible.

We would like to acknowledge the absolutely critical and enthusiastic support provided by the UT-MSI field team, led by Kim Jackson, who was assisted by Travis Bartholomew, Chris Wilson, Karen Bishop, and Nathan McTigue.

Many people provided help during this study as it evolved to its current state. The original ideas for a marsh plant photosynthesis model were provided by Dr. Hae-Cheol Kim while he was at Texas A&M University-Corpus Christi (TAMUCC). Over time, we realized that photosynthesis per se is primarily driven by daylight and nutrient input, which does not help answer our main question, which was “how does freshwater inflow and water levels promote marsh plant growth?” It became clear that the modeling exercise had to encompass not just leaf or stem growth, but also coverage of marsh surface. All of the marsh plant data were supplied by Dr. Kenneth Dunton, University of Texas Marine Science Institute, and it was all in terms of percent cover. When Dr. Kim left TAMUCC for a position at the National Oceanic and Atmospheric Administration, Brittany Blomberg (a TAMUCC doctoral student) took over and developed a cellular automata model to predict marsh plant coverage. This model divided the marsh into cells and occupation of a cell was based on a series of rules. While this approach was successful in populating the marsh with plants, it also was limited in its ability to link inflow and salinity to coverage. A key insight was provided by Dr. Michael Rasser (then a doctoral student at UTMSI and now at the Bureau of Ocean Energy Management) who demonstrated the link between elevation and plant distribution. With this in mind, co-author Dr. Alexey Sadovski developed a diffusion modeling approach, which included functional relationships between marsh plant coverage of cells with salinity and water level elevation. The marsh digital elevation model, which was critical for implementing our diffusion model, was supplied by Dr. James Gibeaut of the Harte Research Institute. Evan Turner, a TAMUCC doctoral student, provided useful suggestions and insights as the model was being developed.

This research project was supported by the Coastal Bend Bays and Estuaries Program (Project 1001), the U.S. Army Corps of Engineers (W9126G-09-P0315 and W9126G-09-T0076) and the City of Corpus Christi through support of CBBEP. Additional support to Montagna’s team was provided by the TAMUCC Texas Research Development Fund, and the Harte Research Institute for Gulf of Mexico Studies as well as CBBEP funding to create databases.

The work herein represents the original studies and analyses of the authors and collaborators. The views expressed herein are those of the authors and do not necessarily reflect the views of supporting organizations or people.

Notes on elevations and data sources

All land and water elevations in this report are based on the North American Vertical Datum of 1988 (NAVD88). “Sea level” is used to refer to the zero value of NAVD88, which corresponds to 0.25 ft below the minimum of the mean daily tide recorded at the Texas State Aquarium on Corpus Christi Bay. Raw tidal data were obtained from the Division of Nearshore Research, Conrad Blucher Institute for Surveying and Science, Texas A&M University-Corpus Christi. The authors are responsible for tidal analyses presented herein.

Tidal data used for modeling in this report are from the Texas State Aquarium tidal gage on Corpus Christi Bay. The data for this gage have a longer time history than the Nueces Bay gage, thus allowing for more complete analysis. Both the daily mean and hourly elevations at the aquarium deviate, on average, less than 0.15 inches from the Nueces Bay elevations (2011 data); the standard deviation of the data differences are 1.01 inches for the daily mean tide and 1.71 inches for the hourly tide. However, during unusual storm events, the instantaneous gage readings have differed as much as 9 inches.

Bathymetric data at a 1x1 m resolution were provided by J. Gibeaut at Texas A&M University-Corpus Christi, based on lidar data collected under the auspices of the Coastal Bend Bays and Estuaries Program. The authors are responsible for data analysis and processing to a 15x15 m model grid.

Table of Contents

1	OVERVIEW	1
1.1	STUDY ORGANIZATION AND GOALS.....	1
1.2	NUECES DELTA IN A LARGER CONTEXT	2
1.3	FEATURES OF THE NUECES DELTA.....	8
1.4	KEY ISSUES FOR ECOSYSTEM SUSTAINABILITY	11
2	ECOSYSTEM RESPONSE TO INUNDATION	13
2.1	THE ECOSYSTEMS	13
2.2	VEGETATION RESPONSE TO SALINITY GRADIENT (TIDAL CREEK TO MARSH)	17
2.3	MODELING PLANT COVER CHANGE.....	21
2.4	FISH AND INVERTEBRATE HABITAT CONNECTIVITY.....	28
3	PHYSICS OF INUNDATION.....	31
3.1	OVERVIEW.....	31
3.2	OVERBANKING AND DRAINING.....	31
3.3	TIDALLY-DRIVEN INUNDATION	32
3.4	OTHER FORCING FOR INUNDATION	35
4	RESTORING THE NUECES DELTA	41
4.1	REQUIREMENTS AND OPTIONS.....	41
5	RECOMMENDATIONS FOR FUTURE RESTORATION WORK.....	43
6	REFERENCES	45
A	APPENDIX: NUECES DELTA HYDRODYNAMIC MODEL.....	51
A.1	INTRODUCTION	51
A.2	METHODOLOGY.....	57
A.3	RESULTS AND DISCUSSION	68
A.4	REQUIREMENTS FOR CALIBRATION AND VALIDATION OF NDHM	83
A.5	CONCLUSIONS FROM HYDRODYNAMICS.....	89
A.6	LITERATURE CITED IN APPENDIX A	91
B	APPENDIX: FIELD RESEARCH.....	97
B.1	INTRODUCTION	97
B.2	POREWATER SALINITY DYNAMICS.....	97
B.3	STATISTICAL ANALYSIS	99
B.4	PLANT PARAMETERS	99
B.5	RESULTS AND DISCUSSION	100
B.6	LITERATURE CITED IN APPENDIX B	113
C	APPENDIX: ECOLOGICAL MODELING	115
C.1	INTRODUCTION	115
C.2	OBJECTIVES.....	119
C.3	METHODS.....	120
C.4	RESULTS	123
C.5	DISCUSSION.....	129
C.6	IMPLICATIONS	130
C.7	LITERATURE CITED IN APPENDIX C	131

This page intentionally blank for two-sided printing.

1 Overview

1.1 Study organization and goals

The goal of this project was to develop the science, data, and modeling to improve our understanding of the Nueces Delta ecosystem functions and the role played by freshwater inflows, for the purpose of restoring the ecological health and functioning of the delta.

This study was initiated as part of the Nueces River and Tributaries Study¹, which developed from the Section 905(b) analysis of the Nueces River Basin (HDR Engineering, 2002) and the subsequent feasibility study². These studies recognized the historic problems of reduced freshwater flows to the Nueces Delta causing ecosystem harm. Because freshwater from the Nueces Basin must serve both human demands and ecological services, an overall management goal must be understanding the relationships between the quantity/timing of freshwater inundation and maintenance of a healthy ecosystem.

Over the last 15 years, significant research and engineering efforts have been undertaken in an attempt to improve ecosystem functioning in the Nueces Delta. The Rincon Bayou Demonstration Project (Bureau of Reclamation, 2000) provided increased flow into the delta through the Nueces Overflow Channel and improved water distribution in the upper marsh through the Rincon Overflow Channel (Montagna et al., 2002; Palmer et al., 2002; Ward et al., 2002). A pipeline connecting the Nueces River above the Calallen salt-water barrier weir to the upper end of the Rincon Bayou was developed to provide a controlled source of fresh water to the delta. This pipeline was first tested in April 2007 and has been used to create 12 freshwater inflow events between September 2009 and August 2012. The salinity monitoring system, salinity effects, and spatial distribution of the Rincon Bayou Pipeline inflows are discussed in Adams and Tunnell (2010), Tunnell and Lloyd (2011), and Hill et al. (2012), respectively.

From an ecological management perspective, the principal questions for the Nueces Delta system are:

1. How much fresh water is needed?
2. Where is the fresh water needed?
3. When is the fresh water needed?

Unfortunately, there are no simple answers because the environmental forcing mechanisms (wind, tide, precipitation, river inflows) are episodic and subject to seasonal/annual/decadal fluctuations with poor predictability. The ecological health of the delta today is an integration of decades of processes affecting the distribution and speciation of plant life; the water needs must be thought of in terms of maintaining robust ecological communities that survive through both drought and flood. Water needs are different for a dry year that is a continuation of a multi-year drought compared to a dry

¹ <http://www.nueces-ra.org/CP/COE/purpose.php> . Accessed Sept. 10, 2012.

² <http://www.nueces-ra.org/CP/COE/ppts/public.ppt> . Accessed Sept. 10, 2012.

year following several wet years. Furthermore, as the present research shows, the impact of freshwater inflows will strongly depend on their distribution across the delta, which depends on both the semi-annual secular tide and the affects of wind-driven flows.

The present study improves our understanding of the functioning of the Nueces Delta ecosystem and provides new models of vegetation, aquatic habitat connectivity, and hydrodynamic inundation that can be used to further develop management strategies for efficient freshwater use. We have developed new insights into the critical role of porewater salinity and the manner in which tidal elevation, wind forcing, and freshwater inflows affect this parameter. This new knowledge provides the foundations for developing quantitative methods and goals for managing the Nueces Delta.

This report provides an overview of our present understanding of the Nueces Delta ecosystem. The body of this report is intended as an overview and interpretation of results developed using methods documented in the appendices. Appendix A contains the hydrodynamics report. Appendix B contains the field research report on porewater salinity. Appendix C contains the marsh ecological modeling report.

1.2 Nueces Delta in a larger context

The Nueces Delta is part of the Corpus Christi Bay system, shown in Fig. 1, which is a complex of interconnected embayments and associated watercourses extending from the main tidal inlet of Aransas Pass to Calallen Dam on the Nueces River (Fig. 2). Geomorphologically, this system is part of a larger connected network of bays ranging from the Laguna Madre on the south to Matagorda Bay on the north. Because the passages and water exchanges between Corpus Christi Bay and the adjacent bays to the north and south – Aransas Bay and the Upper Laguna Madre, respectively – are quite limited, it is appropriate to regard the Corpus Christi system as approximately autonomous. This system is a coastal bay, but, more importantly, it is also an estuary connecting the fresh water of the Nueces River to the salt water of the Gulf of Mexico.

Estuarine dynamics

Estuarine characteristics differ in detail, but are similar in consisting of a semi-enclosed coastal waterbody in which ocean and fresh waters intermix. An estuary is therefore transitional between a continental watercourse and the sea, being influenced by both terrestrial and marine processes as well as processes that are unique to the coastal zone. Among the oceanic factors that influence an estuary are tides, ocean circulations, and marine storms. On the terrestrial side, the single most important factor is surface water runoff from the land, mainly organized into semi-permanent drainage channels, *viz.* rivers. Indeed, the main source of fresh water for almost all estuaries is river inflow. This is certainly the case for the Texas estuaries. The land surface supplies nutrients and sediments (as well as contaminants and toxics) whose transport into the estuary is primarily affected by inflows. Among the influencing factors unique to the coastal zone are land-sea breeze circulations, nearshore wave processes, littoral sediment mechanics,



Figure 1. Corpus Christi Bay system. Imagery from Google Earth, ©2012 TerraMetrics.

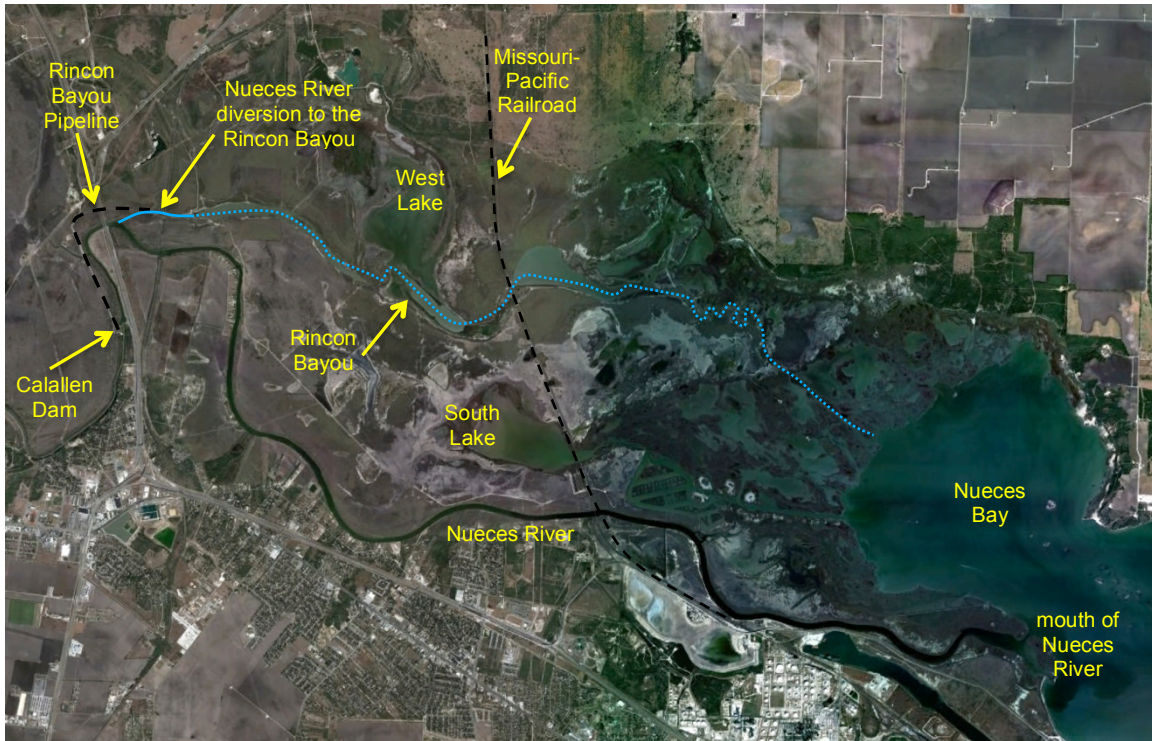


Figure 2. Nueces Delta and environs. The river bypasses the delta except for the narrow diversion (emphasized with solid blue line) and the Rincon Bayou Pipeline (dashed black line). The Missouri-Pacific Railroad cuts across the delta on a dike, which is not visible at this resolution; the path of the railroad is shown with a dashed black line. Imagery from Google Earth.

and water motion generated by the contrasting densities of fresh and ocean water. Estuaries are classified in several ways, one of the most useful being according to their morphology. Corpus Christi Bay is morphologically classified as a lagoonal estuary, characterized as broad and shallow with a limited connection to the sea through tidal passes.

Salinity regime

The salinity of seawater is defined to be the mass concentration of dissolved solids, which is almost entirely salts, and varies around 35 parts per thousand (‰) in the oceans of the world; in contrast, the salinity of freshwater is approximately zero. Therefore, the intermixing of river inflow with ocean water in an estuary establishes a gradient of salinity from zero near the river mouth(s) to oceanic salinity near, or perhaps just offshore from, the estuary mouth. Apart from the *usually* minor effects of landscape salt loading (such as from human effluent discharges) and evaporation³, salinity is a measure of the relative proportion of seawater in a sample of estuarine water. Salinity is therefore a natural water mass tracer for an estuary. It is also an important metabolic determinant for organisms, both plant and animal, living in or adjacent to estuarine waters.

Commercial and ecological value of estuaries

As a coastal waterbody, an estuary is ideally situated to offer access to both fresh water (in the inflow rivers) and the sea. It typically exhibits a range of depths with prominent shoals; it is a nutrient-rich/water-rich environment – in contrast to land, which is nutrient-rich/water-poor, and the oceans, which are nutrient-poor/water-rich – and it affords a degree of protection from the hostile environment of the sea. All of these factors, plus the range of habitats created by the gradient between fresh and salt water, make estuaries attractive to a variety of organisms and the most productive components of the world oceans (e.g., Woodwell et al., 1978; Smith and Hollibaugh, 1993). A central ecological function of estuaries, which extends their importance far beyond their geographical bounds, is that of providing breeding or nursery habitat to a host of marine species. Many species migrate between the sea and the estuary at key stages in their life cycles. It is estimated that approximately 50% (by weight) of the total commercial marine (territorial seas) landings of finfish and shellfish in the U.S. are species that use estuaries during some stage of their life cycle (Lellis-Dibble et al., 2008). For the Gulf of Mexico, this fraction is 97%.

The Texas coastal system

There are nine major bays on the Texas coast extending from Sabine Lake on the Louisiana border to the Lower Laguna Madre in south Texas. These are all estuaries, but river flow diminishes by two orders of magnitude from northeast to southwest along the coast, a reflection of the pronounced gradient in hydroclimatology across the state from humid in the east to arid in the west. The mean freshwater replacement time for these bays (defined as the ratio of bay volume to annual-mean inflow) ranges from weeks for Sabine Lake to years for the Laguna Madre. There is a concomitant range in mean

³ However, along the Texas Gulf Coast in summer, evaporation *cannot* be neglected when using salinity to infer the proportion of seawater.

salinity, increasing down the coast from less than half of seawater for Sabine Lake to 50% greater than seawater (hypersaline) for the Laguna Madre. Other features of the estuarine environment change from northeast to southwest along the coast, such as air temperature, which increases, and inlet cross sectional area, which decreases. Each bay exhibits a different suite of hydrographic characteristics and an associated variation in the animals and plants or their relative proportions. In a northeast-to-southwest progression, the Nueces Delta provides the last freshwater marsh along the Texas coast, thus the southwestern-most habitat for species requiring brackish marsh nurseries.

Two bays on the Texas coast have been recognized as estuaries of national importance by their inclusion in the National Estuary Program: Galveston Bay (Shipley et al., 1994) and Corpus Christi Bay (Volk et al., 1998). The Corpus Christi Bay National Estuary Program (CCBNEP) was organized in the late 1990's, and included a comprehensive assessment of estuarine characteristics and resources as well as original research studies, documented in a series of technical reports, and the formulation of a management plan by a committee of scientists and stakeholders⁴. The CCBNEP was the progenitor of the Coastal Bend Bays and Estuaries Program (CBBEP), which continues to serve as a focus for research and management of the bay system.

Tidal behavior

The dominant connection between Corpus Christi Bay and the sea is Aransas Pass – some limited exchanges also occur through the newly opened Packery Channel near the Laguna Madre to the south and through Cedar Bayou to the north (when it is open) but these are negligible compared to Aransas Pass. The tidal range in the western Gulf of Mexico is small, only about 3 ft (1 m) when lunar declination is maximal, and much of the tidal energy is lost upon passage through Aransas Pass into the bay. The typical daily tidal range inside Corpus Christi Bay is less than 1 ft (0.3 m), and diminishes even more with propagation into the inland reaches of the system. These ranges describe the usual astronomical constituents, which in Corpus Christi Bay are primarily diurnal, semidiurnal and fortnightly in period. More details on the tidal hydrography of Corpus Christi Bay are given by Ward (1997).

There is a longer period rise and fall in water level on the Texas coast, called the secular semiannual tide⁵, which extends into the embayments as exemplified in Fig. 3. This figure illustrates several years of averaged water level variation within Corpus Christi Bay. There are two highs and two lows annually, the highest water levels occurring in the fall and the lowest in winter. The precise elevations and dates of these extrema vary from year to year and are not readily predictable. The mechanics of the semiannual tide are poorly understood, but are considered to be a combination of astronomical forcing, climatology and fluid dynamics of the Gulf of Mexico. What is

⁴ <http://www.cbbep.org/publicationshome.html>

⁵ Technically, a “tide” is a change in water surface elevation associated with gravitational influences of the moon and sun. However, other changes in water surface elevations are commonly referred to as tides, e.g. a “storm tide” is common name for meteorologically-forced changes in water surface elevation. For simplicity, we will use “tide” as the generic name for all forced changes to water surface elevation in Nueces Bay.

important is that the water level excursion between the winter minimum and the autumn maximum shown in Fig. 3 is the baseline about which other tidal components oscillate. This longer-time scale effect is manifested throughout Texas bays, providing an important mechanism for large-scale exchange of water through the bay system and with the Gulf of Mexico.

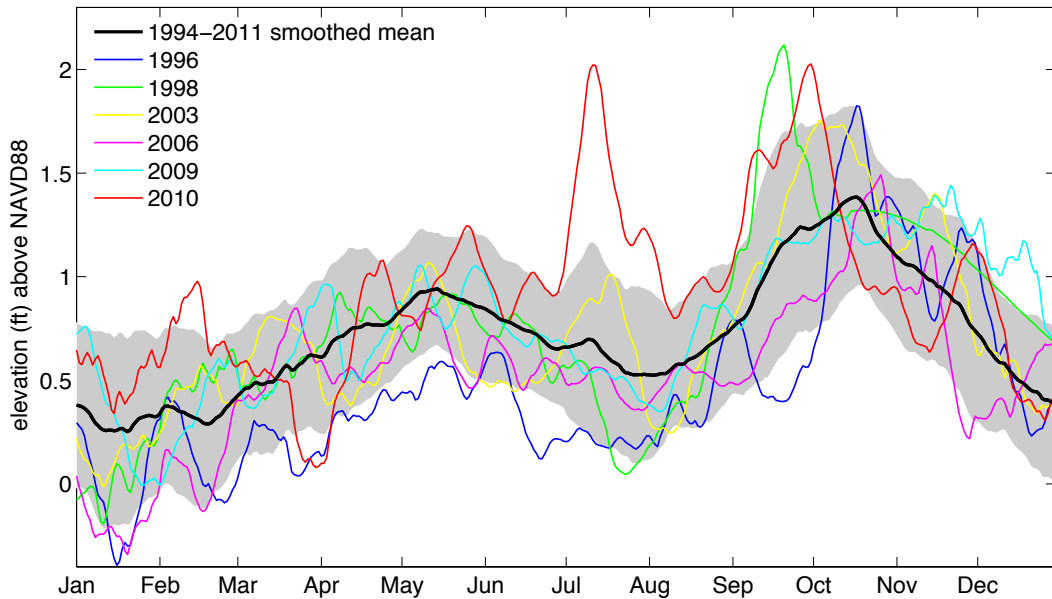


Figure 3. Water levels of Corpus Christi Bay, subjected to a running 14-day average for each year 1994–2011 (only selected years plotted), and the 1994–2011 smoothed daily mean (14 day running average of all data). Gray background is the daily mean \pm one standard deviation. The autumn secular maximum elevation occurs on October 18 at elevations of 1.38 ± 0.13 ft. The spring secular maximum occurs on May 15 at elevations of 0.94 ± 0.08 ft. Individual years may show spring and autumn maximums displaced by as much as 6 weeks on either side of the mean. The unusual peak in July 2010 reflects rainfall from Hurricane Alex in the first week of July and a tropical depression in the second week.

Meteorological forcing

While tidal movement in Corpus Christi Bay is relatively modest by estuarine standards, the large area-to-volume ratio of the bay renders it highly responsive to meteorological forcing. There are several air-sea interaction processes (e.g., storm surge, sea breeze) that manifest themselves through water circulation and associated water-level variation; these meteorological forces undermine the utility of simple astronomical tide predictions. One ubiquitous example is the response of the bay to frontal passages. Fronts initially produce an enhanced onshore (southerly) wind flow followed by an abrupt shift to offshore (northerly) winds. The resulting rise and fall in water levels are typically greater than the astronomical tide and effect a much larger exchange of water volume between the bay and sea.

Corpus Christi Bay is located in the more arid, south reach of the Texas coast. Though the bay itself receives roughly the same annual rainfall as Central Texas, rainfall

events are less frequent, and the higher temperatures and greater insolation often combine to create a net surface deficit (i.e. a negative value for precipitation minus the sum of evaporation and transpiration). Moreover, the watershed of the bay extends west into the arid Brush Country and Edwards Plateau regions, so inflow into the bay is only about 25% of San Antonio Bay and 5% of Galveston Bay to the northeast.

Freshwater inflows

The principal inflow to Corpus Christi Bay is the Nueces River, which debouches into the western end (bay head) of Nueces Bay (Fig. 2, above). A relatively small fraction of this water enters through the Nueces Delta through the diversion channel and through the Rincon Bayou Pipeline (§1.3, below). According to flow data compiled by the Texas Water Development Board, the average annual inflow to Corpus Christi Bay is 57 million cubic meters (46 thousand acre feet), of which nearly 97% is the flow of the Nueces River. The time signal of inflow to Corpus Christi Bay can be succinctly summarized as a sustained low flow upon which are superposed flood pulses separated by long, irregular intervals. On the upper Texas coast, flood hydrographs cluster seasonally, producing a dependable seasonal variation in inflows, with high flows in the spring and fall, and low flows in winter and summer. With distance down the coast, the increasing aridity means these flood hydrographs become smaller in magnitude, sparser in time, and the seasonal variation less dependable. The unpredictable appearance of hurricanes and large tropical storms provides occasional years with extraordinary rainfall that may dominate the river inflows in the annual freshwater budget.

Urbanization

Corpus Christi Bay has been greatly modified to support urban development on its periphery, notably the city of Corpus Christi (Ward, 1997). In the latter part of the nineteenth century, the bay inlet was stabilized by revetment and jetty construction. The shallows between Aransas Pass and the open waters of Corpus Christi Bay were opened by dredging in the 1910's, an action which shifted the main tidal flow away from the natural tidal gorge to the north (the Lydia Ann Channel). In 1925, the Corpus Christi Ship Channel was completed across the bay to the Corpus Christi Inner Harbor to accommodate the drafts of ocean-going vessels. Over the succeeding decades, the ship channel dimensions have been increased by dredging to accommodate larger vessels. Much of the shoreline of the bay has been bulkheaded or revetted, and much of the peripheral watershed has been replaced by impermeable surfaces or converted to agriculture. About 15 percent of the mean inflow of the Nueces River has been diverted for water supply, but the proportion is much higher in the later years of the record and during drought. The bay receives runoff from agriculture and return flows from the municipalities and industries that have developed on its periphery. In 1999, the National Ocean Service in its National Eutrophication Assessment (Bricker et al., 1999) declared Corpus Christi Bay to be eutrophic (a determination that is disputed by some scientists), and among the six most eutrophic estuaries of the Gulf of Mexico.

Nueces Delta study under Senate Bill 3

Most recently, as part of the Senate Bill 3 process to establish flow standards for Texas rivers and inflow standards for the estuaries into which the rivers flow, the Nueces Basin

and Bay Expert Science Team (BBEST) issued a report on its one-year study of the Corpus Christi Bay system (BBEST, 2011). The BBEST found that Nueces Bay is no longer a “sound ecological environment” under the definition of S.B. 3. This finding was based on the determination that species historically supported by conditions in the bay are no longer present. Of the seven major bay systems addressed in the S.B. 3 process, this is the only determination of an unsound ecological environment.

1.3 Features of the Nueces Delta

Most of the marine species utilizing estuaries are catadromous, meaning their young migrate into estuaries to grow out to maturity and take advantage of the estuary’s shelter and food. For many of these organisms, it is wetlands that afford the principal nursery habitats. In the northern Gulf of Mexico, and on the Texas coast in particular, the most important such habitats are salt marshes (e.g., Turner, 1977; Zimmerman et al., 2002). Those salt marshes located in or in the proximity to river deltas are especially valuable. In Corpus Christi Bay, by far the most extensive such habitats are in the delta of the Nueces River, a.k.a. Rincon Bayou and Nueces Delta marsh. Ecologists that have studied Corpus Christi Bay for many years have come to the opinion that the *sine qua non* of the bay’s productivity is Nueces Bay and the Nueces Delta.

Upstream dams on the Nueces River

This deltaic system is located in the head of Nueces Bay. The principal distributary is Rincon Bayou (location shown in Fig. 2, above), which is a relict channel of the Nueces River. The river abandoned this channel rather recently in geological time; the Rincon Bayou serving as the main channel is certainly prehistoric (see, e.g., Superintendent of the Coast Survey, 1862) but within the past 2.5 ka BP (Simms et al., 2008). The present main channel circles the southern periphery of the delta and empties directly into Nueces Bay (Fig 2, above). Despite the diversion of the main river flow, the delta was regularly flooded by high river stages (until hydrologic modification by man). Historically, flood waters entered the delta through several low points in the natural levee that otherwise separates the main channel and the delta. This hydrologic function began to change with the construction of a water supply reservoir on the Nueces River for the city of Corpus Christi. Mathis Dam and Lake Lovenskiold were constructed in 1929, replaced by La Fruta Dam and the first Lake Corpus Christi in 1934, later subsumed by Wesley E. Seale dam and the present Lake Corpus Christi in 1958. The hydrograph was further impacted by Choke Canyon Reservoir, constructed upstream of Lake Corpus Christi on the Frio River in 1982 (Ward, 1997; Hill et al., 2011). Although these reservoirs do not have flood-control storage, the long duration between major flood events coupled with the high evaporation rate and municipal withdrawals routinely results in substantial drawdown of the reservoir volume. Thus, when flood hydrographs do occur, their time base is extended and their amplitude is diminished. Fewer flow events reaching the Nueces River alongside the delta are large enough to overtop the levee, and those that do so carry smaller flood volumes into the delta (Irlbeck and Ward, 2000; Ward et al., 2002; and citations therein).

Past and ongoing efforts to improve Nueces Delta

The modern Nueces Delta is water-starved, which constrains the productivity of Corpus Christi Bay. Since the late 1970's, the possibility has been explored of opening a cut in the east levee of the Nueces River, so that more flow might be intercepted and diverted into the delta during flood events (Ward, 1985). For the period 1995-99, the U.S. Bureau of Reclamation operated a demonstration project in which a cut from the Nueces River below Calallen Dam into the head of Upper Rincon Bayou was maintained (Bureau of Reclamation, 2000; Ward et al., 2002). The response of the marsh to the resulting flood water diversions established that this was a feasible means of improving the conditions of the marsh, particularly vegetation, whose community structure and spatial density are important metrics of the environmental integrity and health of the marsh. This experiment led the City of Corpus Christi to install a permanent diversion from the river into the Rincon Bayou (location shown in Fig. 2, above). However, this diversion is not a panacea, because the less extreme hydrograph of the river (as controlled by upstream dam operations) often leads to the water in the Nueces River near the diversion being tidal Corpus Christi Bay saltwater with only minor dilution. The barrier physically limiting the tidal influence on the main channel of the Nueces River is the Calallen Dam⁶, which is upstream of the diversion and cannot prevent tidal saltwater from entering the Upper Rincon Bayou.

Further efforts to improve and control freshwater flows into the delta were made by building the Rincon Bayou Pipeline (location shown in Fig. 2, above), which takes freshwater upstream of the Calallen Dam and introduces it into the upstream channel of the Rincon Bayou. During pump operation, a gate⁷ is used to close the connection between the Nueces and the Rincon Bayou to prevent backflow into the main channel. Freshwater pumping is certainly helping the marsh, but many questions remain, including the time and space extent of the effects of the diversion and pumping, the relative impacts on the marsh of alternative strategies of water inputs, the volumes of flow necessary for quasi-permanent improvement of the delta, and the ultimate response of biota utilizing the delta. The present study was designed to provide the scientific understanding and tools to address these questions.

Marsh inundation

The distribution of water on the surface of a marsh is dictated by the interaction between two factors: the time signal of the source of water and the physiography of the marsh. For the better-studied salt marshes on the east coast of the U.S., the principal mechanism of inundation is the astronomical tide. The tidal range is on the order of 10 ft (3 m) in the Atlantic, about an order of magnitude greater than for marshes of Texas. This difference has consequences for vegetation. The higher tidal range in the Atlantic means greater spatial extent of inundation on flooding tides and therefore more reliability in water supply for the development of vegetation communities. There is generally a clearer

⁶ The Calallen “Dam” is only about 5 ft above sea level (Ockerman 2001) and should be classified as a weir rather than a dam.

⁷ CBBEP is going through a permitting process with the U.S. Army Corps of Engineers for a permanent hydraulic structure to replace the present gate (Tunnell, *pers. comm.*).

distinction between high marsh and low marsh in Atlantic systems than is seen in Texas marshes. On the other hand, the marsh “edge” on the Atlantic coast (as defined by the encroachment of vegetation into the adjacent water) is typically higher than is the case for Texas marshes (Minello et al., 2011).

For Texas marshes, and in particular the Nueces Delta, meteorological water-level excursions and riverine flooding are more important as a source of inundation than the astronomical tide, except perhaps for the immediate zone on the order of 10 ft (3 m) from the bay into the marsh. The major contrast is that Atlantic marshes have dependable daily flooding mechanisms, whereas Texas marshes have only the secular semiannual tide (Fig. 3, above) providing dependable hydroperiod. Because the main river bypasses the Nueces Delta, its inundation and hence survival depends on floods or meteorological tides driven by wind and storms, whose efficacy depends upon when they occur with respect to the semiannual tide. With the historic hydrographic alteration of the Nueces River flows, flooding depends on extreme events (e.g., hurricanes) causing substantial rainfall either directly on the marsh or in the limited catchment between the delta and Wesley E. Seale Dam.

The effect of physiography is to determine the paths of water movement and retention on the marsh surface during inundation events. The distributary network of “channels” is the main mechanism of conveyance, and when inundated these channels provide both the vehicle for water movement and connectivity between major regions of the marsh. Some indication of the channel network is apparent in Fig. 4, in that the major

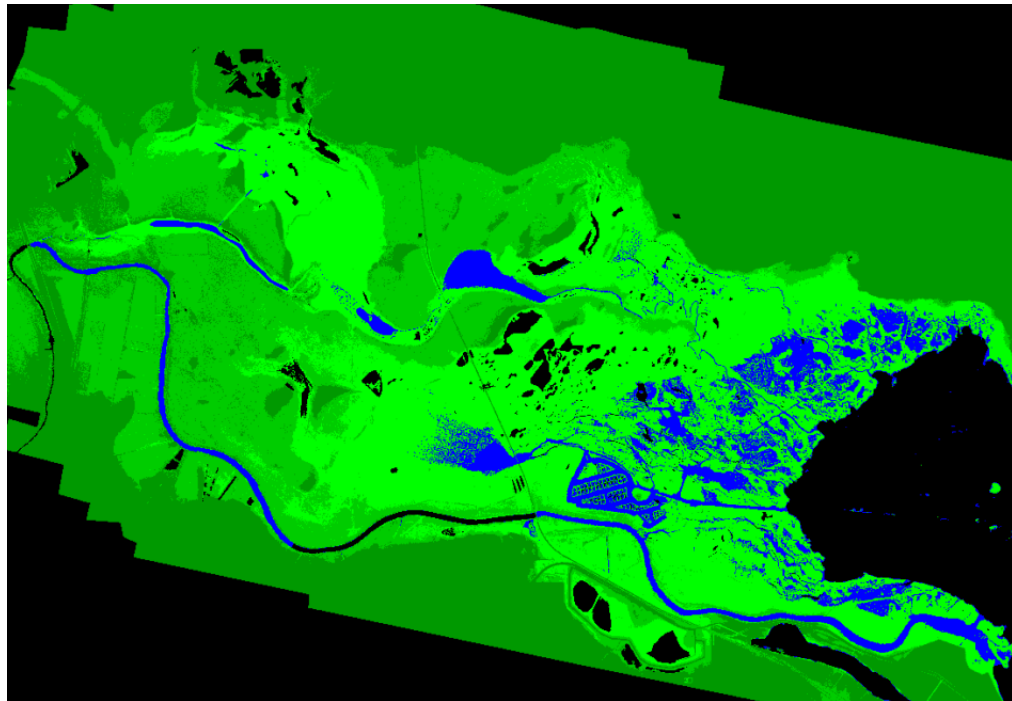


Figure 4. Physiography of Nueces marshes, blue = inundated at sea level, light green = lower marsh, medium green = middle marsh, dark green = high marsh and uplands, black = non marsh areas.

permanent channels are delineated, but the ephemeral channels are not. These may be differentiated from tidal flats by only a few centimeters of elevation difference. The main gradients in vegetation community structure are found on lines normal to the marsh channels (see §2.1). Unfortunately, man has modified the surface of the Nueces Delta over many years, disrupting the natural water-distribution network. This disruption has included installation of roads, soil compaction by cattle trampling, and, most notably, the placement of the railroad bed (Fig. 1, above), whose embankment is bridged in a few places (e.g., Fig. 5a), but otherwise acts as a major barrier to water flow (Fig. 5b) between the upper and lower marshes.

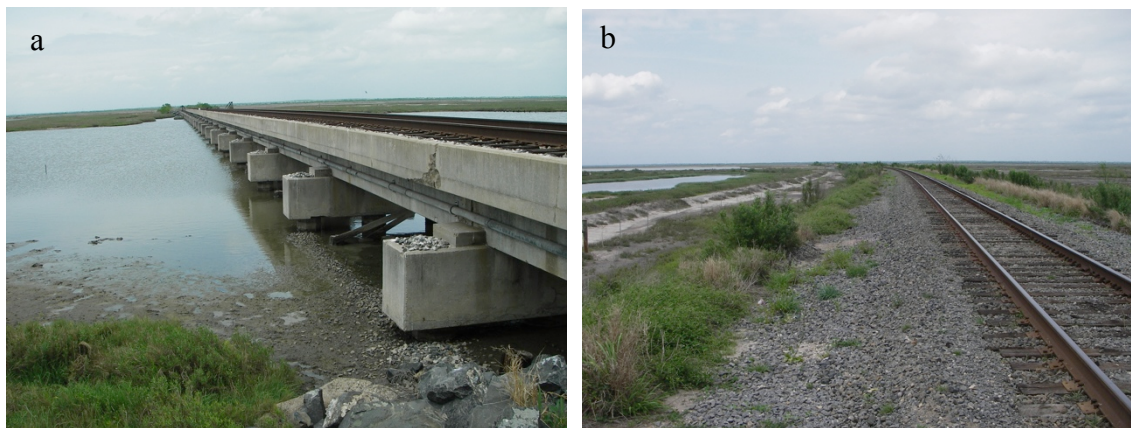


Figure 5. (a) Bridged section of railroad at South Lake; (b) non-bridged railroad embankment.
Photos by B.R. Hodes, 2011.

1.4 Key issues for ecosystem sustainability

Salinity and inundation define community composition and viability

There are several key problems that impact potential management strategies for both the Nueces Delta and the larger Corpus Christi Bay system. For the delta, first, salinity is the defining parameter for vegetation community viability and nursery ecological functions. With the cessation of inundation, the marsh exhibits a water loss to evaporation and transpiration, so that the salinity of whatever water is retained by the marsh increases until the next inundation event. Reducing salinity is the objective of the present program of water releases through the Rincon Bayou Pipeline by the City of Corpus Christi. Second, it is the volume and frequency of inundation events that determine the extent and quality of the delta's surface water. As described above, the important hydrographic mechanisms for inundation are (1) long-period rise and fall of water level on the coast, notably the secular semiannual tide, (2) flood events on the Nueces River, and (3) set-up and set-down of Nueces Bay due to meteorological events. Inundation, of course, is the key mechanism that controls water transport, connectivity, and circulation in the marsh, and ultimately determines salinity. Of secondary importance after salinity are the supplies of nutrients and sediments to the delta. Typically, riverine flooding provides the principal source for these, and retention of flood waters on the marsh surface is necessary to obtain their ecological benefits.

Nursery for the coastal system

For the larger estuarine system, beginning with Nueces Bay, it is the nursery function that is of central importance. Utilization of the shallow, lower-salinity environment of Nueces Bay by a range of biota, especially juvenile, is a prime metric of ecological function. Presence of juvenile shrimp, crab, and finfish in the shallow waters of Nueces Bay are an indicator of the bay's viability. The loss of oyster was specifically identified by BBEST (2011) in its determination of an unsound ecological environment. Oyster reefs are important shallow-water habitats for variety of species, and the reefs also play an important hydrodynamic role in their interception of current flow and extraction of nutrients and other transported constituents.

Trends are in the wrong direction

The prognosis for the Corpus Christi Bay system in the absence of management intervention is not optimistic. Decreasing trends have been reported in Corpus Christi Bay for blue crab, white shrimp, brown shrimp, along with southern flounder and several other finfish (e.g., Choicair et al., 2006). Few oysters are found in Nueces Bay. Water demand in the Corpus Christi area continues to increase, and though other supplies have been secured (e.g., Lake Texana) or are being sought, the Nueces River will continue to be the primary source for the city. Recent intense droughts have raised concerns about climate change effects and sea-level rise, which indisputably threaten to accelerate marsh erosion on the bay side.

2 Ecosystem response to inundation

2.1 The ecosystems

The marshes of the Nueces Delta provide three distinct ecosystems: tidal creeks/pools, lower marshes, and upper marshes, Fig. 6 (also see Fig. 4, above). The key feature of the tidal creeks and pools is their continuous connectivity with Nueces Bay over seasonal time scales. Because of the semiannual secular tide (Fig. 3, above), the extent of these creeks and pools changes with the season. The tidal creek connectivity is critical to the delta's role as habitat for fish and invertebrates, part of the nursery function for the wider coastal bay system. The lower marshes are areas inundated by the semiannual secular tide, as well as episodically inundated by floods, storm tides, and wind-driven events. The upper marshes are areas that may see inundation during the November secular maximum, or during extreme storm and precipitation events – particularly those coinciding with the May secular maximum. The ecological health of the lower and upper marshes directly depends on the frequency and duration of inundation, which controls the accumulation and flushing of porewater salinity. Insufficient flushing leads to the development of salt pans that are inhospitable to plant life (Fig. 7).

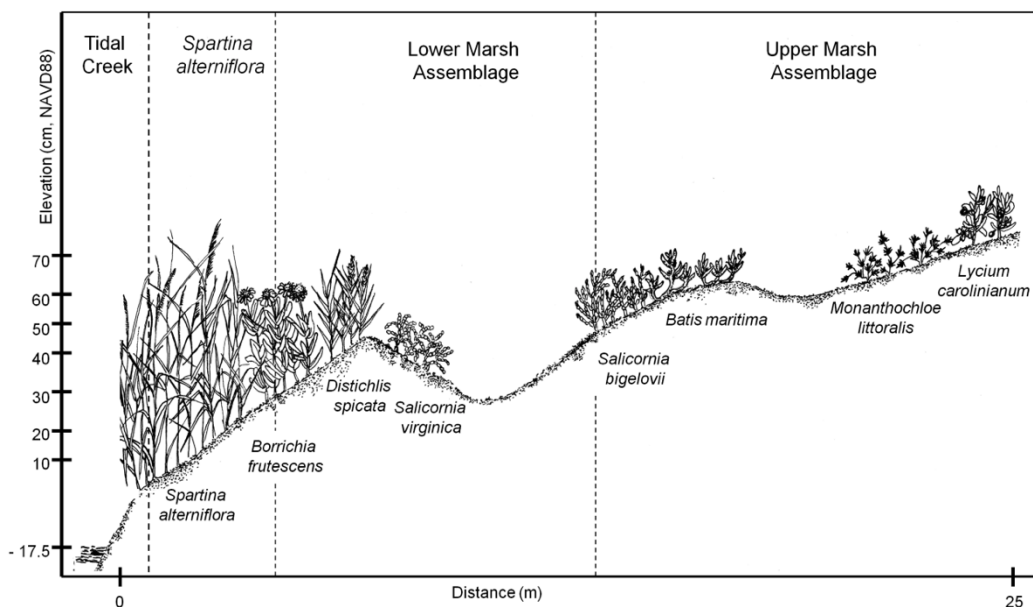


Figure 6. Zonation patterns of emergent vegetation in the Nueces Marsh in relation to vertical elevation. Tidal creek banks are dominated by *Spartina alterniflora* and *Borrichia frutescens*, whereas these species are largely absent in the interior marsh. As marsh species' habitat is separated primarily according to soil moisture and porewater salinity, areas of lower elevation in the marsh interior are characterized by vegetation “gaps”, where high porewater salinity and moisture levels preclude plant establishment. As one moves upstream in the Nueces Delta, the vegetation “gaps” become increasing larger as the frequency of overbanking events related to tidal excursions become attenuated, leading to the occurrence of extensive salt pans. Adapted from Rasser et al., (2013).



Figure 7. Area of the Rincon Bayou in the lower salt marsh showing vegetation near channels, impounded pools, and salt pans. Imagery from Google Earth historical data, 11/22/2011 satellite.

Plant zonation affected by inundation

Salt marshes are characterized by physical gradients, including pore water salinity, inundation frequency (both from freshwater pulses and tidal variation), and nutrient availability. Plant zonation is defined by these gradients (Chapman, 1974; Adam, 1990; Raffaelli and Hawkins, 1996). The high and low areas of the marsh are the extreme points in the physical gradients and are characterized by distinct plant assemblages. The low marsh is characterized by higher tidal energy and is more frequently inundated by tidal flow. Salinities in the low marsh are usually dominated by bay salinities. The high marsh is rarely inundated by bay water and prolonged exposure to dry conditions leads to higher salinities. The mid-marsh, in semi-arid climates, contains plants from both the high and low marsh assemblages (Zedler et al., 1999).

The general patterns of zonation have a strong influence on how plants in the Nueces Marsh respond to elevation (Rasser, 2009). The plant cover and physical characteristics of the Nueces Marsh were identified in a geographic information system using elevation from a lidar digital elevation model (Fig. 8). The plants *Borrichia frutescens* and *Salicornia virginica* dominate cover at the lowest elevations around 50 cm above mean sea level. *Spartina alterniflora* dominates cover at higher elevations between 120 -200 cm (Fig. 9).

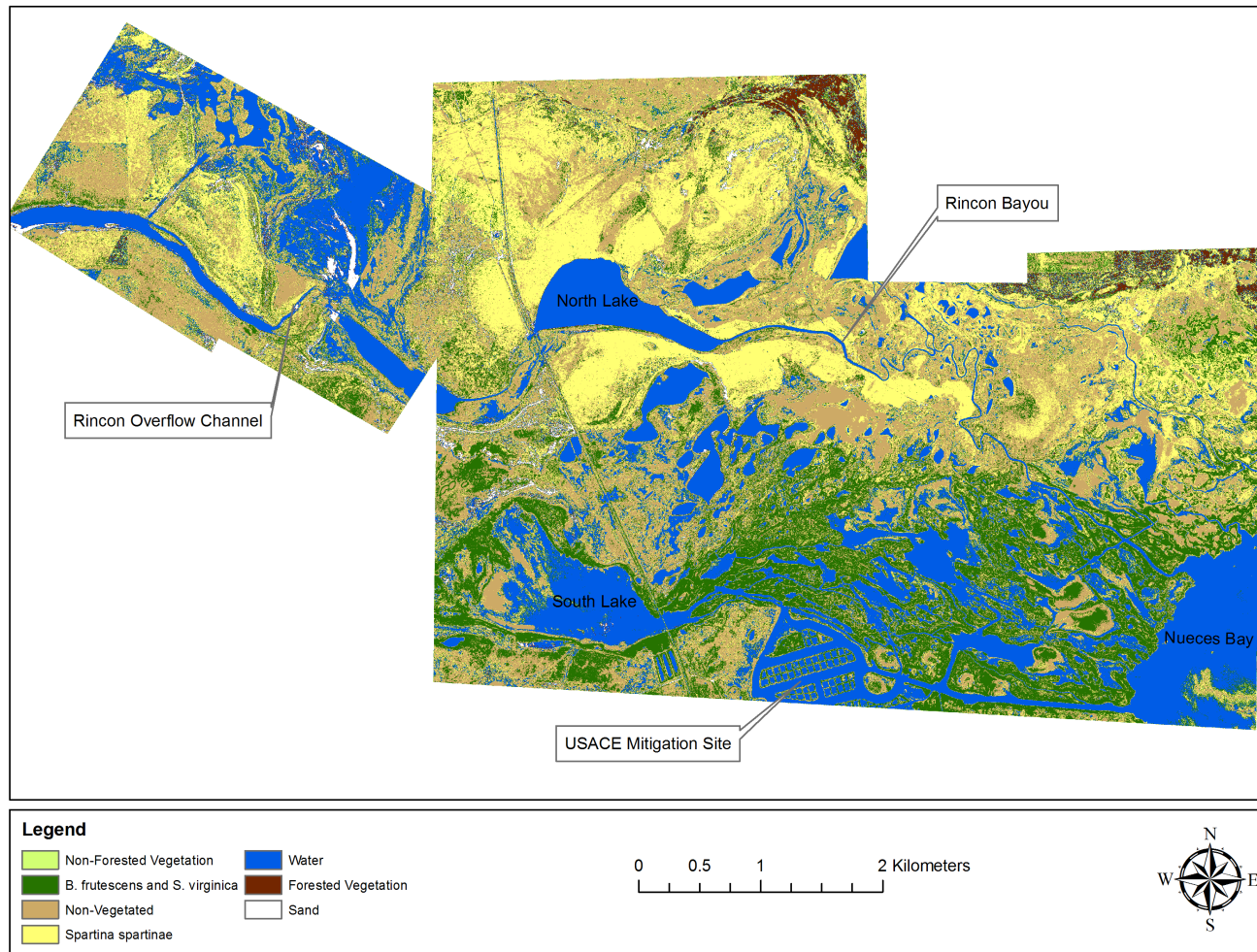


Figure 8. Vegetation distribution across the Nueces Marsh based on classification of digital aerial imagery acquired 1 November 2005 (Rasser, 2009).

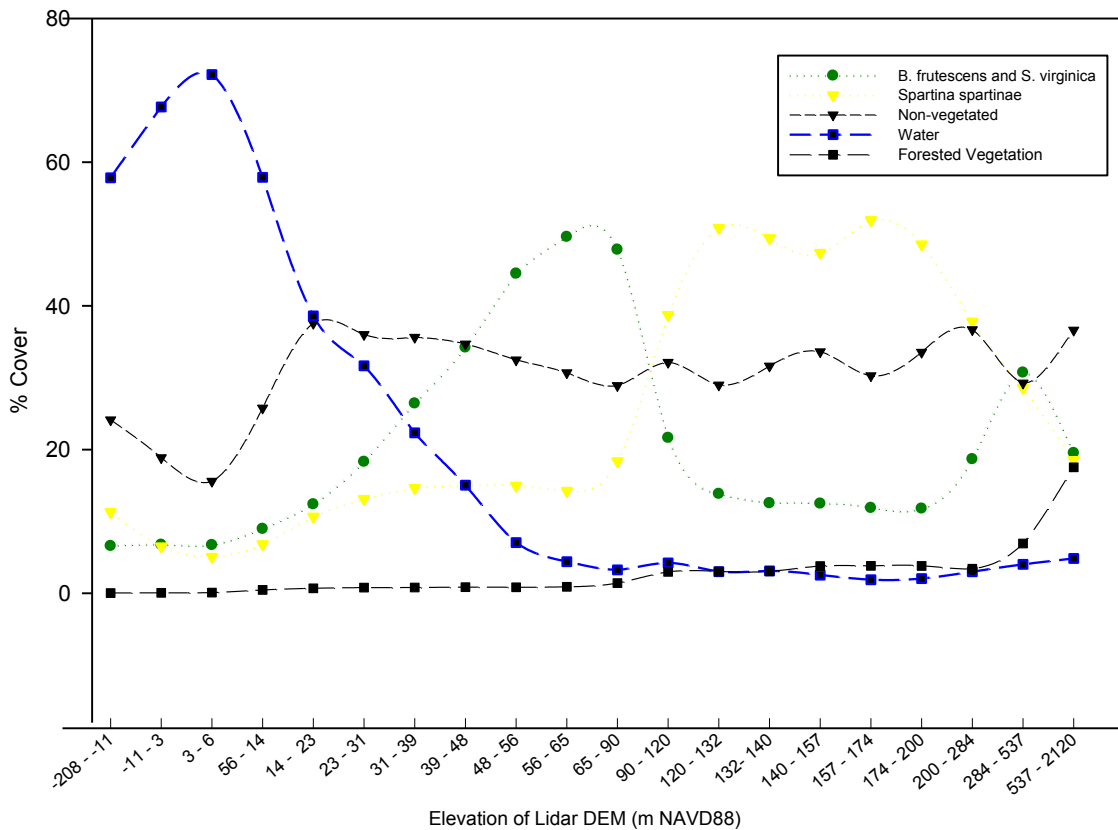


Figure 9. Percent cover of classes from Fig. 8 within the Nueces Marsh as a function elevation (Rasser, 2009).

Decreases in overbanking event frequency in the Nueces Delta, especially during prolonged low water levels in summer and winter, leads to extensive evaporation and drainage of creek bank and interior marsh areas. The resulting gradients in porewater salinity causes distinct zonation of emergent plants in the Nueces marsh (Rasser, 2009). As long as water levels remain below inundation stage and soil moistures remain high (exceeding field capacity), creek bank and interior marsh soils lose water due to evaporation, especially in lower elevation areas. As a result, salts become concentrated in exposed surface sediments, prohibiting plant establishment. The resulting salt pans vary greatly in spatial extent (e.g., white areas in Fig. 7, above).

We believe that alternating periods of regular and irregular inundation produced in response to the phases of the semiannual secular tide are the primary determinant of zonation patterns presently observed throughout the Nueces Delta. During the negative phase of the semiannual tide, the marsh surface is often exposed for long periods of time (weeks to months). Both the low water levels during these periods and extreme flooding events discourage processes that produce distinct zonation patterns. In contrast, periods of regular inundation produce differences between the environmental characteristics of creek bank and interior marsh areas, therefore promoting distinct patterns of plant

zonation (Dunton et al., 2001). This hypothesis is supported by Forbes and Dunton (2006) who noted that the greatest emergent plant diversity in the Nueces Marsh was found during moderate climatic periods. During extremely wet periods, the plant community was dominated by only a few ecologically dominant species. Conversely, during dry periods the plant community was reduced to only a few species capable of tolerating extreme environmental stress. Thus, porewater salinity dynamics in the Nueces Marsh share some characteristics with salt marshes elsewhere, but are uniquely controlled by the conspicuous semiannual secular tide (Ward et al., 2002) and the relatively low amplitude of these tides compared to the U.S. east and west coasts.

2.2 Vegetation Response to Salinity Gradient (Tidal Creek to Marsh)

Separate but related studies by both Rasser (2009) and Stachelek (2012) in the Nueces Marsh have demonstrated the important role of porewater salinity in controlling the abundance and distribution of plants in low latitude salt marshes, especially across elevation gradients from tidal creeks to interior marsh. Stachelek (2012) noted that interior marsh porewater salinities are broadly reflective of discharge and replacement by either rising tidal creek waters or precipitation. Past studies have noted a tight coupling between freshwater inflow events and tidal creek salinities (Alexander and Dunton, 2002; Forbes and Dunton, 2006; Ward et al., 2002). However, in this study, we found that precipitation is often the dominant source of porewater flushing during prolonged seasonal low water events driven by the semiannual secular tides in summer and winter. Porewater salinity dynamics of the Nueces Delta are highly dependent on water level variations and inundation of the interior marsh. High water levels, present in fall and spring, result in more frequent inundation and porewater flushing.

Plant species and salinity

Differing porewater salinities in creek bank versus interior marsh areas may control emergent plant distributions in the Nueces Delta (Forbes and Dunton, 2006; Rasser, 2009). For example, *Spartina alterniflora*, which is only found at extremely low elevations adjacent to creek banks, has a low tolerance for extreme variations in porewater salinity (Touchette et al., 2009). A study by Webb (1983) on Galveston Island, Texas, found that porewater salinities exceeding 25 resulted in significant reduction in density, height, and standing biomass of *S. alterniflora*. Along tidal creeks, the *S. alterniflora* root zone is generally buffered from extreme salinity and soil moisture variations due to consistent inundation. The root zone of *Borrichia frutescens*, in contrast, is found on elevated creek bank levees (Fig. 6, above) where sediments are irregularly inundated and porewater salinity can be highly variable. Porewater salinity dynamics in interior marsh areas, which are dominated by *Batis maritima*, are generally high, but considerably more stable than creek bank porewater salinities (Fig. 10).

As the only salinity-tolerant emergent plant species in the Nueces Marsh, the distribution and abundance of *Spartina alterniflora* reflects environmental conditions in tidal creeks and exhibits a salinity tolerance similar to other faunal estuarine indicator species (BBEST, 2011). Our results clearly show that the coverage of *S. alterniflora* is regulated by porewater salinity. For instance, the cover of this species was substantially

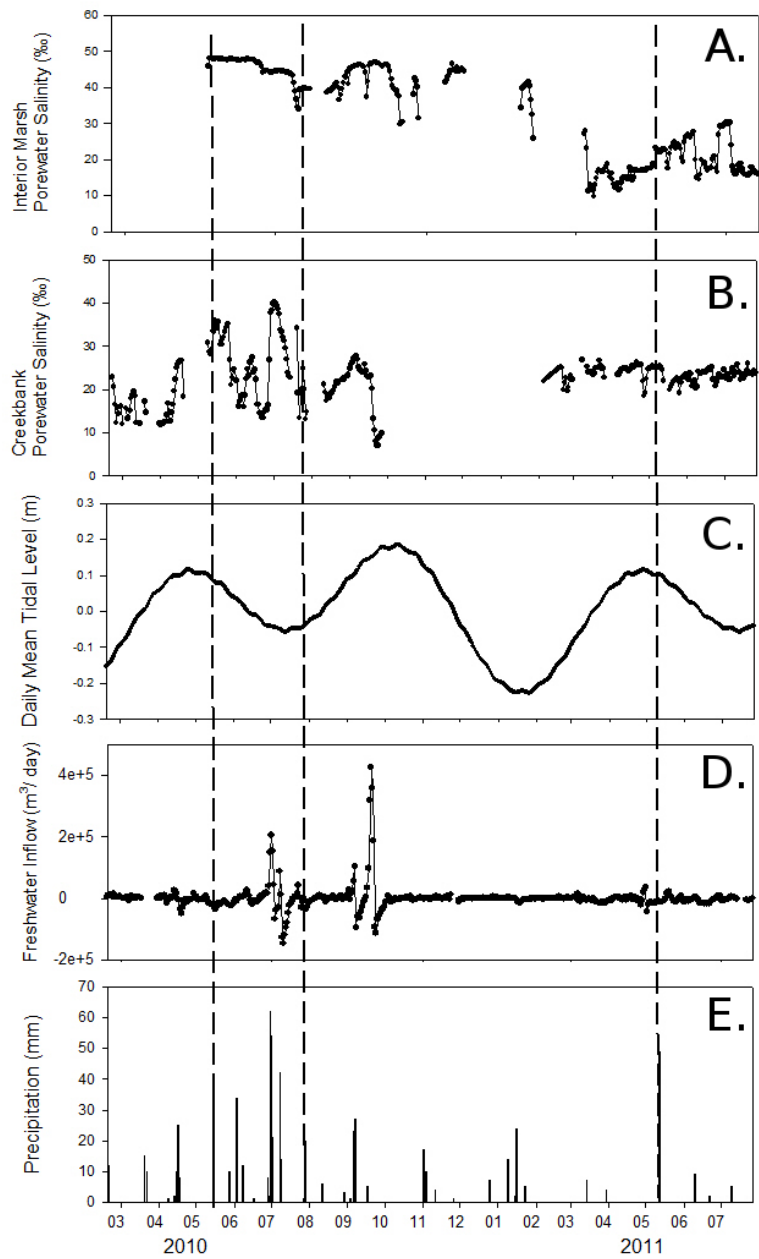


Figure 10. Time-series of porewater salinity at site 450 (A and B), mean water level in Nueces Bay (C), freshwater inflow to the Rincon Bayou (D), and precipitation (E). Local precipitation data were recorded at the Nueces Delta weather station (NUDEWX). Freshwater inflow (discharge) data were taken at the USGS Rincon Bayou gage station (#08211503). Gaps in the porewater salinity data occurred as a result of low soil moisture conditions. Dashed lines highlight precipitation events not accompanied by a freshwater inflow event. From Stachelek (2012).

reduced at salinities exceeding 25 (Fig. 11), whereas percent cover of *B. frutescens*, and *S. virginica* showed no relationship with porewater salinity. Webb (1983) found that porewater salinities exceeding 25 resulted in significant reductions in density, height, and standing biomass in *S. alterniflora*. Integrative studies by BBEST (2011) and TDWR (1982) illustrated that the freshwater inflow needs of *S. alterniflora* are nearly identical to that of other common indicator species such as blue crab (*Callinectes sapidus*), Atlantic croaker (*Micropogonias undulatus*), and eastern oyster (*Crassostrea virginica*). Therefore, one would expect that percent cover of *S. alterniflora* serves as a reasonable proxy for the abundance of these higher trophic level organisms.

Surveys by Forbes and Dunton (2006) and Rasser (2009) reveal that *S. alterniflora* is concentrated at the edge of tidal creeks and in lower elevation areas in the lower Nueces marsh. However, this species is extremely rare in upstream marsh habitats (further from Nueces Bay) beyond the railroad track that bisects the Nueces Delta (Fig. 5, above). This railroad crossing restricts hydraulic flow between the low and high marsh and substantially dampens tidal fluctuations (Ryan, 2011). Similarly, *S. alterniflora* is not found within the interior marsh except at low elevations where frequent inundation via small tidal creeks allows adequate water exchange.

Creek overbanking into the marsh and porewater drainage

Modeling exercises used to evaluate potential replacement and dilution of pore waters revealed that (1) creek bank drainage in the Nueces marsh occurs at a high rate compared to salt marsh soils elsewhere, and (2) porewater replacement likely takes place primarily through vertical percolation. Large porewater salinity fluctuations following either large precipitation events or high water levels exceeding inundation stage confirmed this hypothesis. Since porewater salinity is a major determinant of vegetation abundance and diversity (Rasser, 2009), the value of freshwater inflow events in and of themselves is not viewed as important as the development of inundation (overbanking) events that flood the marsh and promote vertical percolation of sediment pore waters (Ward, 1985; Stachelek, 2012). Thus, freshwater inflows without overbanking (confined to the tidal creeks) will have limited impact on the vegetation health of the saltwater marsh.

Our long-term observations clearly show that freshwater inflow events provide critical moderation and flushing of sediment pore waters. The importance of these events is especially apparent during drought years when the absence of freshwater inflow leads to hypersalinity and extreme soil moisture deficits (Forbes and Dunton, 2006). A substantial portion of this study encompassed a severe drought period beginning in May, 2011, which intensified following the conclusion of monitoring in July, 2011. The Palmer Drought Severity Index values at the conclusion of monitoring (< -2.75) indicated that South Texas was in an exceptional drought⁸. Porewater salinities remained unchanged in 2011 due to a lack of precipitation and freshwater inflow events.

⁸ National Climate Data Center, <http://www.ncdc.noaa.gov/sotc/drought/2011/7>

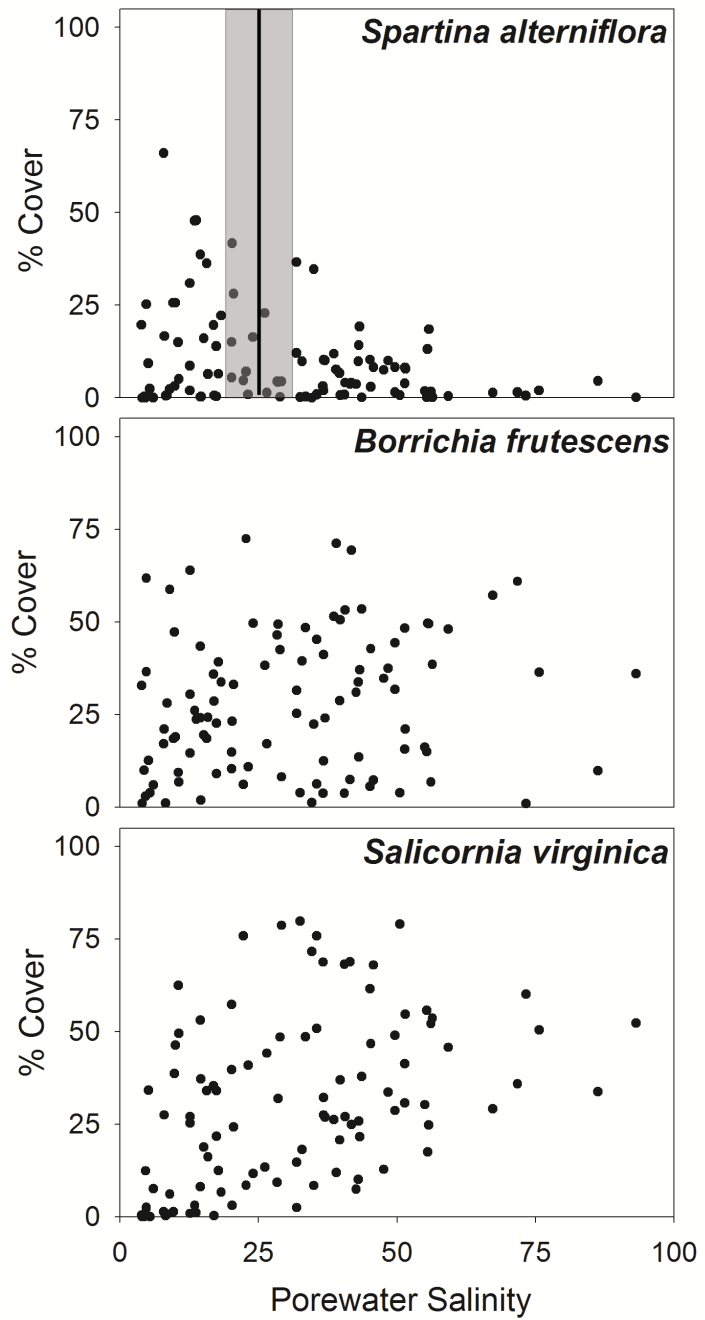


Figure 11. Percent cover of individual plant species (*S. alterniflora*, *B. frutescens*, and *S. virginica*) relative to variations in porewater salinity. The salinity tolerance (shaded box) of *S. alterniflora*, estimated at 25 ± 5 , was estimated from empirical measurements and published literature values (Webb, 1983; Bertness, 1991). From Stachelek (2012).

2.3 Modeling plant cover change

A goal of this project was developing a forecasting system to allow us to determine effects of human activities on marsh structure and function, in particular vegetation. One of the problems facing us in the Nueces Delta is to determine how much water to divert back into the marsh to increase water levels in order to restore the vegetated wetlands. To solve this problem, we have designed mathematical models for marsh ecosystems of the wetlands of the delta (Fig. 12). These mathematical models could be modified as needed and applied to marshes in other regions of the country that are susceptible to the negative ecological and environmental impact from construction and water resource development.



Figure 12. Nueces Marsh surrounding the Nueces River entering Nueces Bay. Photo by Paul Montagna during high flow conditions (July 1997).

Marsh model capabilities

In the model developed for this project (see Appendix C for details) the definition of marsh regions is based on elevation. For this report, water areas are designated by areas of elevation less than 0.0 m. The low marsh is all points between 0.0 m to 1.0 m, the mid marsh from 1.0 m to 2.0 m and the high marsh anything above 2.0 m. While three elevation ranges were used in this study, the number of ranges and the size of the elevation bins can be varied in the model. Elevation was used for grouping plant species in this study. Other grouping schemes could have been used, such as distance from continuously-inundated tidal creek, or salinity tolerance.

The model can be tailored to represent individual species or groups of species based on any group definition. Following a previous study in the Nueces Delta (Forbes and Dunton, 2006), plants were divided functionally into two groupings: 1) clonal stress tolerant (CST) plants, and 2) clonal dominants (CD). Clonal stress tolerant plants are

small, slow-growing plants including *Batis maritima*, *Distichlis spicata*, *Monanthcloe littoralis*, and *Salicornia virginica*. The clonal dominant plants are taller, faster-growing species, which include *Borrachia frutescens* and *Spartina alterniflora* (Grime 1979; Boutin and Keddy 1993). Facultative annuals, which do not spread clonally, were not included in this study, but with suitable growth rate estimates, could be easily included.

Marsh model results

The model predicts mostly reductions in plant cover for various initial plant coverage conditions (Fig. 13). In both drought and moderate conditions⁹ the model predicts a decline in plant coverage. Marsh plant coverage increases in area only during the wet conditions when there is space available. If the initial conditions are that there is already 100% coverage – as on the far left of Fig. 13 – then there is no room for plants to grow and fill more space. It is not until there is about 20% space vacant that plants will grow and fill the remaining space.

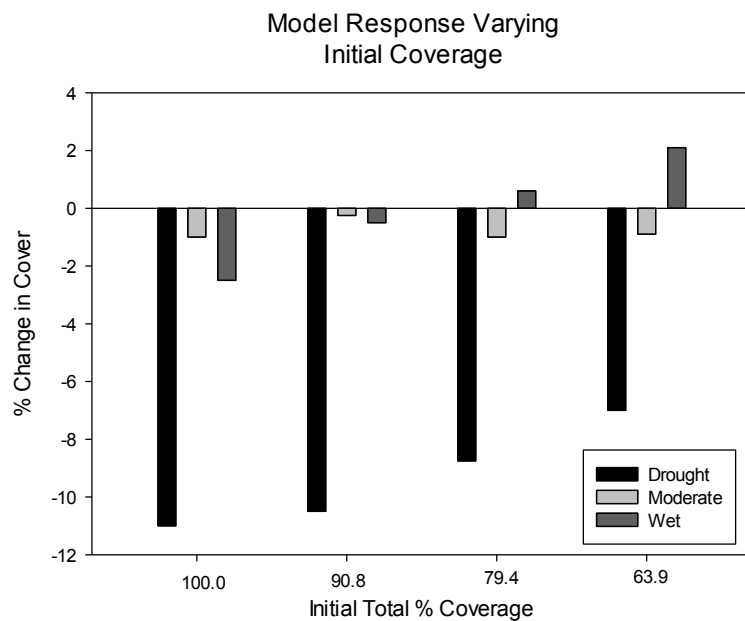


Figure 13. Change in percent coverage based on various initial coverage conditions. Run duration was 3 months, and climate defined in Table C.1 (Appendix C).

The modeling experiment was run for a 10-year period nine times: three climate periods for three initial coverage conditions (Fig. 14). The three climate conditions were dry, moderate, and wet. The three initial starting plant coverage conditions were 2%, 50%, and 100% (Fig. 14, solid lines, thick lines, and dotted lines respectively). It was assumed that the initial conditions contained equal amounts of each functional group, thus two species starting at 25% cover (the thick lines) have a total coverage of 50%. The marsh plants consistently approach a steady state of maximum coverage during wet periods for all starting conditions. Coverage decreases during moderate conditions and more dramatically during drought conditions.

⁹ Defined in Appendix C, Table C.1

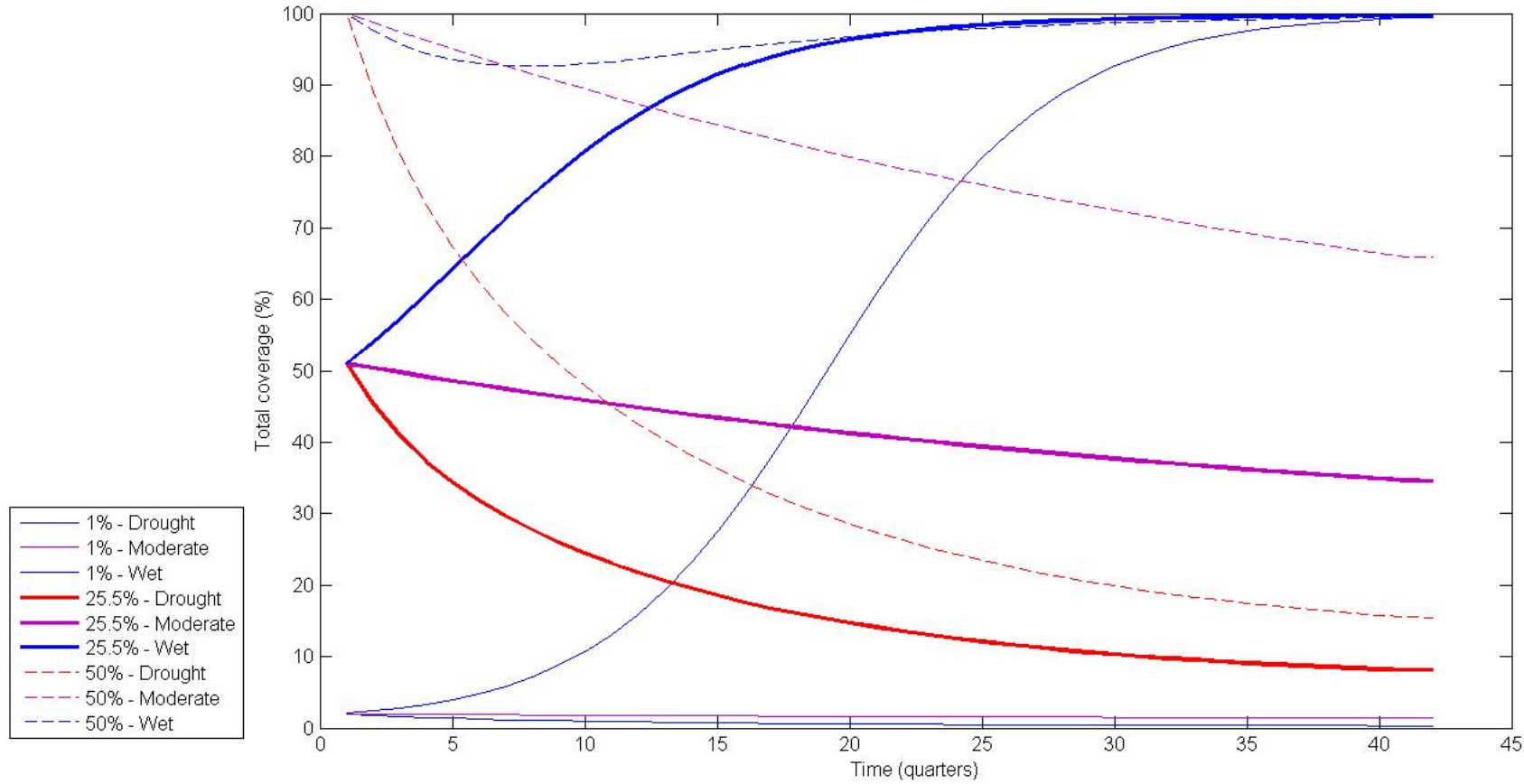


Figure 14. Modeled marsh coverage over 10-year run starting with 2%, 50% and 100% initial coverage

The simulation of plant cover change over the entire Nueces Marsh was run at 10 m resolution using the two functional groups: clonal stress tolerant (CST) plants and clonal dominant (CD) plants. There was about a 1% difference in outcome between the 10 m and the 100 m resolution, and between 0.1% and 1% difference when running the model at the highest resolution of 1 m. The simulation was run for a 10-year period with daily time steps and on a high-end laptop the simulations took about 5 seconds to run at 100 m resolution, 15 minutes at 10 m resolution, and about a full day at 1 m resolution. Because of the small differences in changes at the different resolutions, but significant time savings at 10 m, the simulations at run at 10 m resolution for reporting here.

The relative spatial coverage of the two functional groups was different under different climate regimes, as presented in detail in Appendix C. Fig. 15 provides a color scale, used in Figs. 16-18, for illustrative results from 3 simulations. The clonal dominate (CD) plant group is denoted in red and the clonal stress tolerant (CST) plant group is denoted in green. Pure red or green denotes 100% coverage of that functional grouping while shades of yellow/orange/brown denote a mix of members from each functions grouping.

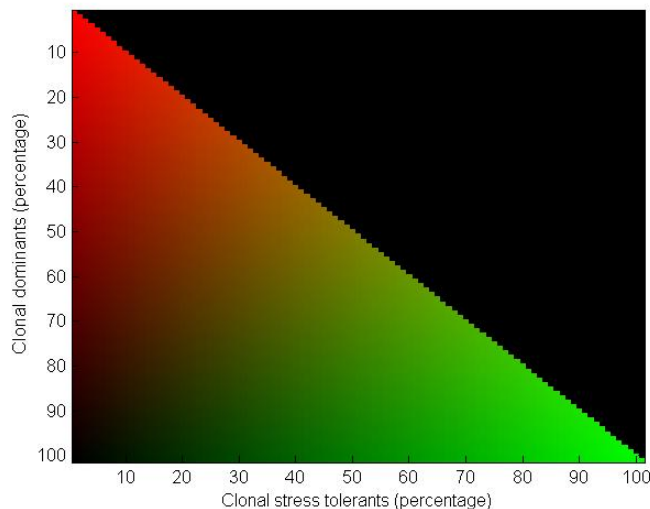


Figure 15. Color scale for for simulations in Figs. 16-18 where 100% cover of clonal dominant species is red, and 100% of clonal stress tolerant species is green.

There is more coverage of CD after 10 years of wet conditions (Fig. 16) than moderate climate conditions (Fig. 17), but virtually no CD during dry conditions (Fig. 18). While there is little diversity during dry conditions, moderate climate conditions yield mixtures of the two plant community groups, thus higher plant diversity. Under dry conditions the area of bare marsh without vegetation is quite large because marsh vegetation coverage decreases by 84.1%.

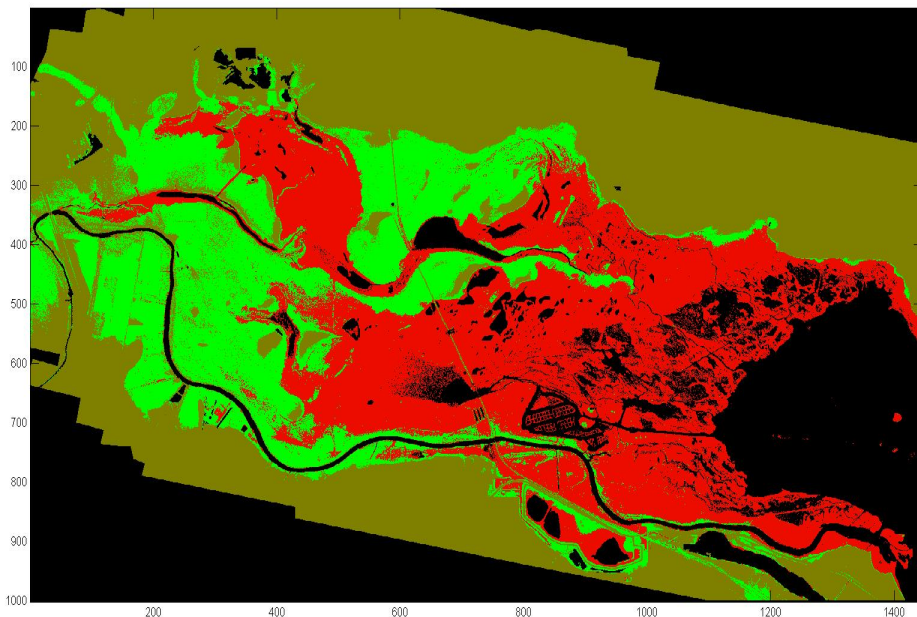


Figure 16. Modeled marsh coverage over 10-year run during wet conditions for two species. Clonal dominant (CD) species is red, and clonal stress tolerant (CST) species is green. At full red, that species is at 100% coverage, cells with both species will be combinations of red and green colors (yellow when equal). See Fig. 15 for color scale.

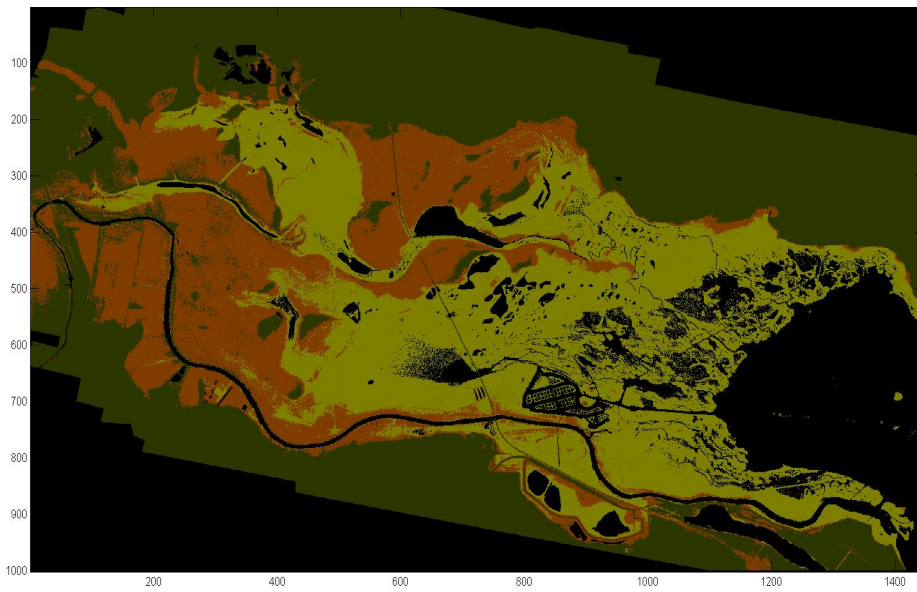


Figure 17. Modeled marsh coverage over 10-year run during moderate conditions for two species. CD species is red, and CST species is green. At full red, that species is at 100% coverage. Yellow and orange are different mixes of the two species. See Fig. 15 for color scale.

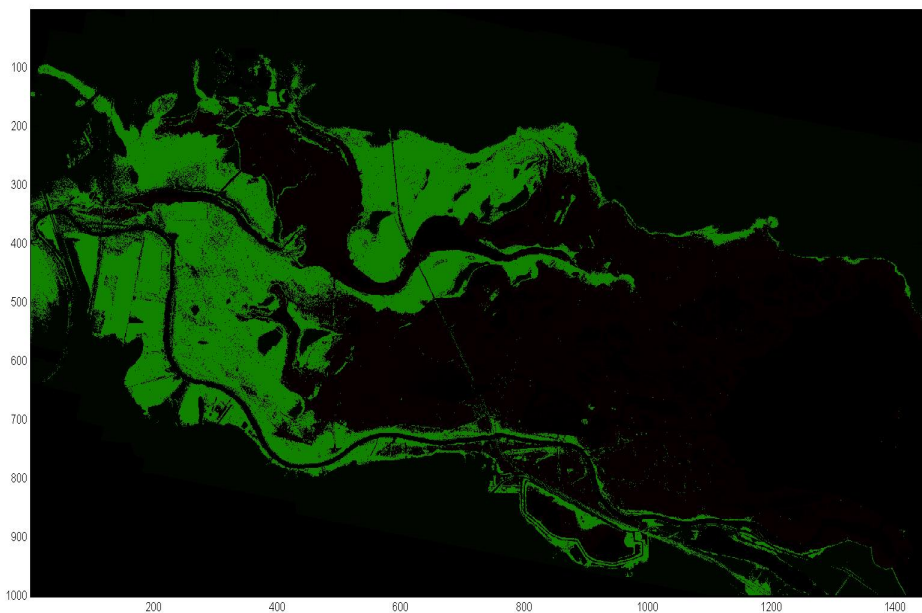


Figure 18. Modeled marsh coverage over 10-year run during dry conditions for two species. CD species is red, and CST species is green. At full green, CST species is at 100% coverage. See Fig. 15 for color scale.

Discussion of marsh model results

To provide for marsh growth and development, the freshwater flow must be sufficient to overbank the berms along the marsh edge and fill the marsh. The results from the modeling study appear to indicate that there are rarely sufficient flows to promote full connectivity along the complete axis of Rincon Bayou, nor provide for overbanking. Only during the wettest periods do we see increases in marsh areal coverage. One would expect the marsh coverage to expand when there is a transition from dry to moderate conditions. But under the moderate climate case, there is still not enough water entering the marsh to increase plant coverage in the short term. This condition could become worse as climate change is likely to affect coastal south Texas with higher temperatures in the summer (greater evaporation), less frequent rainfall, and longer dry periods between wetter periods (Twilley et al., 2001).

The model shows decreasing plant coverage during wet conditions under some initial starting conditions (Fig. 13, above). This could be because some plants, particularly in the lower marsh decrease coverage during wet conditions when salinity declines. Additionally, since the growth rates used for this model are aggregate rates for functional groupings, different species can dominate the growth rate in a grouping (depending on differences in zonation and climate). Such differences within a functional grouping are not reflected in the model. In essence, a decline in one species could be offset by an increase in another within a functional group leading the aggregate rate being near zero.

One would expect that during moderate or wet conditions, the marsh vegetation coverage would expand. However, cannot happen if the marsh is in healthy conditions such as near 100% cover (Fig. 13, above). If the plants have already filled the area, then the growth rates are very small because cover cannot exceed 100%. There are also decreases in coverage during wet conditions under some starting conditions. This result likely occurs because some salt-preferring plants, particularly in the lower marsh, decrease coverage during wet conditions when salinity declines. While the model allows for diffusion from one grid to another, it does not account for competition or the propensity for some plants (such as pioneer species) to move more aggressively into bare areas.

Further, marsh coverage approaches equilibrium in the long-term only during wet periods (Fig. 14, above). The temporal simulation also shows that several years, depending upon the model's initial conditions, are required for the marsh to return to full coverage. This result seems to contradict shorter-duration empirical measurements (Forbes and Dunton, 2006). The current modeled growth rates are based on long-term observations of plant cover. However, actual growth rates are influenced by shorter-term events like inundation and the following recovery. During these times, the growth rates could be different due to the lack of competition and other species-specific factors.

Implications of marsh model results

From the spatial-temporal model of vegetation growth in Nueces Marsh, it is apparent that growth in areal extent of the marsh largely depends on water flow and elevation, which in turn depends on the quantity of fresh water in marshes and also drives marsh water salinity. This fresh water has two sources: flows down the Nueces River from precipitation in the watershed or pass-through releases from Lake Corpus Christi. The next logical step is to determine whether it is possible to control releases of fresh water to produce the most desirable quantity and quality of marsh restoration. The modeling system is governed by partial differential equations and a stochastic factor, namely, precipitation and storm events. This problem can be formulated as one of optimal control, where we have to clearly quantify the objectives of the control problem. A short but incomplete list of objectives might include:

- Minimize time of restoration of vegetation cover
- Maximize the area of vegetation cover or habitat
- Promote a species abundance or functional group to enhance ecosystem services
- Minimize fresh water use
- Minimize the cost of restoration

An objective function for optimal control can be formulated from weighted combinations of any (or all) of the above. Developing the “best” objectives for optimal control will require a combination of expert judgment, quantification of processes, and evaluation of costs and benefits for human vs. environmental water use.

2.4 Fish and invertebrate habitat connectivity

The Rincon Bayou, as described in §1.3 above, is the connector for nutrient-laden fresh water in the Nueces River and the salt water of Nueces Bay within the delta. Under present conditions, where dam operations provide an inflow that is approximately 1% of historic levels, freshwater inflow from the Nueces River rarely reaches Nueces Bay through the Rincon Bayou (Irlbeck and Ward, 2000). Tidal inflows of salt water from Nueces Bay enters the Rincon Bayou, which is concentrated by evaporation and a reverse estuary forms. A reverse estuary is where salinity increases upstream rather than decreasing, as would occur in a normal estuary. The salinity gradient between the Upper Rincon Bayou and Nueces Bay reverts to a normal pattern (i.e. salinity increases downstream) periodically after large overbank events from the Nueces River (Irlbeck and Ward, 2000) or through freshwater pumping from the Rincon Bayou Pipeline (Barajas, 2011; Tunnell and Lloyd, 2011; Hill et al., 2012). A return to a normal pattern of decreasing salinity in Rincon Bayou is evidence of lateral mixing across the Nueces Estuary, which has positive effects on the connectivity of aquatic fauna.

Connectivity, with respect to fishes and invertebrates, implies “the enhanced storage of genetic and energetic pools due to variable migration and dispersal patterns across habitats and ecosystems” (Secor and Rooker, 2005). Connectivity within estuaries and between estuaries and marine areas is especially important for mobile marine fauna that utilize different habitats along a salinity gradient in different parts of their life cycles, or utilize tides or other flow as mechanisms for larval dispersal (e.g., Riera et al., 2000; Gillanders et al., 2003; Vasconcelos et al., 2010). Analysis techniques – such as comparing carbon and nitrogen isotopes of tissues with those of potential food sources (Riera et al., 1996; Herzka, 2005) and comparing elemental signatures in otoliths of fish found in similar and different habitats (Gillanders, 2005) – confirm that connectivity within estuaries and between estuaries and marine waters are important in the life cycles of some mobile aquatic species.

Several aquatic invertebrate and fish species use the connectivity of the Rincon Bayou, especially when freshwater inflows are favorable enough to create a positive salinity gradient (Barajas, 2011; Kalke, *pers. comm.*). Juvenile brown shrimp (*Farfantepenaeus aztecus*) enter Rincon Bayou in late winter (February-March) and usually peak in abundance in April, before migrating back downstream in May and June as sub-adults (Hill and Nicolau, 2007; Kalke, *pers. com.*). The main sources of food for brown shrimp are *S. alterniflora* and *S. spartinae* detritus and benthic diatoms; organic matter carried by river flow into the marsh greatly contribute to the brown shrimp diet (Riera et al., 2000).

White shrimp (*Litopenaeus setiferus*) also utilize Rincon Bayou in juvenile stages of their lives. White shrimp enter Rincon Bayou in late spring and leave at the start of winter. Both brown and white shrimp forage in the top 2 cm of the sediment, and are known to prey on infauna, such as polychaete worms, in addition to having other food sources (Hunter and Feller, 1987; Beseres and Feller, 2007). Infauna biomass and

diversity are strongly correlated with temporal changes in salinity in Rincon Bayou (Montagna et al., 2002), which in turn are directly related to freshwater inflows and tidal flushing.

Various other invertebrate and fish species (red drum, *Sciaenops ocellatus*; black drum, *Pogonias cromis*; menhaden, *Brevoortia patronus*; croaker, *Micropogonias undulates*; blue crab, *Callinectes sapidus*) are ecologically connected to Rincon Bayou, however the link to freshwater inflow is less direct. Red and black drum feed on shrimp and other invertebrates, and can get temporarily isolated in shallow pools in Rincon Bayou if the flow into Rincon Bayou decreases to the extent that the water is not deep enough to easily swim. High blue crab abundances often coincide with low salinities in Rincon Bayou, however the data are not always consistent (Hill and Nicolau, 2007).

The flow required for large-scale ecological connectivity in Rincon Bayou does not occur often enough in the recent hydrograph of the Nueces River because of the high upstream extraction of water for municipal and agricultural uses. Operation of the Rincon Bayou Pipeline to pump water from the Nueces River into the delta at more frequent intervals (see §1.3) has decreased salinities in mid-Rincon Bayou and therefore shows the potential to increase ecological connectivity in the area. However, the effects of these inflows on salinity are much shorter than historic overbank flooding events, and the flows appear largely restricted to existing channels (although this remains to be confirmed by wider data collection efforts across the delta). Overbanking of the existing channels both dilutes salts in the surface sediments of surrounding areas, making it more suitable for marsh plants to grow, and washes detritus into the channels, which provides food for brown shrimp. It is inconclusive whether there is enough flow from these pumping events to increase the amount of connectivity for species that inhabit Rincon Bayou for part of their life cycles. However, it is assumed that an increase in pumped and overbanking freshwater inflows would increase the amount of food available and accessibility into and out of Rincon Bayou, thereby increasing the habitat available and connectivity in the system for mobile aquatic species.

This page intentionally blank for two-sided printing.

3 Physics of inundation

3.1 Overview

The physics of the Nueces Delta are driven by competition between freshwater flows and tidal/wind-driven saltwater flows. Freshwater flows are mainly precipitation, storm events (flooding) and pumping from the Rincon Bayou Pipeline. Outside of extreme storm events, Nueces Bay is the principal driver of water levels in the delta, providing the inundation patterns that dominate the interchange between tidal creeks and episodically-flooded interior marshes. As a tool for understanding the physics of inundation, the Nueces Delta Hydrodynamic Model (see Appendix A) was constructed to model the interactions of wind, tide, inflows and salt transport through the delta.

Understanding the processes concentrating and transporting salt through the delta is critical to predicting the ecosystem behavior in response to management actions.

Evaporation rates ranging from 15 cm/month in April and October to a typical peak of 25 cm/month in July (Ward, 1997) imply a physical salt load ranging from 5 to 9 ppt/month that will build up through processes described below if flushing is insufficient.

Additional salt loading results from transpiration, which we measured directly in the field on several species of emergent vascular plants. As noted in a number of field surveys and experimental studies (see §2.2), salinity regimes regulate plant zonation, production, and overall diversity over the entire delta, from tidal creeks to the marsh interior, with ultimate effects on habitat utilization by estuarine organisms.

3.2 Overbanking and draining

A marsh inundation cycle described by Stachelek (2012) for the Nueces Delta, based on field measurements and modeling of porewater salinity, is illustrated in Fig. 19. With rising water level in the tidal channels a hydraulic pressure gradient is developed across the embankment, creating pore water and salt fluxes illustrated in Fig. 19A. Once the tidal creek overtops its embankment the low-lying marshes and salt pans are flooded, such that their water surface levels are continuous with the tidal creek. With falling water levels the creek embankments physically trap water, such that evaporation and transpiration lead to increasing porewater salinities. The hydraulic gradient now may be reversed, with porewater fluxes of water and salt from the interior towards the tidal creek (Fig. 19B). Note that waters trapped behind embankments slowly evaporate, transpire, and percolate, which removes freshwater and leaves salt behind. Both surface water and porewater salinities slowly increase as the flooded area slowly reduces. In particular, plant transpiration leads to porewater salt build up that leads to porewater salinities significantly exceeding surface water salinities. Lower-lying areas develop higher porewater salt concentrations (and may become salt pans) whereas higher areas are typically flushed by episodic rain and brief overbanking events. With prolonged low water levels, the water/salt fluxes into the areas behind embankments are strictly pore/groundwater fluxes (Fig. 19C), leading to drying out of the embankments and slow migration upward of accumulated salt.

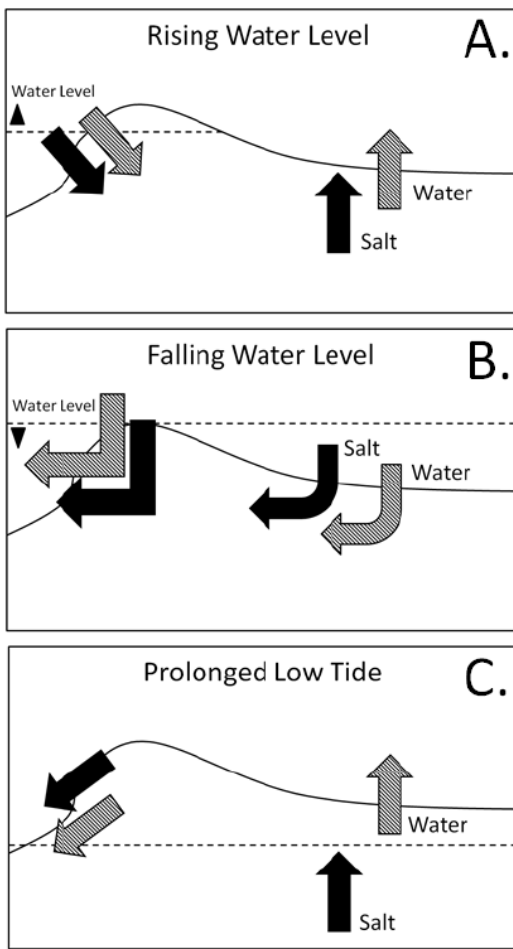


Figure 19. Exchanges between tidal creek and interior marshes that affect porewater salinity (From Stachelek 2012, Fig. 1.6)

3.3 Tidally-driven inundation

Model estimates

The daily tidal excursion in Nueces Bay is typically less than 1 ft (0.3 m) from minimum to maximum tide. This short time-scale tidal signal is moderated within the marshes, such that the mean daily elevation in Nueces Bay is a good indicator of the tidal forcing. Fig. 20a shows the 18-year smoothed daily mean tide (1994-2011 data) along with the daily mean tide and a 14-day smoothed tide for 2003 data. Note that for 2003, the smoothed daily mean is entirely within one standard deviation of the long-term smoothed daily mean; however, this is not always the case. As shown in Fig. 3, above, in 1996 the smoothed tide was significantly below the 18-year mean until October, which contrasts with a July 2010 peak (hurricane and subsequent tropical depression) that was above the 18-year mean and equivalent to the typical autumn secular rise.

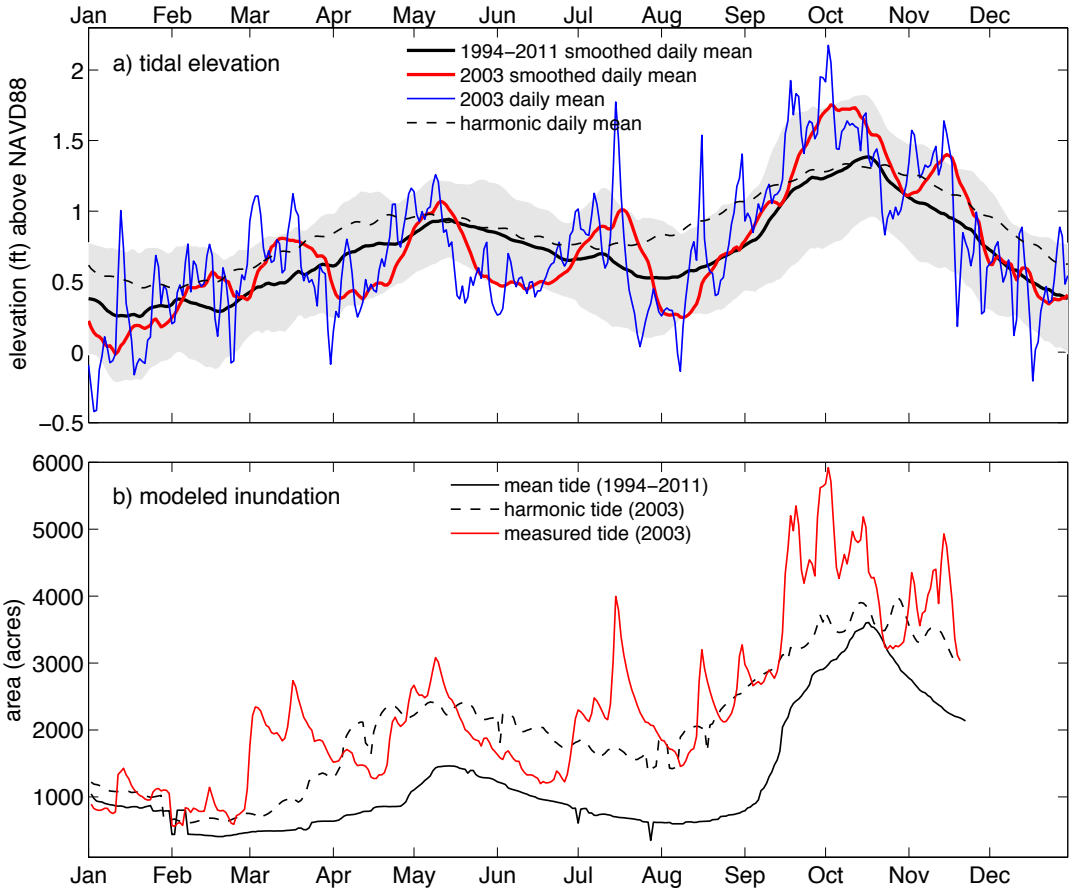


Figure 20. (a) Tidal elevations with 14 day smoothing and the unsmoothed daily means. Gray background is the daily mean \pm one standard deviation; (b) inundation areas using the smoothed daily mean tide, harmonic tide and measured tide as forcing for the Nueces Delta Hydrodynamic Model. Harmonic and measured tides in the model use 6-minute intervals (data not shown) to capture short time-scale excursions.

The overall scale of tidal inundation can be estimated by comparing model results forced with the measured tide and model results forced with the 1994-2011 smoothed mean daily tide, as shown in Fig. 20b. The effective inundation area is computed with two adjustments to the total inundated area from the model: first, the inundated areas of tidal creeks and ponds flooded at sea level (approximately 2000 acres) are removed; secondly, areas without connectivity through surface water paths are removed. As discussed above, the unconnected areas provide transport through porewater movement; however, these slow transport effects cannot be represented in the present version of the Nueces Delta Hydrodynamic Model. The trapped areas are estimated as those whose water levels change less than 0.4 mm/day.

The 3-4 week peaks in the 2003 smoothed daily mean tide (Fig. 20a) during March, May and July are correlated with 3-4 week peaks in modeled inundation (Fig. 20b). This result indicates that inundation is principally driven by the longer-time scale changes in

the tidal elevation. That is, short-term events causing excursions of tide significantly above the smoothed daily mean value merely provide episodic overbanking without improving marsh connectivity or providing significant flushing.

Comparison of the real tide and harmonic tide inundation areas in Fig. 20b provides clear evidence that the meteorological tides – i.e. effects of frontal systems and wind set-up in Corpus Christi and Nueces Bay – are critical to inundation. Results with the harmonic tide include inundation effects of the daily tidal excursions, but miss the meteorological effects included in the model results using the measured tide.

Inundation vs. elevation

The results from Fig. 20b can be used to develop a comparison of inundation against the driving tidal elevation, as shown in Fig. 21. When forced by the 18-year secular mean tide, the inundated area outside the tidal creeks and pools flooded at sea level (blue dots) is consistent with the inundation computed by considering a simple flat free surface across the marsh (solid line). When the real (measured) tide is used to drive the model, results show substantially greater inundation and significant variability. Because of the

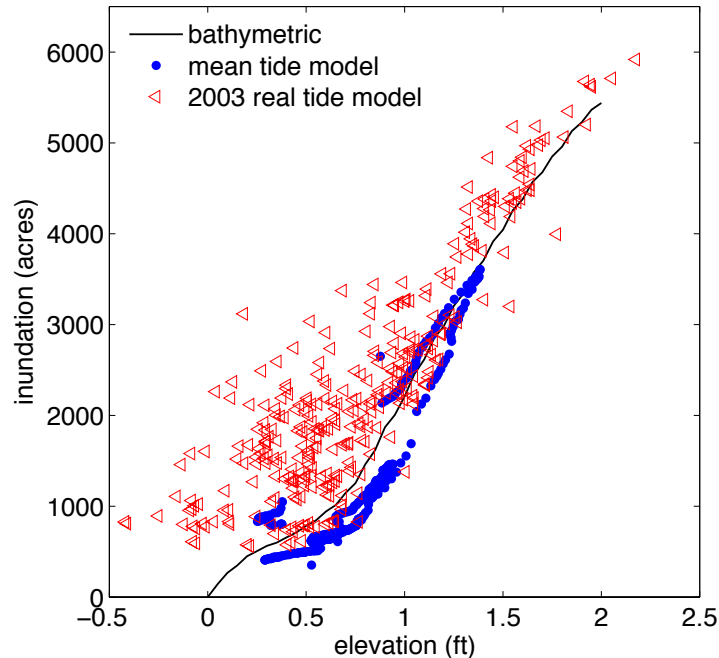


Figure 21. Added inundation area outside of sea-level-flooded creeks and ponds (2000 acres) as a function of elevation. Solid line represents added inundation by a flat water surface at the given elevation. Symbols are model-predicted values using the 14-day smoothed daily average tide (see Fig. 20a) and the 2003 measured tide (6-minute intervals). Elevation for the model runs is the tidal elevation. Note that the minimum added inundation for the daily mean tide model result is 350 acres. The minimum added inundation for the 2003 measured tide is 620 acres. The autumn secular peak of 1.38 ft for the mean tide model provides 3600 acres of additional inundation. The spring secular peak of 0.94 ft for the mean tide model provides 1500 acres of additional inundation.

slow draw-down of marginally connected regions after overbanking events, the inundation area loses correlation with the forcing tidal elevation over the broadest range of elevations. Nevertheless, we suspect that both the bathymetric and mean tide models provide a good estimate of the additional inundated areas with strong connectivity to the continuously-inundated tidal creeks and pools.

Connectivity and inundation

Connectivity of the tidal creeks and pools is a necessity for aquatic habitat (§2.4). Because the tidal regime (Fig. 3, above) covers a narrow range, a majority of the delta is only episodically flooded and continuity with the creeks is insufficient for aquatic habitat. Based on modeling completed to date, only about 2500 acres (of approximately 25,000 acres) within the Nueces Delta remain continuously flooded, of which ~2000 acres are channels and pools whose bottom elevations are below sea level (Fig. 4, above). The remaining ~500 acres (with land elevations above sea level) are continuously inundated because of a bias in tidal transport, as evidenced by the minimum inundations in Fig. 21, above. Water pushed up into the delta, driven by tides and winds, leads to overbanking and relatively rapid inundation for a small subset of the marsh area (depending on tidal elevation). In contrast, water drainage from the delta is impeded by creek banks and marshes, leading to temporary impoundments that drain more slowly (as illustrated in Fig. 19 above). Marsh waters impounded during overbanking events provides continuous seepage through banks, enabling water flows in some creeks that would otherwise be dry. This cycle is substantially different than a classic river delta, where a hydraulic gradient between freshwater in the upstream river water and the downstream tidal waters drives a continuous flow through the tidal network.

In addition to the 2500 acres of continuously-flooded marsh, model results (Fig. 20b) indicate another 3000-6000 acres may be flooded during an autumn secular peak over a period of 4-6 weeks. The spring secular peak has a more modest effect, on the order of 1000-2000 additional flooded acres. At these spring and autumn secular peaks, the connected area in the marsh is significantly increased for the duration of the peak. Of course, Fig. 3 shows that secular peaks may vary substantially year-to-year, which will in turn vary the inundated area. These effects can be quantified with the hydrodynamic model. Of interest is the possibility of other inundation peaks through the summer that are on the same order as the spring secular peak. Fig. 20b shows early spring and summer inundation peaks in 2003 that are similar to the May peak. The daily mean tide (Fig. 3, above) indicates such peaks are less likely; nevertheless, they may occur and provide important opportunities for freshwater pumping or other restoration strategies.

3.4 Other forcing for inundation

Wind

The prior discussion considers only tidal inundation without compounding local effects of wind. That is, the measured tide used to drive the model results of Fig. 20b includes the measured effects of wind in setting up water levels in the Gulf of Mexico and Corpus Christi Bay, but not the additional effects of local wind-driven transport within the delta. Results of the model indicate that the wind plays a non-trivial role in moving water

through the Rincon Bayou, especially in the West Lake and South Lake regions where southeasterly winds can cause substantial upstream transport. However, quantification of these wind effects requires further calibration and testing of the model.

Precipitation

Precipitation remains one of the most variable and important factors in the health of the Nueces Delta. Localized ephemeral thunderstorms appear to be of limited impact, although no doubt of importance in the areas where rain falls. In particular, precipitation plays a vital role in flushing the South Lake region, which otherwise has minimal connections to the Rincon Bayou (Fig. 2, above). In the absence of rainfall, the South Lake has poor flushing characteristics and will experience significant salinity increases. Broader rainstorms are associated with flushing of porewater salinity, as well as reducing accumulated salt load in surface waters caused by evaporation and transpiration. Below some critical threshold (dependent on antecedent soil moisture) rainfall's impact is mostly localized and simply reduces local salinity without causing any significant transport of salt out of the marshes. Beyond the critical threshold, rainfall begins to change the flushing of the delta, and move salt from porewater towards the tidal creeks and Nueces Bay.

Freshwater pumping

The NDHM can be used to evaluate the effectiveness of pumping strategies for use of the Rincon Bayou Pipeline and effect of different tidal conditions¹⁰. As shown in Fig. 22, the additional inundation contributed by the pump for different types of tidal forcing are qualitatively comparable, with peak inundation at the real tide slightly higher. However, Fig. 23 indicates that the tidal stage when the pumping takes place affects the overall total inundation achieved. Effective inundation from the pumps is highly dependent on the overbanking achieved, which is driven by the tidal elevation rather than the pumping itself. Note that both 1 and 2 pump strategies in Figs. 22-23 introduce the same amount of water (1600 acre-ft) but over two different time spans. Two pumps results in a more rapid development of the peak inundation but, as shown in Fig. 24, the different pumping strategies do not significantly affect the overall space-duration of added inundation – both achieving about 7000 acre-days of added inundation. These results should be considered qualitative and provisional, as the model has not been calibrated.

Implications of hydrodynamic modeling

Although the Nueces Delta Hydrodynamic Model is not presently calibrated¹¹, it is clear from the model results that the interaction of wind, water elevation and freshwater

¹⁰ Although the Rincon Bayou Pipeline did not exist in 2003, this year was chosen for the pump exercise for consistency and comparison to other model results. The base year of 2003 was chosen for analysis because its daily mean was within one standard deviation of the long-term daily mean during the year.

¹¹ During model development, it became apparent that the existing monitoring data was insufficient to calibrate and validate the model. In early 2012, the Texas Water Development Board was funded by the U.S. Army Corps of Engineers to place additional sensors in the delta to gain adequate data. These sensors are in place and operating as of September 2012 (C. Schoenbaechler, pers. comm.) based on an initial scoping developed by PI Hodges (see §A.4).

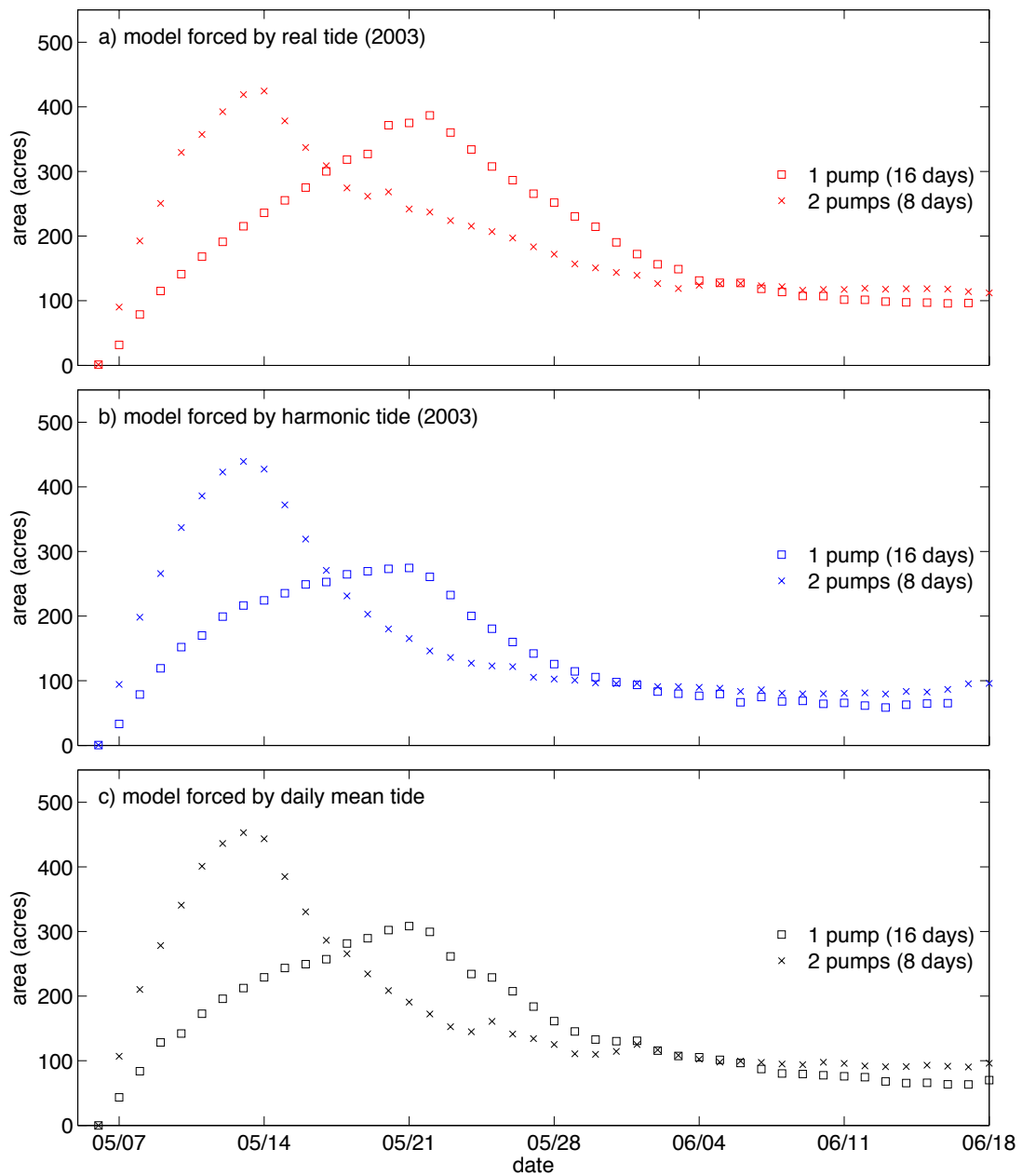


Figure 22. Model results for additional area inundated during the spring peak for theoretical use of Rincon Bayou Pipeline. The additional area inundated is computed as the difference between modeled inundation with pumping and an identical model without pumping.

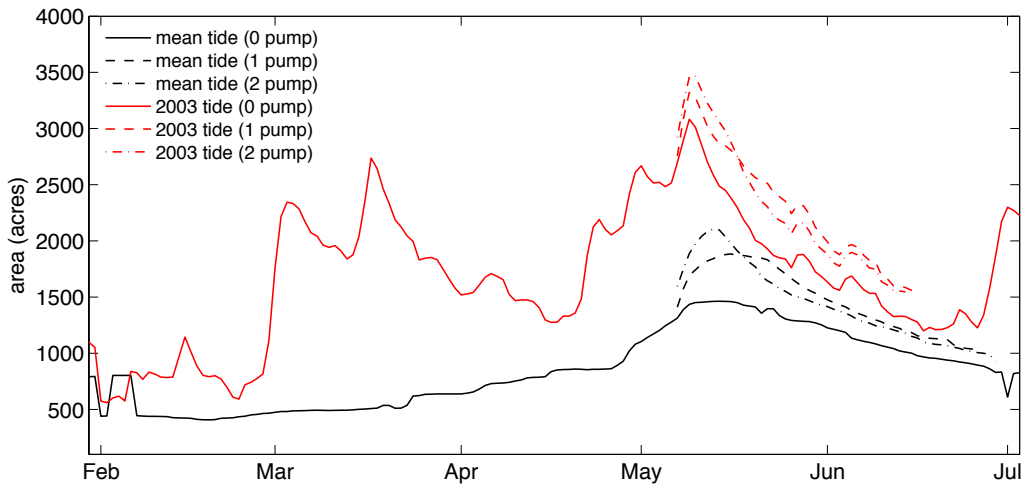


Figure 23. Total inundation predicted for different pumping strategies with different model forcing conditions.

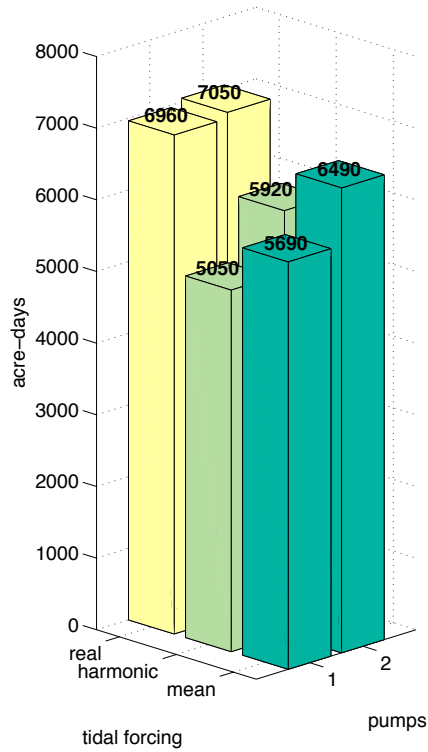


Figure 24. Total additional acre-days of inundation predicted for different pumping strategies with different model forcing conditions for 31 days of simulation (May 7 – June 6). Note that the mean tide does not include daily tidal fluctuations in the model forcing, whereas both harmonic and real tides use 6-minute interval data. The difference between the real and harmonic tides is in meteorological changes in the water elevations forced by wind and weather systems.

inflows exert important controls on both freshwater and saltwater distributions in the delta. Pumped freshwater inflows are readily distributed into the West Lake region through both the Rincon Overflow Channel and backflow from the Central Rincon Bayou. The model can readily represent these fluxes, and with further calibration can be used to predict the scales of pumping necessary to flood West Lake and maintain inundation under different wind conditions. The flooding extent in the South Lake region is critically dependent on wind, as steady forcing can easily move water over extensive areas of the relatively flat landscape. Again, the model can represent these processes, but there are critical gaps in the calibration of wind-driven shallow flows that need to be addressed.

In the eastern delta, the distributed effects of freshwater pumping are strongly dependent on the water elevation in Nueces Bay and wind forcing that speeds up the spread of the water over flat areas beyond embankments of the tidal creek. The characteristics of the inundation beyond the tidal creeks plays a critical role in porewater dynamics and hence the ecosystem health. Although the Nueces Delta Hydrodynamic Model does not include a porewater module at this time, the model presently can compute the time it takes to physically fill and drain marsh and salt pan areas through the combination of overbanking, wind-driven flows and evaporation. Future improvements of the model should focus on linking plant communities, transpiration, and mobilization of salt. Modules for these processes are relatively easy to implement, but will require significantly more data collection and an understanding of local process scales for accurate calibration.

This page intentionally blank for two-sided printing.

4 Restoring the Nueces Delta

4.1 Requirements and options

What happens without restoration?

Without any action, the Nueces Delta will continue to degrade. The most obvious loss is the ongoing erosion at the interface between the delta and Nueces Bay, with the consequent loss of marshlands at a significant rate. Continuing this erosion will further reduce the aquatic habitat in the lower salt marsh, reducing the nursery ecosystem service provided by the delta as well as the migratory bird refuge. Without any action, the delta to the east of the railroad embankment will eventually disappear as the plant community withers and wave-driven erosion removes the sediments that are not bound by root systems. Erosion of the eastern delta will effectively expand the shallow Nueces Bay to the west of where the Nueces River enters. This increased area will have relatively poor flushing and will likely see increasing hypersalinity. To the west of the railroad embankment, rising salinities in Nueces Bay will lead to increased salt pan development and reduction of brackish marsh region. The overall connected aquatic habitat will be reduced, as will be the total vegetated area. The no-action scenario may lead to the complete collapse of Corpus Christi commercial and sport fisheries as the decline of nursery habitat irreparably damages the food web.

What does restoration require?

Restoration of the Nueces Delta has two critical aspects: 1) improving flushing of salt build up in the pore waters of emergent vegetation, and 2) improving area connectivity within salt marshes for aquatic habitat. These two aspects are related through inundation. In the former, inundation is both the source of pore water salt and a key flushing mechanism. The difference between healthy and unhealthy vegetation is in the duration of dry spells (e.g., the time between overbanking events). In contrast, effective connectivity for aquatic habitat depends on the duration of inundation itself as short-duration inundation provides little opportunity for developing aquatic habitat for invertebrates and fish. Thus, restoration strategies must focus on both increasing inundation duration and decreasing time between inundation events.

What are possible restoration approaches?

There are two obvious restoration approaches to improving inundation: 1) pumping freshwater through the Rincon Bayou Pipeline, and 2) diverting more (or all) of the Nueces River back into the delta. The former provides for hands-on management of the system, whereas the latter may provide larger flows during storm events to help flush salinity from pore waters. Note that simply increasing the depth and/or breadth of the existing Nueces River diversion channel (location shown in Fig. 2, above) is unlikely to be a complete solution, as during much of the year this would simply introduce saltwater from Nueces Bay into the Upper Rincon Bayou. Any substantial diversion of water from the Nueces River main channel would entail building a new saltwater barrier on the main channel downstream of the present diversion, which would change the existing main river

channel into a lagoonal reach of Nueces Bay. The appropriate barrier height and resulting flow conditions in the delta can be analyzed with the Nueces Delta Hydrodynamic Model.

Additionally, it may be possible to increase connectivity, particularly between the upper and lower marshes, by installing new culverts under the railroad dike and/or through selective creek banks. There is an open question whether man-made tidal creeks could be developed to improve connective habitat and/or improve drainage behind banks to reduce impoundment duration and evaporative salinization. Another open question is whether a wave-breaking structure across the delta frontage could reduce the front erosion rate caused by wind-driven waves.

5 Recommendations for future restoration work

Lessons learned from this research

We now have a deeper understanding of the key drivers of ecosystem health in the Nueces Delta and the relationships between freshwater, saltwater, porewater, and environmental forcing. The porewater salinity appears to be a key driver of ecosystem health, with a slow concentration and episodic flushing of the porewater salinity part of the natural cycle that has been exacerbated by anthropogenic reduction of freshwater inflows. The critical issue for management is determining how to evaluate the rate of salt increase and the rate of flushing expected for different management actions under different multi-year cycles of drought and wet years. Restoring the delta will require careful consideration of management options and further development of the scientific tools to manage the long-term restoration.

Vegetation

Based on our increased understanding of the importance of inundation events to the interior marsh and the flushing of sediment pore waters for emergent vegetation, we recommend that future work focus on (1) updated vegetation maps that accurately depict vegetation patterns in relation to both elevation and distance to tidal creeks, and (2) accurate estimates of factors controlling surface water interactions rather than those controlling atmospheric water interactions. Spatially-based models of net production would benefit from more detailed estimates of factors describing the interaction between tidal creek water and sediment pore water, such as inundation frequency and soil hydraulic conductivity. The Nueces Delta Hydrodynamics Model should be used to develop inundation maps to identify expected duration of drying across the marsh. The effects of different restoration strategies should be analyzed under a variety of tidal conditions to produce predictions of net area changes under different restoration strategies.

Improvements can be made to the existing marsh development model. The diffusion equations employed in the current study allows for dispersal of plants from one grid to another, however it does not account for competition between plants or the ability of some plants (such as pioneering species) to colonize bare areas rapidly. Adding competition and distinguishing between pioneer and climax species could improve model performance. The marsh model can be further extended using ideas of optimal control as a tool for evaluating effectiveness and cost-benefits of different fresh water strategies.

Aquatic habitat

The connectivity and duration of aquatic habitat area under different historic environmental conditions should be mapped using the Nueces Delta Hydrodynamics Model. Effects of different restoration strategies on the connected habitat area under different historic tidal conditions should be analyzed to predict effective area changes under different restoration strategies. Effects on habitat connectivity through use of additional man-made creeks and use of culverts through the railroad embankment should be explored.

Hydrodynamics

The Nueces Delta Hydrodynamic Model (NDHM) needs to be calibrated using data presently being collected by the Texas Water Development Board. Once this calibration is completed, the model can be used to evaluate inundation under different environmental forcing conditions. A number of studies and improvements to the Nueces Delta Hydrodynamic model are possible to provide long-term use as a management tool:

- *Pump operational planning.* Use the NDHM to develop operational plans for freshwater pumping that maximizes the inundation area and duration over the marsh.
- *Quantify large-scale effects of transpiration on water and salt budget.* Using the plant-based study that we have accomplished, upscale these measures to quantify transpiration rates across the landscape as a function of plant communities. Link this ecosystem model with NDHM to predict effective freshwater loss to rates to the atmosphere and resulting increases in salinity.
- *Add a porewater module.* A module for the NDHM that represents porewater fluxes (including mobilization and storage of salt) as affected by plant communities and hydraulic gradients, and precipitation should be created to close the loop between surface water fluxes and through-bank fluxes.
- *Improve model of subgrid-scale topography.* The existing 1-m resolution lidar data can be used in conjunction with the 15-m resolution model results for better estimates of water retention (overbanking) and inundation areas affected by marsh plants.
- *Study localized rainfall effects.* The existing model provides new capabilities for representing the rainfall from the uplands that forms ephemeral streams and enters the delta. Future studies should use this capability to quantify the scale of storms that are required to have a significant flushing impact. Below some critical threshold (dependent on antecedent soil moisture) rainfall's impact is mostly localized and simply reduces local salinity without causing any significant transport of salt. Beyond the critical threshold, rainfall begins to change the flushing of the Delta, and move salt from porewater towards the tidal creeks and Nueces Bay.

Completion of the above will result in a coupled Ecosystem-Hydrodynamics model, which we might call E-NDHM. This model can be applied to quantify the rate of salt build up and flushing in the system, which can be used to develop effective management guidance for optimal freshwater flushing of the Nueces Delta.

6 References

- Adam, P. 1990. *Salt Marsh Ecology*. Cambridge, U.K., Cambridge University Press.
- Adams, John S., and J. Tunnell 2010, *Rincon Bayou Salinity Monitoring Project*, CBBEP Publication 66, Project Number 0921.
- Alexander, H.D., K. Dunton. 2002. Freshwater inundation effects on emergent vegetation of a hypersaline salt marsh. *Estuaries* 25: 1426–1435.
- Barajas, M.J. 2011. *Effects of Enhancing Freshwater Inflow on Macrofaunal Communities in a Marsh*. Master's Thesis. Texas A&M University-Corpus Christi.
- BBEST 2011. Nueces River and Corpus Christi and Baffin Bays Basin and Bay Expert Science Team. 2011. *Environmental Flows Recommendations Report*, Final Submission to the Environmental Flows Advisory Group, Nueces River and Corpus Christi and Baffin Bays Basin and Bay Area Stakeholders Committee, and Texas Commission on Environmental Quality. Available at http://www.tceq.texas.gov/permitting/water_rights/eflows.
- Berseres, J.J., and R.J. Feller. 2007. Importance of predation by white shrimp *Litopenaeus setiferus* on estuarine subtidal macrobenthos. *Journal of Experimental Marine Biology and Ecology* 344: 193-205.
- Bertness, M.D. 1991. Zonation of *Spartina patens* and *Spartina alterniflora* in a New England salt marsh, *Ecology* 72: 138–148.
- Boutin, C. and P. A. Keddy (1993) A functional classification of wetland plants. *Journal of Vegetation Science* 4: 9.
- Bricker, S., C. Clement, D. Pirhalla, S. Orlando, and D. Farrow, 1999: *National Estuarine Eutrophication Assessment: Effects of nutrient enrichment in the Nation's estuaries*. National Ocean Service, National Oceanic and Atmospheric Administration, Silver Spring, Maryland.
- Bureau of Reclamation, 2000: *Concluding report: Rincon Bayou Demonstration Project*. Bureau of Reclamation, U.S. Department of the Interior, Austin, TX.
- Chapman, V. J. (1974) *Salt Marshes and Salt Deserts of the World*. Lehre, Germany.
- Choucair, P., K. Spiller and K. Meador, 2006: *Status and trends of selected marine fauna in the Coastal Bend Bays and Estuary Program study area, 1984-2004*. Report CBBEP-43, Project 0504, Coastal Bend Bays & Estuaries Program, Corpus Christi, Texas.
- Dunton K., B. Hardegree, T.E. Whitledge. 2001. Response of estuarine marsh vegetation to interannual variations in precipitation. *Estuaries* 24: 851–861.

- Forbes M.G. and K. Dunton. 2006. Response of a subtropical estuarine marsh to local climatic change in the southwestern Gulf of Mexico. *Estuaries and Coasts* 29: 1242-1254.
- Gillanders, B.M. 2005. Using elemental chemistry of fish otoliths to determine connectivity between estuarine and coastal habitats. *Estuarine, Coastal and Shelf Science* 64: 47–57.
- Gillanders, B., K.W. Able, J.A. Brown, D.B. Eggleston, P.F. Sheridan, 2003. Evidence of connectivity between juvenile and adult habitats for mobile marine fauna: an important component of nurseries. *Marine Ecology Progress Series* 247: 281-295.
- Grime, J. P., 1979. Evidence for the existence of three primary strategies in plants and its relevance to ecological and evolutionary theory. *The American Naturalist* 111: 25.
- HDR Engineering (2002), *Nueces River Basin Section 905(b) Analysis Reconnaissance Report*, Prepared for U.S. Army Corps of Engineers Ft. Worth and Galveston Districts, August, 2002. 54 pgs.
- Herzka. S. Z. 2005. Assessing connectivity of estuarine fishes based on stable isotope ratio analysis. *Estuarine, Coastal and Shelf Science* 64: 8-69.
- Hill, E.M. and B.A. Nicolau. 2007. *Rincon Bayou diversion project. FY 2006 Annual Report October 2005- September 2006*. Center for Coastal Studies ,Texas A&M University-Corpus Christi. p. 1-60.
- Hill, E.M., B. Nicolau, and P. Zimba, 2011: History of water and habitat improvement in the Nueces estuary, Texas, USA. *Texas Water Journal* 2(10), 97-111.
- Hill, E.M., J.W. Tunnell and L. Lloyd. 2012. *Spatial Effects of Rincon Bayou Pipeline Freshwater Inflows on Salinity in the Lower Nueces Delta, Texas*. CBBEP Publication 81, Project Number 1202.
- Hunter, J., Feller, R.J. 1987. Immunological dietary analysis of 2 penaeid shrimp species from a South Carolina tidal creek. *Journal of Experimental Marine Biology and Ecology*. 107: 61-70.
- Irlbeck, M. J. and G. H. Ward, 2000: Analysis of the historic flow regime of the Nueces River into the upper Nueces delta and of the potential restoration value of the Rincon Bayou Demonstration Project. Appendix C, in *Rincon Bayou Demonstration Project Concluding Report, Volume II – Findings*. Oklahoma-Texas Area Office, Bureau of Reclamation, U.S. Dept. of the Interior, Austin, TX, pp. C.1- B.24.
- Lellis-Dibble, K., K. McGlynn, and T. Bigford, 2008: *Estuarine fish and shellfish species in U.S. commercial and recreational fisheries: Economic value as an incentive to protect and restore estuarine habitat*. NOAA Tech. Memo. NMFS-F/SPO-90,

National Marine Fisheries Service, National Oceanic and Atmospheric Administration.

Minello, T., L. Rozas, and R. Baker, 2011: Geographic variability in salt marsh flooding patterns may affect nursery value for fishery species. *Estuaries and coasts* 35, 501-514.

Montagna, P.A., R.D. Kalke, and C. Ritter. 2002. Effect of restored freshwater inflow on macrofauna and meiofauna in upper Rincon Bayou, Texas, U.S.A. *Estuaries* 25 (6B):1436-1447.

Ockerman, D.J. 2001. *Water Budget for the Nueces Estuary, Texas, May-October 1998*. USGS Fact Sheet 081-01, pp. 1-6. Available at: http://pubs.usgs.gov/fs/fs-081-01/pdf/FS_081-01.pdf

Palmer, T.E., P.A. Montagna, and R.D. Kalke, 2002. Downstream effects of restored freshwater inflow to Rincon Bayou, Nueces Delta, Texas, USA. *Estuaries* 25: 1448-1456.

Raffaelli, D. and S. Hawkins (1996). *Intertidal Ecology*. London, Chapman and Hall.

Rasser, M. 2009. *The Role of Biotic and Abiotic Processes in the Zonation of Salt Marsh Plants in the Nueces River Delta, Texas*. PhD. Dissertation. University of Texas at Austin, Austin, Texas, USA.

Rasser, M.K., N.L. Fowler, and K. H. Dunton. 2013. Elevation and plant community Distribution in a microtidal salt marsh of the western Gulf of Mexico. *Wetlands*: in press.

Riera R, P.A. Montagna, R.D. Kalke and P. Richard. 2000. Utilization of estuarine organic matter during growth and migration by juvenile brown shrimp *Penaeus aztecus* in a south Texas estuary. *Marine Ecology Progress Series* 199: 205–216.

Riera, P., P. Richard, A. Grémare, and G. Blanchard. 1996. Foods source of intertidal nematodes of the Bay of Marennes-Oléron (France), as determined by dual stable isotope analysis. *Marine Ecology Progress Series* 142: 303–309.

Ryan, A. 2011. *Modeling hydrodynamic fluxes in the Nueces River Delta*. M.S. Thesis. University of Texas at Austin, Austin, Texas, USA.

Secor, H. J.R. Rooker, 2005. Connectivity in the life histories of fishes that use estuaries. *Estuarine, Coastal and Shelf Science* 64: 1-3.

Shipley, F., and GBNEP staff, 1994: *The Galveston Bay plan*. Report GBNEP-49, Texas Natural Resources Conservation Commission, Austin.

- Simms, A., J. Anderson, A. Rodriguez and M. Taviani, 2008: Mechanisms controlling environmental change within an estuary: Corpus Christi Bay, Texas, USA. *Geol. Soc. Am. Sp. Pap.* 443, 121-146. doi:10.1130/2008.2443(08).
- Smith, S., and J. Hollibaugh, 1993: Coastal metabolism and the oceanic organic carbon balance. *Reviews of Geophysics* 31 (1), 75-89.
- Stachelek, J.J. 2012. *Freshwater Inflows in the Nueces Delta, TX: Impacts on Porewater Salinity and Estimation of Needs*. M.S. Thesis. The University of Texas at Austin, Austin TX.
- Superintendent of the Coast Survey, 1862: Sketch 19 showing the progress of the Survey in Section Number IX, *Annual report, 1861*. Ex. Doc. No. 41, U.S. House of Representatives, 36th Congr. 1st Sess, Washington.
- TDWR. Texas Department of Water Resources. 1982. *The influence of freshwater inflows upon the major bays and estuaries of the Texas Gulf Coast: Executive Summary*, LP-115 (second edition). Texas Department of Water Resources, Austin, TX. 51 pp.
- Touchette B.W., G.A. Smith, K.L. Rhodes, and M. Poole. 2009. Tolerance and avoidance: two contrasting physiological responses to salt stress in mature marsh halophytes *Juncus roemerianus* Scheele and *Spartina alterniflora* Loisel. *Journal of Experimental Marine Biology and Ecology* 380: 106-112.
- Tunnell, J. and L. Lloyd. 2011. *Effects of Rincon Bayou Pipeline Inflows on Salinity Structure Within the Nueces Delta, Texas*. CBBEP Publication 76, Project Number 1106.
- Turner, R.E., 1977: Intertidal vegetation and commercial yields of penaeid shrimp. *Trans. Am. Fish. Soc.* 106, 411-16.
- Vasconcelos, R.P., P. Reis-Santos, A. Maia, V. Fonseca, S. França, N. Wouters, M.J. Costa and H.N. Cabral. 2010. Nursery use patterns of commercially important marine fish species in estuarine systems along the Portuguese coast. *Estuarine and Coastal Shelf Science* 86: 613–624
- Volk, R. and CCBNEP staff, 1998: *Coastal Bend bays plan*. Report CBBEP-1, Texas Commission on Environmental Quality, Austin.
- Ward, G.H., 1985: Evaluation of marsh enhancement by freshwater diversion. *J. Water Res. Planning Mgmt, ASCE*, 111 (1), 1-23.
- Ward, G.H., 1997: *Processes and trends of circulation within the Corpus Christi Bay National Estuary Program Study Area*. Report CCBNEP-21, Corpus Christi Bay National Estuary Program, Corpus Christi, Texas.

- Ward G.H., M.J. Irlbeck, P. Montagna, 2002. Experimental river diversion for marsh enhancement. *Estuaries* 25: 1416-1425.
- Webb, J.W. 1983. Soil water salinity variations and their effects on *Spartina alterniflora*. *Contributions in Marine Science* 26: 1-13.
- Woodwell, G., R. Whittaker, W. Reiners, G. Likens, C. Delwiche, and D. Botkin, 1978: The biota and the world carbon budget. *Science* 199 (No. 4325), 141-146.
- Zedler, J. B., J. C. Callaway, J. S. Desmond, G. Vivian-Smith, G. D. Williams, G. Sullivan, A. E. Brewster and B. K. Bradshaw, 1999. California salt marsh vegetation: An improved model of spatial pattern. *Ecosystems* 2: 16.
- Zimmerman, R., T. Minello and L. Rozas, 2002: Salt marsh linkages to productivity of penaeid shrimps and blue crabs in the northern Gulf of Mexico. In: *Concepts and controversies in tidal marsh ecology* (M. Weinstein and D. Kreeger, eds.), 293-314. New York: Kluwer Academic Publishers.

This page intentionally blank for two-sided printing.

A Appendix: Nueces Delta Hydrodynamic Model

A.1 *Introduction*

A.1.1 Overview and Background

This appendix presents results and analyses of the Nueces Delta Hydrodynamic Model (NDHM)¹², which was designed to simulate the hydrodynamic conditions in the Nueces Delta near Corpus Christi, Texas. This model addresses the effects of freshwater pumping from the Rincon Diversion Pipeline, tidal inundation, wind-driven flows, and rainfall runoff from the nearby uplands. The model was built on the framework of the PC2 Hydrodynamic Code, v6.0, developed at the Center for Research in Water Resources (CRWR), University of Texas at Austin. The NDHM was created as part of a series of projects focused on restoring the Nueces Delta ecosystem and understanding the movement of fresh and saltwater through the system. This report demonstrates how the NDHM provides a framework for investigating the transport and fate of freshwater introduced in restoration projects.

The Nueces River estuarine system includes the Nueces Delta, the Nueces River tidal segment, Corpus Christi Bay, Nueces Bay, Oso Bay, and Redfish Bay (Figure A.1). The estuary is fed by the river systems impounded in the Choke Canyon Reservoir and Lake Corpus Christi (Figure A.2). The former was completed in 1982, the latter in 1958 (Bureau of Reclamation 2000b). A smaller impoundment at Calallen near the upstream end of the Nueces Delta was constructed in the late 1800's by the Corpus Christi Water Supply Company to prevent saltwater from intruding upstream and contaminating the city's drinking water (Cunningham 1999).

This report focuses on the Nueces Delta, also known as the Nueces Marsh, covering approximately 75 square kilometers of vegetated marshes, mudflats, tidal creeks and shallow ponds (Bureau of Reclamation 2000b). A river delta is commonly the principal path through which a river enters into the broader embayments of an estuary. However, a combination of natural and anthropogenic alteration around Corpus Christi has left the Nueces Delta substantially cutoff from the main flow of the Nueces River into Nueces Bay by embankments that limit flooding (Heilman, et al. 2000). See Bureau of Reclamation (2000a) for a more detailed description of the Nueces Delta and its environs.

An estuary is the transition zone where salt water from the sea mixes with freshwater inflows from rivers, typically with low salinity where the river enters the estuary and increasing salinity towards the sea (Montagna, Merryl, et al. 2002). The balance of freshwater inflow working against tidal forcing generally determines the upstream estuarine salinity distribution (Alber 2002). However, high evaporation rates in hot climates, combined with limited rainfall and low freshwater inflows can create inverse estuary effects, where salinity patterns are reversed with hypersaline conditions upstream. Inverse estuary conditions have been documented in the Nueces Delta (Montagna, Kalke

¹² This appendix was previously published in substantially similar content as Ryan and Hodges (2011) and is presented herein without further quotation or attribution.

and Ritter 2002, Palmer, Montagna and Kalke 2002), arguably due to the combination of climate, landscape changes, and freshwater inflow reductions.

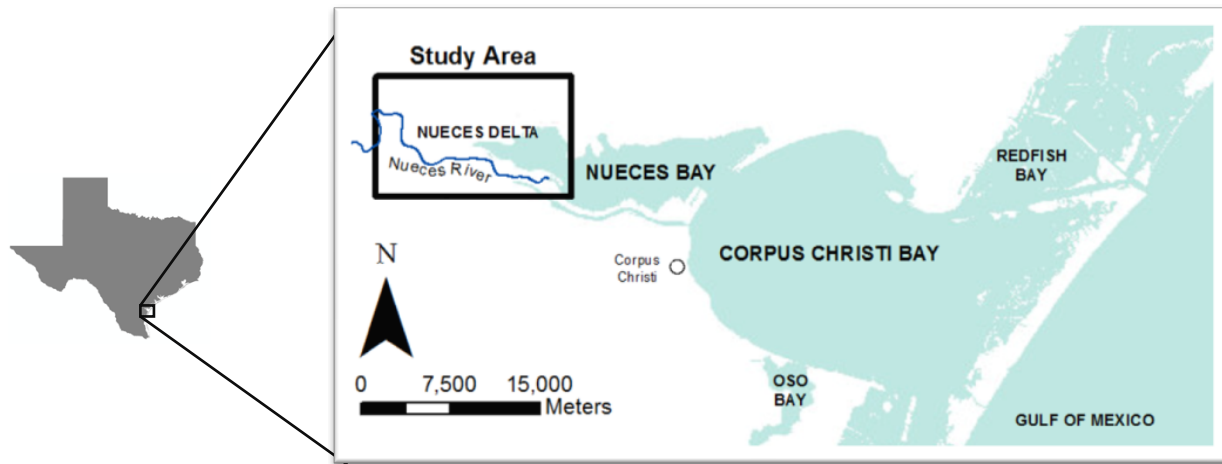


Figure A.1: Location of the Nueces Delta



Figure A.2: Major Rivers and Reservoirs in the Nueces Basin

Since the final dam was completed in 1982, the average annual freshwater inflow to the upper Nueces Delta has decreased by 99% compared to pre-impoundment conditions, i.e. before 1958 (Irlbeck and Ward 2000). Decreasing freshwater inflows often has a negative effect on estuarine ecology through increasing salinity (Copeland 1996), which

has been documented for the Nueces Delta; the Rincon Bayou, a creek located in the upper Nueces Delta, has seen salinities ranging from 0 - 160 ppt and temperatures as high as 40° C (Montagna, Kalke and Ritter 2002). The hypersaline conditions have had demonstrable negative ecosystem effects (Alexander and Dunton 2002). From a simple heat and salt balance perspective, it can be argued that increasing hypersaline episodes will continue in the upper Nueces Delta unless the overbank flooding frequency is increased and/or sufficient freshwater can be introduced through the Rincon Pipeline Diversion.

A.1.2 Nueces Delta Projects

Since 1987, several projects have focused on restoring aspects of the Nueces Delta ecology (Figure A.3). The Nueces Delta Mitigation Project excavated an area to restore a salt marsh habitat in the lower delta. The Rincon Bayou Demonstration Project, the reopening of the Rincon Overflow Channel, and the Rincon Pipeline Diversion were each designed to increase freshwater inflows to the upper delta. The Allison Wastewater Treatment Plant Diversion involved piping nutrient-rich water to the middle delta.

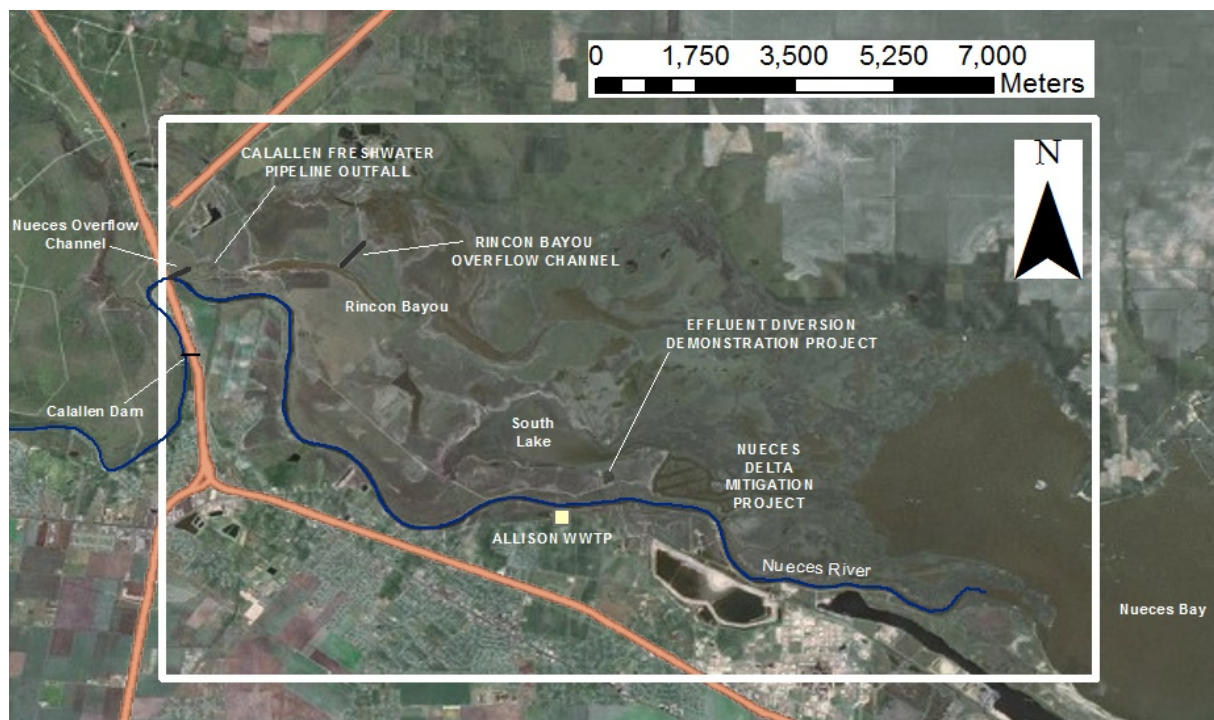


Figure A.3: Nueces Delta restoration and mitigation projects

Nueces Delta Mitigation Project

The United States Army Corps of Engineers (USACE) and the Corpus Christi Port Authority conducted the Nueces Delta Mitigation Project in March 1987 as an effort to reduce wetland losses due to dredging in the Corpus Christi Ship Channel (Alan Plummer Associates, Inc. 2007). The objective was to create a salt marsh that could provide a

wetland habitat. An area of 198 acres was excavated to create a network of levees, channels and ponds simulating natural salt marshes (Nicolau, et al. 1996). While the Nueces Delta Mitigation Project did not provide new *Spartina alterniflora* habitat (an important marsh species in the delta), the project did produce significant non-vegetated bay bottom habitat (Nicolau, et al. 1996).

Rincon Bayou Demonstration Project

The U.S. Bureau of Reclamation conducted the Rincon Bayou Demonstration Project in October 1995 to increase freshwater inflows from the Nueces River to the Nueces Delta (Bureau of Reclamation 2000a). Within the demonstration project, the connection between the Nueces River downstream of the Calallen dam and the Rincon Bayou was excavated to form the Nueces Overflow Channel. The bottom elevation in the excavation was approximately mean sea level (Bureau of Reclamation 2000b). A second channel, the Rincon Overflow Channel, was excavated further downstream in the Rincon Bayou, providing a spillway to tidal mudflat areas located north of the bayou. The resulting increase in freshwater inflows had positive ecological effects in the Rincon Bayou and upper Nueces Delta. Over time, the freshwater inflows reduced salinities in the delta. However, the project did not have permanent easements over private property so the channel was closed in September 2000 (Montagna, Hill and Moulton 2009).

Reopening the overflow channels

Because of the success of the Rincon Bayou Demonstration Project, a program to purchase property and obtain easements from property owners was undertaken, with the overflow channels from the Demonstration Project re-opening in October 2001. The overflow channels are now permanent features of the Nueces Delta (Alan Plummer Associates, Inc. 2007).

Rincon Pipeline Diversion from Calallen

Only two estuarine systems on the Texas Gulf Coast, the Nueces Estuary and the Colorado Estuary, have explicit bay and estuary freshwater inflow volume requirements attached to water rights (Tolan 2007). Based on the 1995 Agreed Order with the Texas Natural Resource Conservation Commission, the City of Corpus Christi is required to pass through freshwater to sustain the ecosystems (Adams and Tunnell 2010). To manage the Agreed Order freshwater inflows to the Nueces Delta, in 2008 the City of Corpus Christi constructed a pipeline and pumping station to divert water from the Calallen pool to the upper Rincon Bayou. Three pumps are installed, each capable of pumping approximately $1.5 \text{ m}^3/\text{s}$ (109 acre-ft/day). Under normal operation only one or two pumps are typically in used (J. Tunnell, pers. comm.)

Allison Wastewater Treatment Plant Diversion Project

The Allison Wastewater Treatment Plant, located on the south bank of the Nueces River tidal reach, has historically discharged secondary treated municipal wastewater effluent to the Nueces River since the plant's construction in 1966 (Alan Plummer Associates, Inc. 2007). In an effort to provide high-nutrient freshwater to the delta, the City of Corpus Christi created a pipeline under the Nueces River to divert water from the treatment plant to the delta. In August 1997, the City constructed three earthen cells to

receive treated effluent in the Lower Nueces River Delta. The diversion began in October 1998, diverting approximately 2.0 MGD (Montagna, Hill and Moulton 2009). A study on the effects of the wastewater diversion project found that there were no detrimental impacts on the marsh, but that more wastewater must be diverted if substantial reduction in downstream salinity downstream is to be achieved (Alexander and Dunton 2006). The Allison Wastewater Treatment Plant Diversion Project was completed in August 2003 (Nicolau, et al. 2002).

A.1.3 Hydrodynamic model

Introduction

Prior to the present study, a comprehensive numerical model of flow and transport in the Nueces Delta using the shallow-water equations had not been attempted. The Bureau of Reclamation report for the Rincon Bayou Demonstration Project notes the opportunity for a numerical model to integrate the data components of the study and improve understanding of the marsh under various conditions (Bureau of Reclamation 2000b). The study presented here fills the need for a hydrodynamic model of the Nueces Delta to examine the impacts of changes in flow to the delta, including inflows from the Rincon Pipeline, tidal flows, and rainfall.

Other estuarine models

A variety of numerical models have been used to simulate hydrodynamic conditions in estuaries (e.g. Table A.1). For estuarine embayments and rivers without significant estuarine marshland the key modeling challenges are in representing tidal and river fluxes (e.g. Spillman et al 2008, Zhan et al 2004, respectively). However, marshland with significant wetting/drying of the landscape provides numerical challenges addressed in fewer models, most notably Yang and Khangaonkar (2009), Battjes (2006), Ji, et al (2001), Oey (2006), Casulli and Zanolli (2002).

PC2 Method

The estuarine models in Table A.1 all use the hydrostatic Navier-Stokes equations (also known as the shallow water equations) to solve conservation of momentum and mass. A common numerical approach in several models is the semi-implicit algorithm using implicit discretization for the free surface (barotropic mode) and explicit discretization for the velocity and baroclinic forcing (internal wave), e.g. Casulli and Cheng (1992). This approach is generally implemented in a first-order accurate scheme for unsteady and baroclinic flows (Hodges 2004). By restructuring the semi-implicit algorithm for a predictor-corrector sweep, the semi-implicit θ -method (Casulli and Cattani, 1994) can be improved to 2nd order for both barotropic and baroclinic flow (Hodges and Rueda 2008). The PC2 Hydrodynamic Code used for the NDHM employs predictor-corrector methods using two time-levels of information (Hodges and Rueda 2008). It has volume-consistent discretization of both barotropic and baroclinic modes, along with mass-conserving scalar transport. The model can be implemented in either 2D or 3D, and using either first-order or second-order accurate numerical algorithms. During development of the NDHM, the PC2 Hydrodynamic Code was applied in 2D (depth-averaged) with first-order algorithms. This approach ensured the fastest model simulation time, which is an advantage during model development.

Table A.1: Prior numerical models created for simulating estuarine environments

Model	Area	Dimension	Focus	Used by:
FVCOM	Skagit River Estuary, Puget Sound, WA	3D	Tidal circulation & transport processes	Yang and Khangaonkar 2009, Chen, Liu and Beardsley 2003
ECOM-si	Satilla River Estuary, Georgia	3D	Semi-implicit finite difference scheme; realistic vertical turbulent mixing parameters	Zheng, Chen and Zhang 2004
ELCIRC	Columbia River Estuary	3D	Turbulence closure schemes; includes terms for the tidal potential and atmospheric pressure gradients, and provides a detailed description of air-water exchanges	Zhang, Baptista and Myers 2004
Environmental Fluid Dynamics Code (EFDC)	Morro Bay, James River Estuary	3D	Provides a hydrodynamic model with water quality model, sediment transport model, and toxics model capabilities	Ji, Morton and Hamrick 2001
Princeton Ocean Model (POM)	Cook Inlet, Alaska	3D	Movable land-sea boundaries	Oey 2006
Delft-FLS	Polders of Tiel and Culemborg, Netherlands	2D	Specifically suited to simulate overland flow over initially dry land	Stelling, Kernkamp and Laguzzi 1998
TRIM	Barbamarco Lagoon, Italy	3D	A stable semi-implicit finite difference method of discretization computationally suitable for spatially fine grids with relatively large time steps	Casulli and Cattani 1994, Casulli and Cheng 1992
ELCOM-CAEDYM	Barbamarco Lagoon, Italy	3D	Provides a hydrodynamic model coupled with an aquatic ecosystem model; includes external environmental forcing	Spillman, Hamilton, Hipsey and Imberger 2008

Hydrodynamic study objectives

The main objectives of this study were

1. Create a model of flow and transport through the Nueces Delta.
2. Examine the model sensitivity to different forcing conditions.

Organization of this appendix

This appendix provides documentation of the approach used in applying the NHDM to the Nueces Delta and an analysis of results. Section A.2 presents the modeling methodology, including sources of input data, selection of modeled scenarios and analysis metrics. Detailed information on input sources and data analysis techniques are provided in appendices of Ryan and Hodges (2011). Analysis of model results is provided in §A.3. Findings and recommendations for future work are provided in §A.5.2, with additional technical details in appendices of Ryan and Hodges (2011). The complete Matlab™ programming scripts used for data analysis are also provided in appendices of Ryan and Hodges (2011).

Caveat

Due to the lack of sufficient field data, the NDHM could be neither calibrated nor validated for the present study. Recommendations regarding the types of data needed for calibration and validation are provided in §A.5.2. However, because the model is mechanistic, the present uncalibrated results are still useful in model-model comparisons to investigate the system's sensitivity to different forcing conditions, which is the focus of this report.

A.2 Methodology

A.2.1 Introduction

This section provides: 1) an explanation of the types of input data required to run the NDHM, 2) a discussion and documentation of the scenarios modeled, and 3) details on the data analysis methods. The model input files are developed to reflect bathymetric, inflow, and meteorological conditions in the delta, but these are inherently limited by the availability of data and its spatial/temporal distribution. Hydraulic effects, such as overtopping of dikes or flow through bridge piers, are not readily represented by the shallow water equations at the practical model resolution and are handled by customized sub-models of the NDHM. Scenarios were selected to exercise a range of conditions to ensure NDHM responded appropriately to changes in forcing. Analysis methods were designed to compress the 3-dimensional data set (space, time, transported variables) into statistical representations that can be readily compared.

A.2.2 Model input data

Overview

There are several types of input: boundary data, forcing data, parameters, and initial conditions. Boundary data, such as land surface elevation (bathymetry) and surface roughness, vary across space but are constant over time for a model run. Forcing data accounting for wind, tide, precipitation and inflows vary in time, but are provided either at fixed points in space (e.g. tide) or are uniformly distributed over the entire domain (e.g. wind). Parameters are used to change the model representation of the physics, such as the time step and the wind drag coefficient. Initial conditions are the distribution of salinity and water depth across the delta at the start of the simulation.

The methodology for determining the boundary data, initial conditions, and forcing data for the Nueces Delta is outlined below. Details for data preparation, are provided in appendices of Ryan and Hodges (2011).

Data for land surface elevation (bathymetry)

A river delta is an intersection between wet and dry land, and thus where topographic descriptions of “land surface elevation” meet a bathymetric description of “water depth.” Herein we will generally use the term “bathymetry” to indicate the elevation above the zero datum of the landscape (NAVD88), whether covered with water or dry.

The best available bathymetry for the Nueces Delta is a 1 x 1m raster data set prepared by J. Gibeaut at Texas A&M Corpus Christi from LiDAR data collected under a

project funded by the Coastal Bend Bays and Estuary Program. This bathymetry was previously processed and validated against field measurements by J. Gibeaut (personal comm.). The 1 x 1 m data set consists of 105×10^6 elevations within the Nueces Delta and the nearby uplands. Extrapolating from recent experience, in its present configuration the PC2 Hydrodynamic Code running on a 3 GHz processor would require about 1500 GB of memory and 10 minutes of computer time for every second of model simulated time (i.e. only 1/600th of real time so that 600 hours on the computer would model only one hour of flow and transport in the delta). By creating a coarser 15 x 15 m bathymetry data set for the NDHM, the computer memory requirements are more manageable (5 GB) and the computational time is 0.14 seconds for every second modeled in the delta (i.e. 7 times faster than real time, so that 1 hour of computation will model 7 hours in the delta).

Upscaling from the 1 x 1 m data to the 15 x 15 m data was accomplished as detailed in appendices of Ryan and Hodges (2011). The result is shown in Figure A.4. The upscaling method used the mean elevation value in a 15 x 15 m grid cell with adjustments for subgrid scale features. Channelization effects along grid cell diagonals for subgrid features was approximated using a statistical analysis to identify affected cells in the 15 x 15 m data set and adjust to the cell elevation to the mean of the lowest 15 data points in the 1 x 1 m grid. The PC2 Hydrodynamic Code has cell edge features to represent for subgrid-scale blocking topography that is otherwise lost in the upscaling process for a grid cell. The two railways crossing the Nueces Delta are 3 to 4 m wide would be lost in the mean elevation of a 15 x 15 m grid, so they are represented by PC2 cell edges. Where piers allow flow under the railways, the computed mean elevation in the grid cell was used without cell edge elevations; a hydraulic model applied to represent the drag associated with the piers.

Data for surface roughness

The 2D shallow water flow equations in NDHM require a drag coefficient (C_D) or an equivalent Manning's 'n' to model frictional losses in the depth-averaged water column. For NDHM, we used a Manning's 'n' approach, where the roughness coefficient was developed from the 2001 National Land Cover Dataset using the approach developed by Hossain, Jia and Chao (2009) for remotely-sensed data. The baseline result is shown in Figure A.5 and explained in more detail in appendices of Ryan and Hodges (2011). The impacts of piers and culverts under barriers are incorporated into the land cover matrix as adjusted Manning's roughness coefficients.

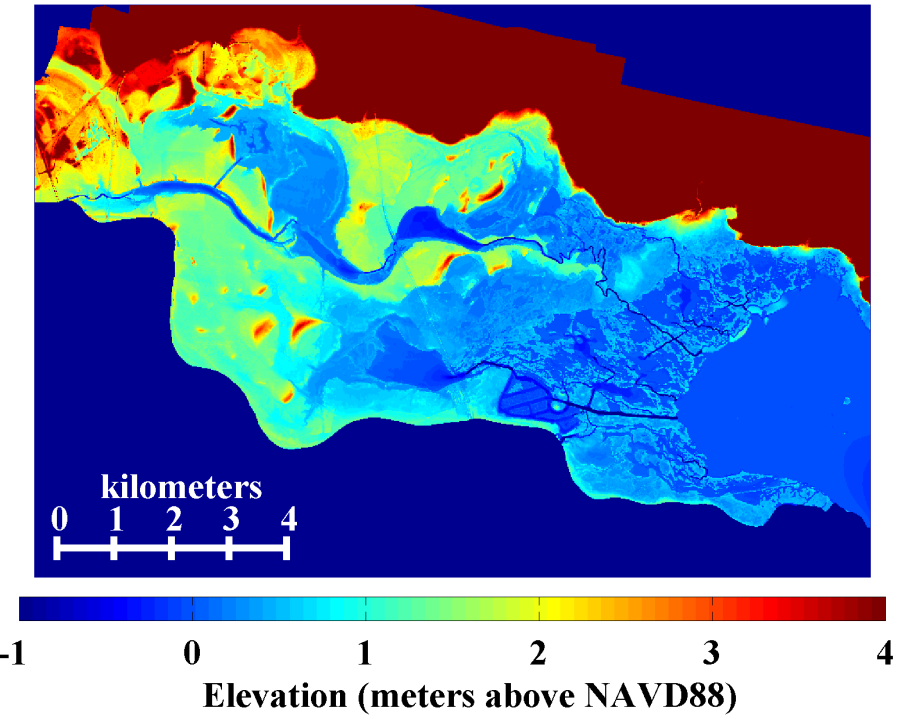


Figure A.4: Image of the bathymetry used in the model. The color scale is selected to show details in the marsh lowlands, however the uplands higher than 4 m are also well-resolved in the data set (q.v. Figure A.1)

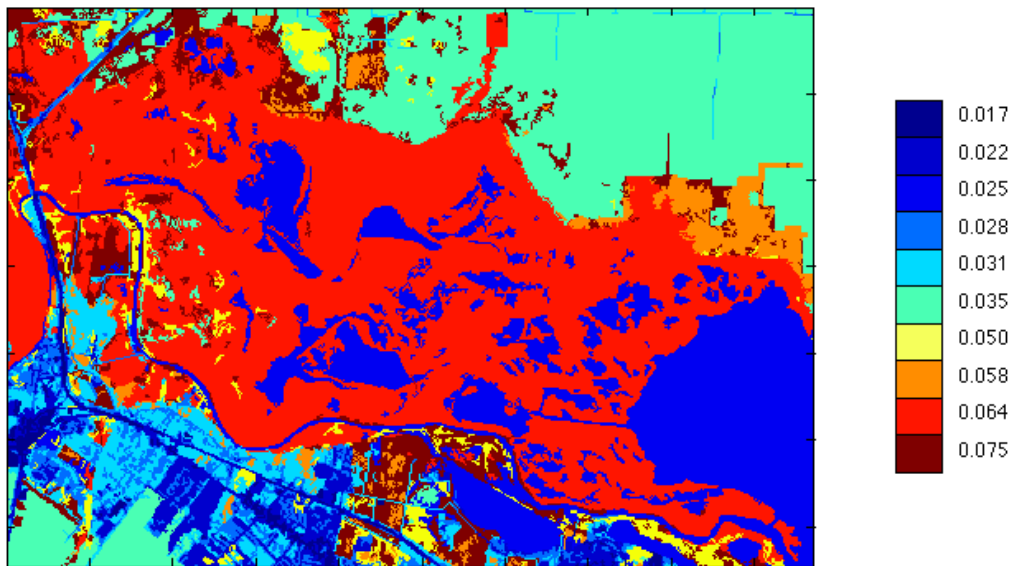


Figure A.5: Manning's 'n' based on land-cover

The methodology described above is fairly common in the modeling literature, usually described as applying a grid-cell average elevation with surface roughness based on accepted literature values. However, as technology improves our data, we are faced with increasing evidence of shortcomings in this traditional approach. Because the 15 x 15 m grid was rasterized from the 1 x 1 m grid, we can analyze the subgrid-scale topography, which shows that topographical roughness can dominate the surface roughness developed from landcover in the Nueces Delta. Figure A.6 gives an example of two 15 x 15 m grid cells, each containing two-hundred and twenty-five 1 x 1 meter data values. The two grid cells have the same mean elevation of 2.1 m, but the cell on the left has a standard deviation of 0.70 m whereas the cell on the right has a standard deviation of 0.02 m. Given the same free surface gradient and antecedent conditions, it seems obvious that the flow across these two grid cells should be different because of the different subgrid-scale topography within the cell. Clearly, cell with the higher variability in elevation should have greater subgrid-scale frictional effects for flows through the upper face of the cell, although the lower elevations along the lower and right faces of the cell might provide a preferential low-friction path. However, no one has developed a method for representing known subgrid-scale topological roughness in terms of either an effective Manning's 'n' or a drag coefficient for this type of modeling. This issue is a subject for future research as discussed in §A.5.2.

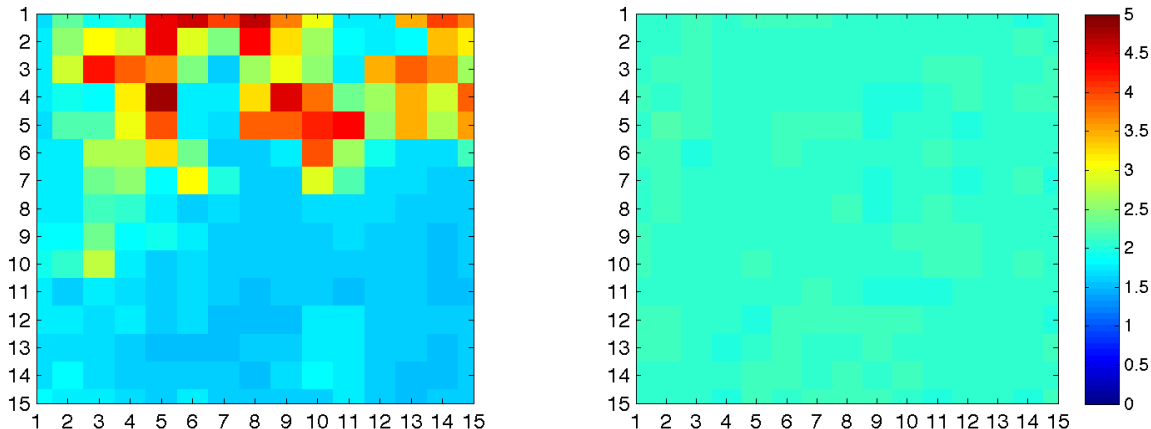


Figure A.6: Examples of two 15 x 15 m grids and their subgrid-scale topography.

Nevertheless, we can gain some insight into how subgrid topography might affect the flow field by changing the roughness in grid cells having a relatively large standard deviation in the subgrid elevation. Localized and global changes to the baseline surface roughness set (R_B) are used to evaluate model sensitivity. The different surface roughness sets tested to date are outlined in Table A.2. For local changes, we adjust the roughness only in grid cells having a large standard deviation in subgrid scale elevation, using twice the baseline surface roughness ($R_{\sigma 2}$) and ten times the baseline surface roughness ($R_{\sigma 10}$). As a comparison to this localized affect, in the global approach the baseline surface roughness for every cell is multiplied by a factor of ten (R_{10}) and one hundred (R_{100}).

Table A.2: Roughness sets; $n_B(k)$ is the baseline Manning's n roughness for $k=\{1...N\}$ grid cell, i.e. the 15 x 15 m cells in Figure A.6; $\sigma_z(k)$ is the standard deviation of the subgrid elevation, c_σ is the standard deviation cutoff value (set at 10 cm, see appendices of Ryan and Hodges 2011)

Surface roughness set identifier	Roughness algorithm
R_B	$n_B(k)$
R_{σ_2}	$n_{\sigma_2}(k) = \begin{cases} 2n_B(k) & : \sigma_z(k) \geq c_\sigma \\ n_B(k) & : \sigma_z(k) < c_\sigma \end{cases}$
$R_{\sigma_{10}}$	$n_{\sigma_{10}}(k) = \begin{cases} 10n_B(k) & : \sigma_z(k) \geq c_\sigma \\ n_B(k) & : \sigma_z(k) < c_\sigma \end{cases}$
R_{10}	$n_{10}(k) = 10n_B(k)$
R_{100}	$n_{100}(k) = 100n_B(k)$

Data for initial conditions

The NDHM requires the spatial distribution of water depth, salinity and velocity across the entire simulation domain as initial conditions. A model approximation of the initial conditions must be made from the limited available data. For velocity, the initial velocity is set to zero. For salinity, data from Conrad Blucher Institute (CBI) observation stations SALT and NUDE (Figure A.7) are used as discussed in appendices of Ryan and Hodges (2011). For water depth, the initial tidal elevation at the Nueces Bay boundary is applied as a uniform water surface across the entire delta. As discussed in §A.3.2, the uncertainty associated with these approximations of the initial conditions are reduced by using an extended model spin-up time.

Forcing data

The model forcing data are tidal elevation, wind speed and direction, inflows, salinity, and precipitation. Data sources, time periods of data availability, and data manipulation are discussed in appendices of Ryan and Hodges (2011). Table A.3 gives the data sources for the years simulated. Section A.2.3 below describes how forcing data were modified for different scenarios.

Of the salinity observation stations in Figure A.7, only SALT03 is used as forcing data, providing the salinity for inflows through the open tidal boundary of Nueces Bay. The other stations are used for both initial conditions and for analysis of model results (§A.3.3)



Figure A.7: Locations of TCOON salinity monitoring stations in the delta

Table A.3: Data sources for model forcing for the scenarios

Forcing Data	Source
Tide	TCOON
Salinity	CBI
Precipitation	NOAA
Wind	NOAA
Inflow	USGS
Rincon Pipeline Pumping	Nueces River Authority

A.2.3 Simulation scenarios

Different model scenarios with different sets of initial, boundary, and forcing conditions were selected to test and evaluate various aspects of the model. Forcing data that were *not* altered were tidal elevation, initial and inflow salinity, and the USGS gauged inflow inflows from the Nueces River into the delta; measured values for these data were used in all simulations. Using measured data as a baseline, additional forcing data sets were created for rain, wind speed, surface roughness and the Rincon Diversion pumping. Development of these data sets is discussed in detail in appendices of Ryan and Hodges (2011).

Based on data availability, the model was run for 7 to 17 days for simulations using data from the first half of April in years 2008, 2009 and 2010. Table A.4 provides an overview of the scenarios. In this table “baseline” conditions use only observed values from field data. For sensitivity testing, three wind speed conditions were considered: zero, baseline, and twice the baseline. Similarly, three rain conditions were considered, zero, baseline, and a heavy rain; the latter corresponding to a week of severe rainfall (computed as described in appendices of Ryan and Hodges 2011). Five surface roughness conditions were modeled, as outlined in Table A.1. Four different flow conditions for the Rincon Diversion Pipeline were modeled, corresponding to a single pump operating, reduced flow conditions of 2/3 and 1/3 of a single pump capacity, and zero flow¹³. Using three baseline years, these data sets provide 324 different possible combinations. The selected 17 scenarios are considered screening scenarios that evaluate the change of a single variable from the baseline.

A.2.4 Analysis methods

Overview

The analysis of model results focuses on a few metrics: inundated area, total volume of water in the system, volume of freshwater in the system, volume of brackish water in the system, mean difference in depth between two simulations, and the mean depth across the delta from north to south.

Computing the inundated area

The inundated area (A_i) is used to integrate the model behavior over all space into a single metric that evolves through time and has practical meaning for water management. However, the wetting and drying algorithms in the hydrodynamic model will include infinitesimally thin layers (e.g. 10^{-6} m), which may not represent important inundated area and should not be included. As a practical measure, the inundated area can be defined as a sum over the N grid cells with individual cell areas $a_k = 225 \text{ m}^2$ for the evolution of the water depth over time $d_k(t)$ as

$$A_i(t) = \sum_{k=1}^N a_k H\{d_k(t) - c_i\} \quad (\text{B.1})$$

where $H\{\}$ is the Heaviside step function and c_i is a cutoff, chosen as 0.02 m for the present study. The methodology for setting the cutoff is presented in appendices of Ryan and Hodges (2011).

¹³ Note that the Rincon Bayou Pipeline pumps cannot be run at 1/3 or 2/3 of their normal capacity, so these scenarios only examine the relative effects of different flow conditions. The original intent was to model 0, 1, 2 and 3 pumps operating. However, miscommunication with the Nueces River Authority over the units used in their online data set resulted in NDHM being applied with flow rates that were 1/3 of the intended conditions.

Table A.4: Conditions used in the simulations of the Nueces Delta

For computing the inundated area affected by pumped water, only those cells containing a significant fraction of pumped water should be used. The computation is

$$A_{pi}(t) = \sum_{k=1}^N a_k H\{d_k(t) - c_i\} H\{P_k(t) - c_p\} \quad (\text{B.2})$$

where $P_k(t)$ is the fraction of pumped water in the k^{th} grid cell and c_p is a cutoff for the minimum water fraction that is considered significant. The cutoff choice affects the computation of A_{pi} , as discussed in §A.3.7.

Computing the total volume

The evolution of the total water volume V_T in the delta is computed without a cutoff, as small depths will not significantly distort the computation:

$$V_T(t) = \sum_{k=1}^N a_k d_k(t) \quad (\text{B.3})$$

Changes in V_T and A_i provide two slightly different ways to evaluate the amount of water in the delta.

Computing the freshwater volume

The water volume can be divided into saline and fresh, which is helpful for isolating the effects of pumping. At grid cell k , the fraction of the local volume that can be considered fresh water, F_k , diluting salt water of with reference salinity S_R to the local salinity, $S_k(t)$, is

$$F_k(t) = \frac{S_R - S_k(t)}{S_R} \quad (\text{B.4})$$

The total volume of freshwater in the system, V_{FW} , is then

$$V_{FW}(t) = \sum_{k=1}^N a_k F_k(t) d_k(t) \quad (\text{B.5})$$

Computing the brackish water volume

The natural complement to a freshwater volume would be a saltwater volume, which we could define simply as $V_T - V_{FW}$. However, of more interest is the volume of brackish water in the system, V_B , i.e. the water with reduced salinity. Herein, V_B can be defined as sum of the volume of brackish water in the individual cells v_{Bk}

$$V_B(t) = \sum_{k=1}^N v_{Bk}(t) \quad (\text{B.6})$$

where the cell brackish water is calculated with reference to a salinity cutoff, c_s . The volume of brackish water in a cell, v_{Bk} , is calculated as

$$v_{Bk}(t) = \begin{cases} a_k d_k(t) & : S_k(t) \leq c_s \\ 0 & : S_k(t) > c_s \end{cases} \quad (\text{B.7})$$

For the present study we use 15 ppt as the cutoff for defining brackish water; this selection is illustrative only, and does not reflect salinity levels that might be important for ecological concerns.

Depth statistics for cross-delta slices

The spatially-averaged depth over the entire delta does not provide any more information than computation of V_T and A_i . However, we can use a more refined depth metric to evaluate how the model represents wind-forced transport from Nueces Bay into the upper delta (§A.3.5). The wind is typically from 120 to 150 degrees during the modeled periods, which roughly coincides with the main flow axis of the delta. Ideally, a depth metric should compute the mean depth and standard deviation in slices perpendicular to an axis of 135 to 315 degrees, i.e. providing the characteristic depth at cross-sections moving upstream in the delta. However, as the model grid is aligned north-south, it is convenient to define a metric based on slices perpendicular to an east-west axis as shown in Figure A.8, which provides reasonable cross-sections for analysis. The delta is divided into 48 slices, each 300 m wide (20 grid cells) along the east-west axis and containing the entire domain (up to 600 grid cells) along a north-south axis. The mean and standard deviation of the depth for slice p are computed from the set of depths D_j (without any minimum cutoff) as

$$\mu_{300D}(p) = \frac{1}{N} \sum_{j=1}^N D_j(p) \quad (\text{B.8})$$

$$\sigma_{300D}(p) = \sqrt{\frac{1}{N-1} \sum_{j=1}^N [D_j(p) - \mu_{300D}(p)]^2} \quad (\text{B.9})$$

Metrics for depth comparison across scenarios

Comparing the local difference between the depths in two different scenarios provides insight into how different forcing conditions affect the modeled response. Such metrics are particularly useful in evaluating when two models produce similar responses, which is necessary for evaluating model spin-up (§A.3.2). The mean difference in depth between two simulations can be defined as:

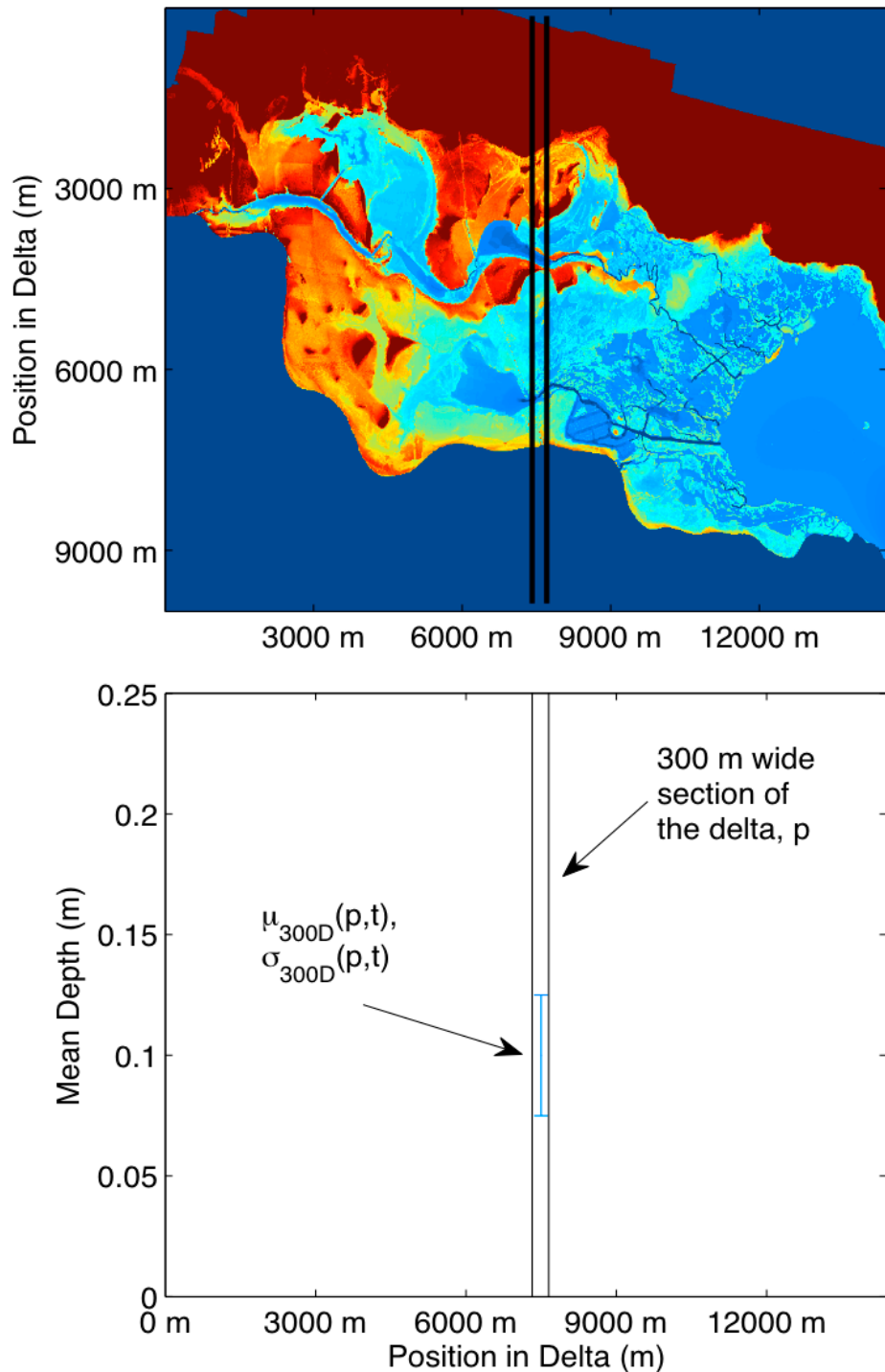


Figure A.8: Slices of 300m width for computing mean depth (μ_{300D}) and standard deviation (σ_{300D})

$$\mu_{\Delta D}(t) = \frac{1}{N} \sum_{k=1}^N \Delta D_k(t) \quad (\text{B.10})$$

where $\Delta D_k(t)$ is the local difference between the k^{th} grid cell depths in two simulations at time t . The standard deviation is

$$\sigma_{\Delta D}(t) = \sqrt{\frac{1}{N-1} \sum_{k=1}^N [\Delta D_k(t) - \mu_{\Delta D}(t)]^2} \quad (\text{B.11})$$

Computing spin-up time

Spin-up time is the interval from the model start until some time when the model results are sufficiently independent of the initial conditions. We can think of this as the time it takes to clear the system's memory. The initial conditions for velocity, depth and salinity are approximations of the unknown real values, with uncertainty that affects results over the spin-up time. However, as tidal, wind and inflow forcing move water through the delta, by the end of the spin-up interval the effects of the initial conditions will be washed out of the system. Beyond the spin-up time, the modeled results are principally determined by the modeled forcing. Thus, estimating the model spin-up time is a necessary exercise in determining the time range over which model result should be compared to field data for calibration and validation. A comprehensive evaluation of spin-up time requires comparison of depth, velocity and salinity metrics. The present study has focused spin-up time on the water depth, using the V_T , A_i , $\mu_{\Delta D}$, and $\sigma_{\Delta D}$ metrics described above. Spin-up is analyzed by starting simulations at two different physical times and evaluating convergence of statistical metrics. Results for spin-up analysis are presented in §A.3.2.

Methods for comparison to field data

For insight into model behavior, in §A.3.3 the water surface elevations are compared with data from the SALT and NUDE stations (q.v. Fig. A.7). Unfortunately, these stations are not benchmarked to a vertical geodetic datum. Without a vertical reference datum, the depth measurements cannot be quantitatively compared to the model. That is, we do not know the exact height of the sensor relative to the model bathymetry so we cannot diagnose either magnitude or direction of any error in water surface elevations. Thus, calibration becomes impossible. However, we can obtain an estimate of sensor elevations by neglecting the mean horizontal gradient in the surface elevation as discussed in appendices of Ryan and Hodges (2011). Using this estimated datum, we can make qualitative comparisons of the water surface behavior between the model and observations.

A.3 Results and discussion

A.3.1 Overview

The NDHM was run to simulate scenarios outlined in §A.2.3. The model spin-up time (§A.3.2), comparison to field data (§A.3.3), response to different forcing conditions

(§A.3.4, A.3.5, A.3.6) and effects of pumping (§A.3.7) are analyzed below. Details on metrics for these analyses are found in §A.2.4.

A.3.2 Spin-up results

Scenario 12 (q.v. Table A.3) was run for 17 days, beginning from 3 April 2009. Scenario 11 commenced on 10 April 2009, seven days into the Scenario 12 run, but using initial conditions developed from measured field data (i.e. without reference to Scenario 12 results).

In Figure A.9 the daily mean depth difference between these two scenarios, μ_{AD} , and standard deviation, σ_{AD} , are computed for the time period when both simulations were running (see §0 for definitions). When Scenario 11 begins μ_{AD} is of the order of 10 cm with similar variability across the domain. However, after Scenario 11 has computed 9 days (i.e. day 16 of Scenario 12 in Figure A.9), the μ_{AD} is reduced to 1.32 mm and σ_{AD} is 2.62 mm, indicating that the different initial conditions for the two scenarios are causing only minor differences in the water surface elevations across the entire delta.

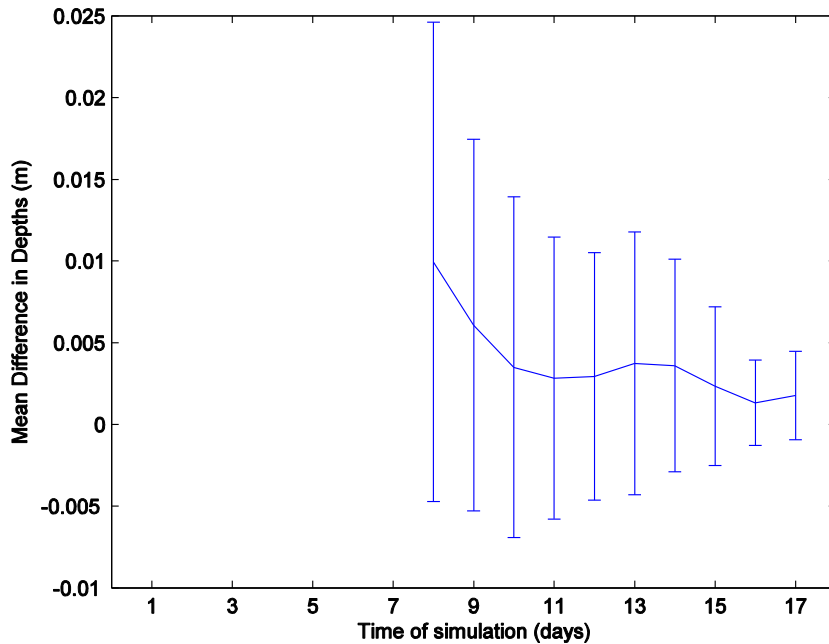


Figure A.9: Mean depth difference (μ_{AD}) with error bars of σ_{AD} for 10 day (Scenario 11) and 17 day (Scenario 12) simulations. The X-axis is simulation days for Scenario 12.

A more qualitative comparison of convergence between the 10 day and 17 day simulation results can be obtained using the inundated area (A_i) and total volume (V_T) metrics. As shown in Figure A.10, after day 14 of Scenario 12 (i.e. the 7th day of Scenario 11) the inundated area and total water volume have converged, indicating that there are no large-scale differences between the models. Thus, the spin-up time for water surface elevation is estimated to be on the order of 7 to 9 days. Spin-up times associated with salinity and velocity have not yet been analyzed.

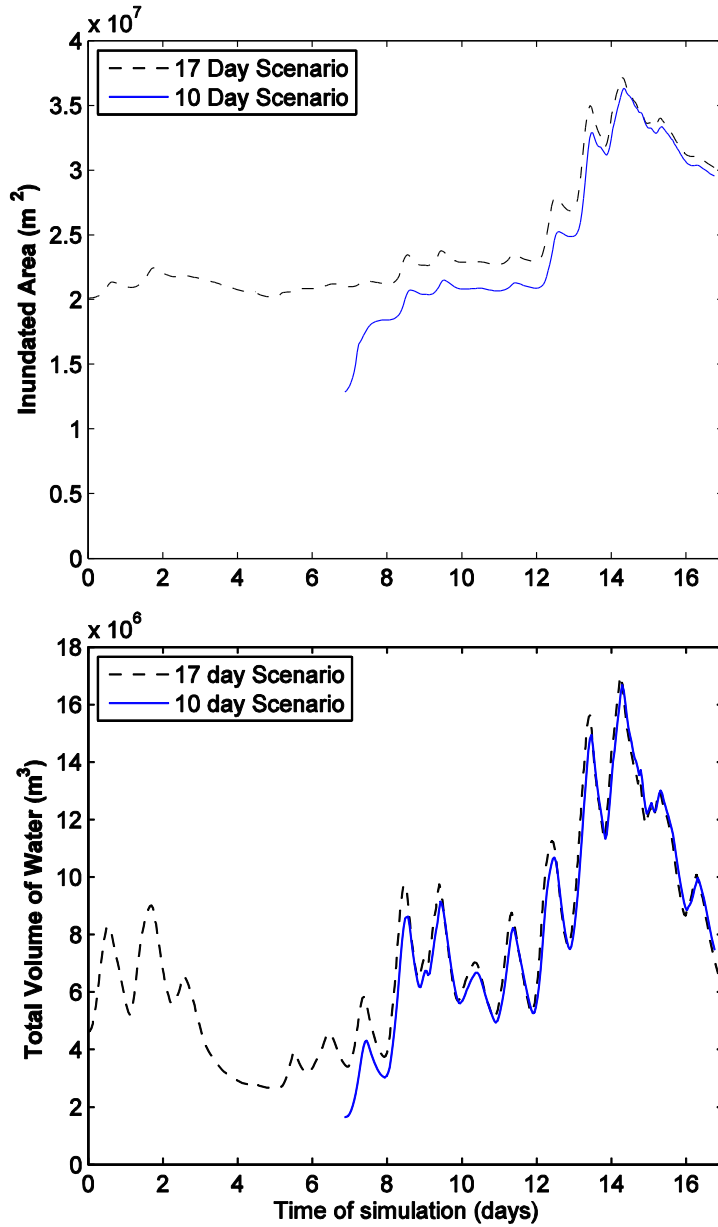


Figure A.10: Comparison of A_i (upper panel) and V_T (lower panel) for 10 day (Scenario 11) and 17 day (Scenario 12) simulations. The X-axis is simulation days for Scenario 12.

A.3.3 Comparison to field data

Field data comparisons are made to 2010 observations using Scenario 13 (q.v. Table A.4) with the baseline roughness R_B and a total of 14 simulation days. Allowing for 7 days of spin up, the field and model free surface elevation data can be compared for days 7 through 14 as shown in Figure A.11.

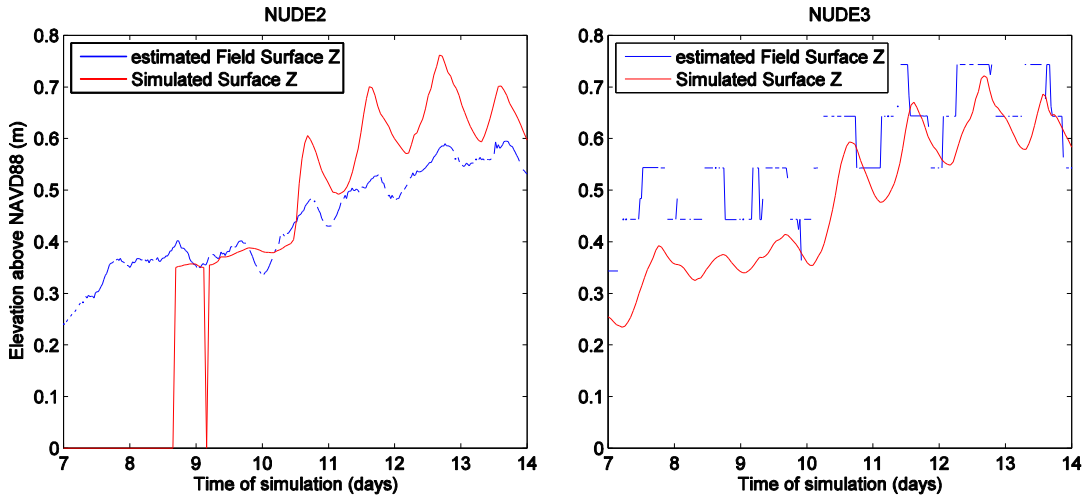


Figure A.11: Comparison of simulated surface elevations with field data estimated elevations.

The overall increasing trend appears to be in reasonable agreement at both stations, indicating that the lowest frequency forcing of the tide and wind are correct. The sharp behavior change at day 10 for NUDE3 is apparent in both field and model data, indicating the model is capturing the transitional features. However, at NUDE2, which is further upstream in the delta compared to NUDE3 (q.v. Figure A.7) the field data daily tidal amplitude is less than 5 cm, but is more than 15 cm in the model. In contrast, the tidal amplitudes appear reasonable at NUDE3 in the lower delta. Thus, it appears that the model surface roughness between the NUDE2 and NUDE3 stations is not sufficiently damping the daily tidal motions. Better agreement could likely be obtained through comprehensive calibration (see §A.5.2). See §A.2.4 for a discussion of the qualitative comparison between model and field data and appendices of Ryan and Hodges (2011) for methods used in estimating the surface elevation for field data from the observed depth with unknown vertical datum.

A.3.4 Model response to rainfall

Rainfall effects on inundated area (A_i) for Scenarios 5, 6, and 7 (q.v. Table A.4) are shown in Figure A.12. The baseline rainfall (Rain) increased the A_i by only $7.29 \times 10^2 \text{ m}^2$ (0.180 acre) over the zero-rain (0) simulation, whereas the heavy rainfall scenario (HR) increased the inundated area by over $1.56 \times 10^4 \text{ m}^2$ (3.85 acre). Although the increase in inundated area is negligible for the baseline scenario and only 0.1% of the flooded marsh for the heavy rain scenario, the effects are more dramatic as measured by total water volume, V_T shown in Figure A.13. The baseline rainfall increases V_T by 2%, whereas the heavy rainfall increases V_T by 24%.

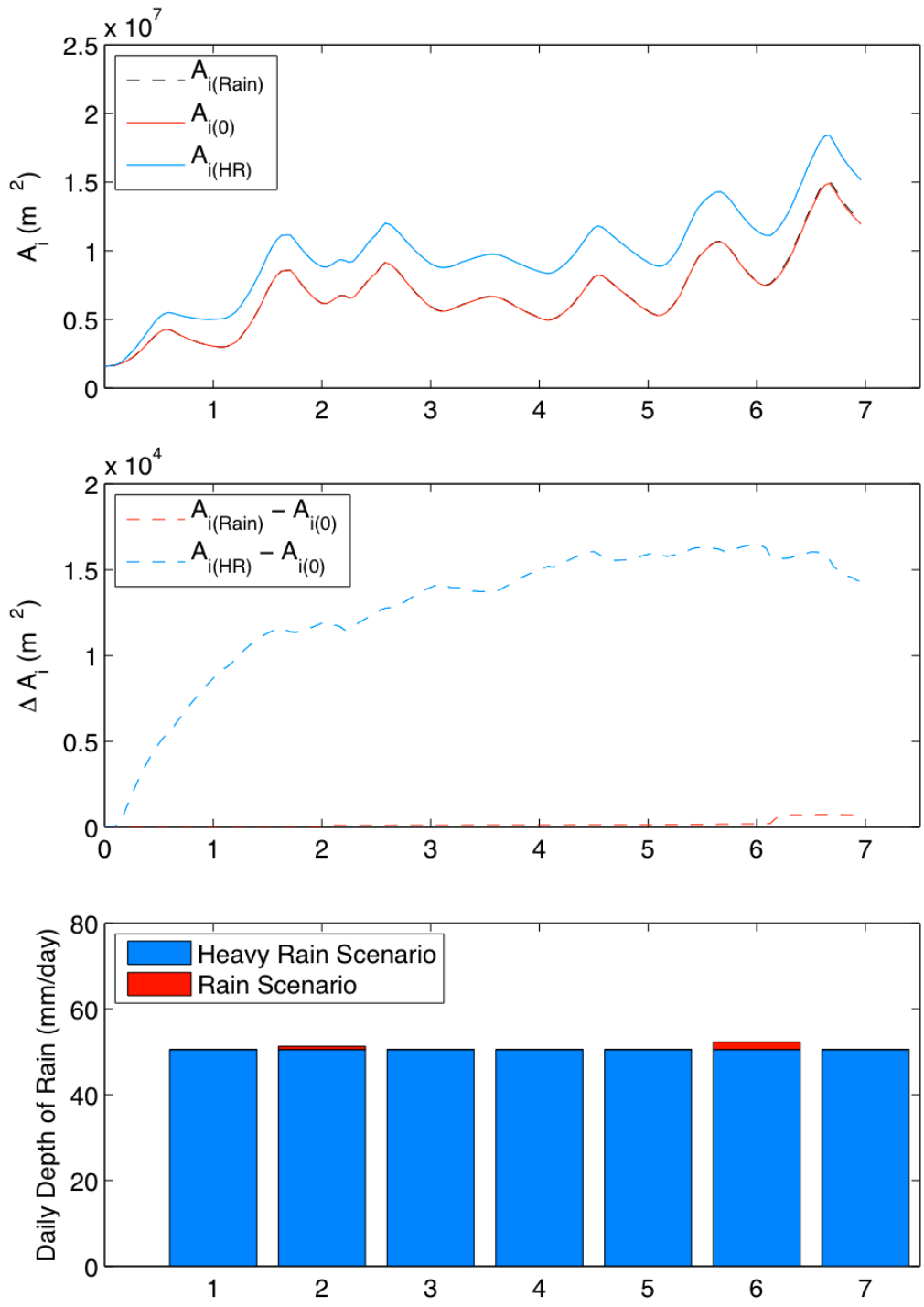


Figure A.12: Rainfall comparisons of inundated area for the seven days of rainfall simulations in Scenario 5 (0 = no rainfall), Scenario 6 (Rain = baseline rainfall) and Scenario 8 (HR = heavy rainfall). Inundated area (A_i) evolution in upper panel; difference between scenarios ΔA_i in middle panel; depth of rainfall on each of seven simulation days in lower panel.

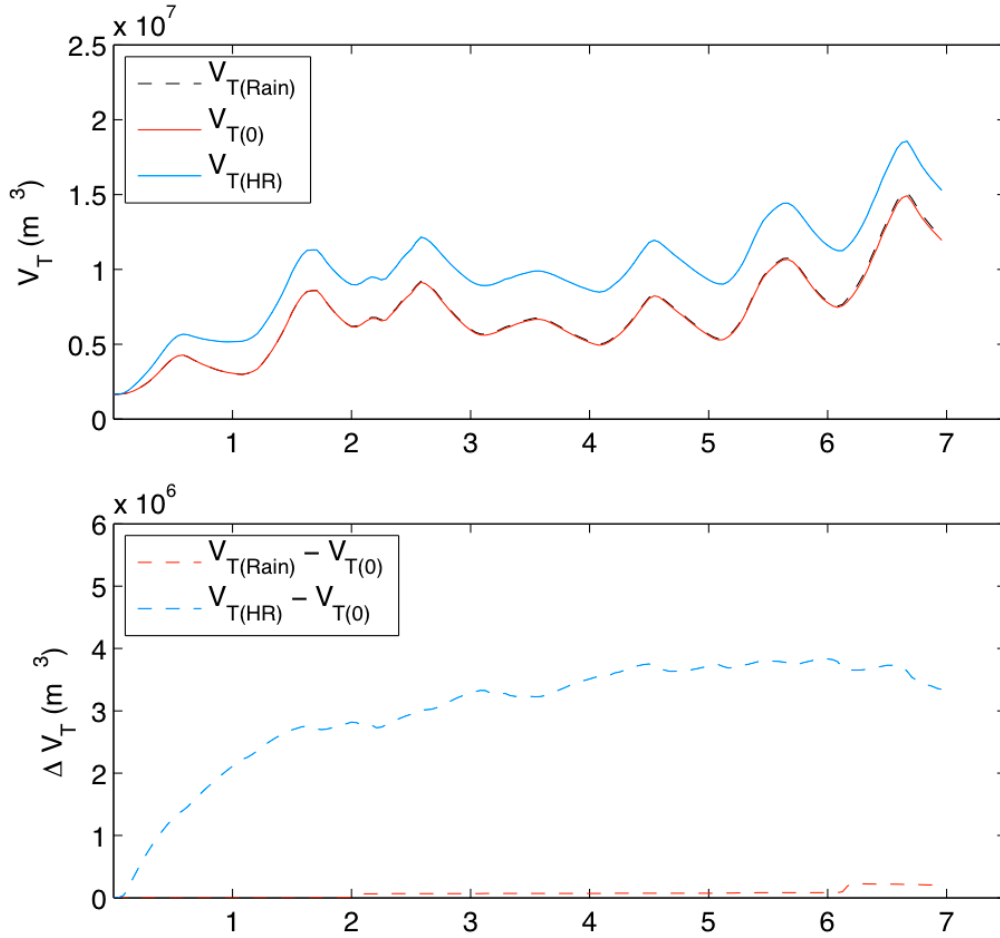


Figure A.13: Rainfall comparisons of total water volume for the seven days of rainfall simulations in Scenario 5 (0 = no rainfall), Scenario 6 (Rain = baseline rainfall) and Scenario 8 (HR = heavy rainfall). Total Volume (V_T) evolution in upper panel; difference between scenarios ΔV_T in lower panel.

These scenarios demonstrate that the NDHM represents the collection of sheet flow from dry-land runoff into stream flow, which is a computational challenge for hydrodynamic models. Rainfall in the dry uplands of the Nueces Delta is channelized into streams and rivulets as it flows down to join the flooded marsh (Figure A.14). Because the cutoff depth for defining an inundated grid cell was 2 cm (see appendices of Ryan and Hodges 2011), the A_i computation does not represent areas temporarily wetted by the rain, but reflects the collection of rainfall into streams and rivulets in the uplands, as well as increased flooded area in the marsh. A portion of the rainfall onto dry landscape is absorbed through infiltration (appendices of Ryan and Hodges 2011), so the baseline Rain Scenario in Figure A.14 shows negligible contributions in the uplands that is above the depth cutoff for computing A_i . In contrast, the Heavy Rain Scenario shows significant ponding and stream formation deeper than 2 cm, which contributes to calculated A_i .

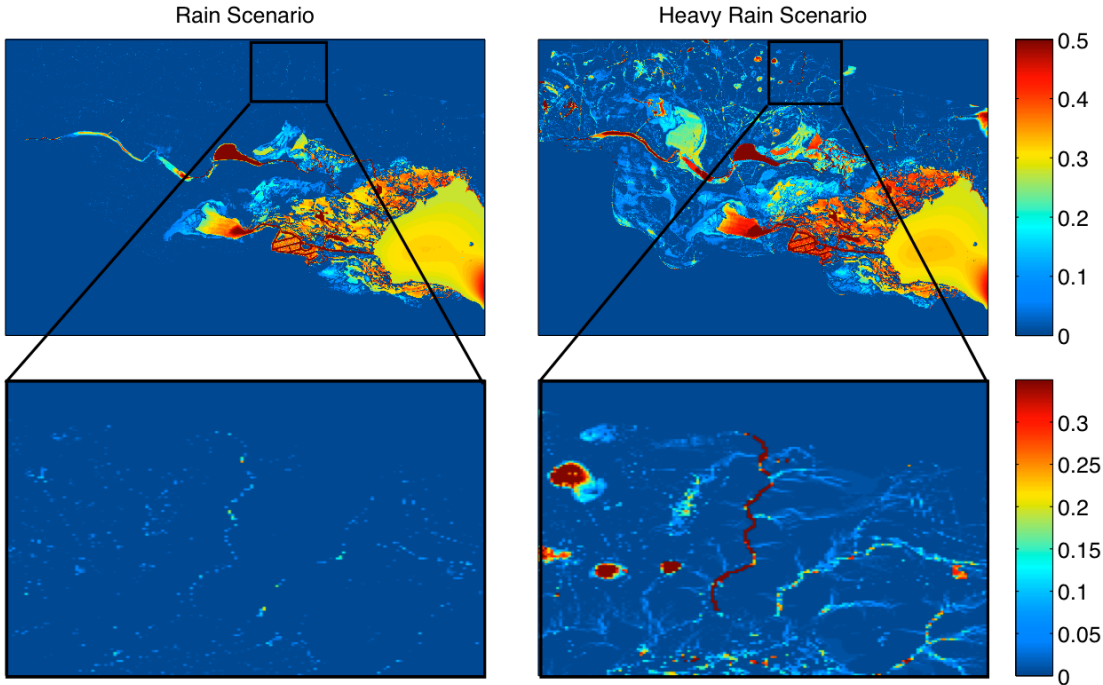


Figure A.14: Modeled water depth during a rainstorm for the baseline Rain Scenario (Scenario 6) and the Heavy Rain Scenario (Scenario 7).

A.3.5 Model response to wind

Simulations 8 through 10 (q.v. Table A.4) use zero wind speed (No Wind), the observed wind speed (Normal Wind), and twice the observed wind speed (2x Wind), respectively. Observations of the Nueces Delta (J. Tunnell, pers. comm.) indicate that steady winds from the south-southeast tend to push water further up into the delta, an effect that the NDHM must be able to capture. Modeling wind-driven flows over shallow marshland is a computational challenge (see §A.5.2). A comparison of the different wind scenarios in Figure A.15 and A.16 indicates the model is able represent wind-driven flows into the upper Nueces Delta. In Figure A.15, both the Normal Wind scenario and the stronger 2x Wind scenario show increased depths through both the lower and upper marsh as compared to the No Wind scenario. This result is echoed in Figure A.16, which shows the total volume of water in the delta after 7 days of simulation is 12% greater for the Normal Wind scenario and 49% greater for the 2x Wind scenario compared to the No Wind scenario.

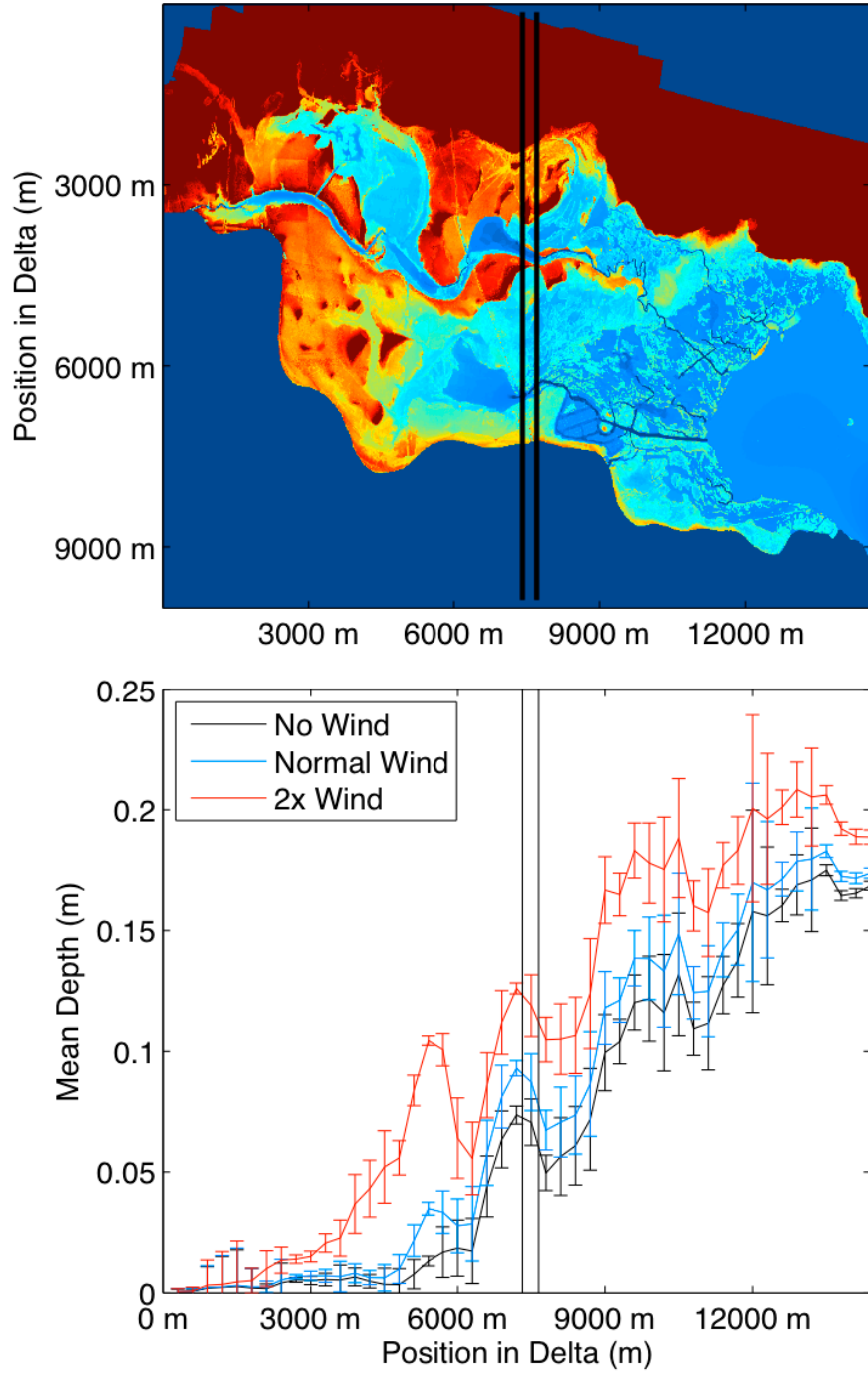


Figure A.15: Wind speed effects on depth from positions upstream in delta to Nueces Bay. Mean depth (μ_{300D}) with error bars of one standard deviation (σ_{300D}) for north-south cross-delta slices (see §A.2.4) after 7 days of simulation for Scenario 8 – No Wind, Scenario 9 – Normal Wind (baseline), and Scenario 10 – Twice the observed wind speed.

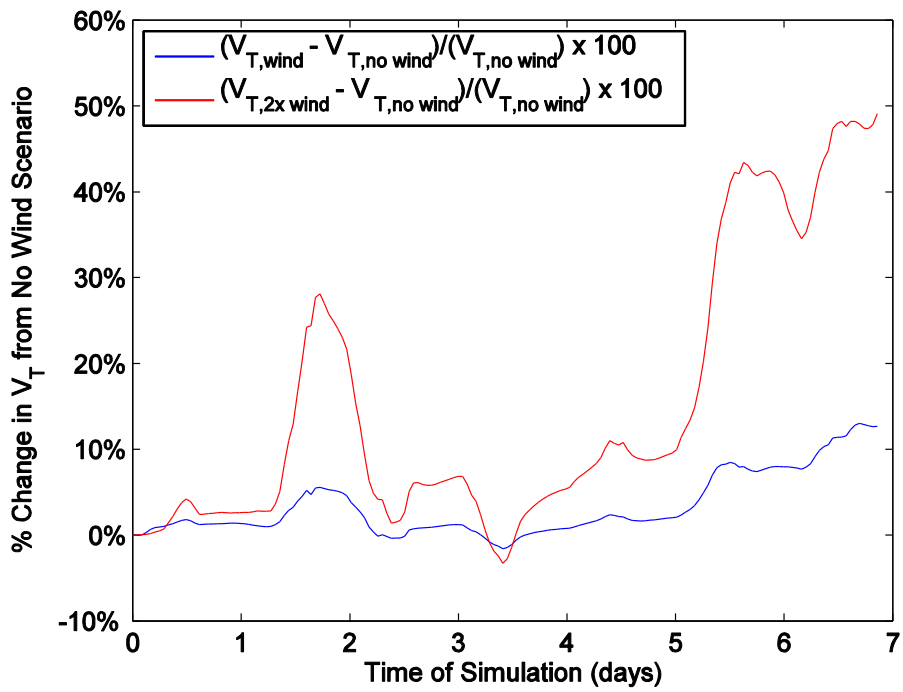


Figure A.16: Total water volume (V_T) change caused by wind forcing for Scenario 9 (Normal Wind) and Scenario 10 (2x Wind) compared to Scenario 8 (No Wind)

A.3.6 Model response to surface roughness

Surface roughness affects the flow rate of water through the delta. Higher surface roughness values should result in slower water motion and should damp tidal oscillations, particularly in the upper Nueces Delta. The evolution of total water volume (V_T) over a seven-day simulation, shown in Figure A.17, indicates that increasing roughness does result in damping tidal oscillation and reducing fluxes through the delta. Comparing these results with Figure A.11 (q.v.), a logical conclusion is that the model's exaggerated tidal oscillations at the NUDE2 observational station is likely caused by surface roughness values that are set too low. Correctly setting roughness values is a challenge for future calibration efforts (§A.5.2).

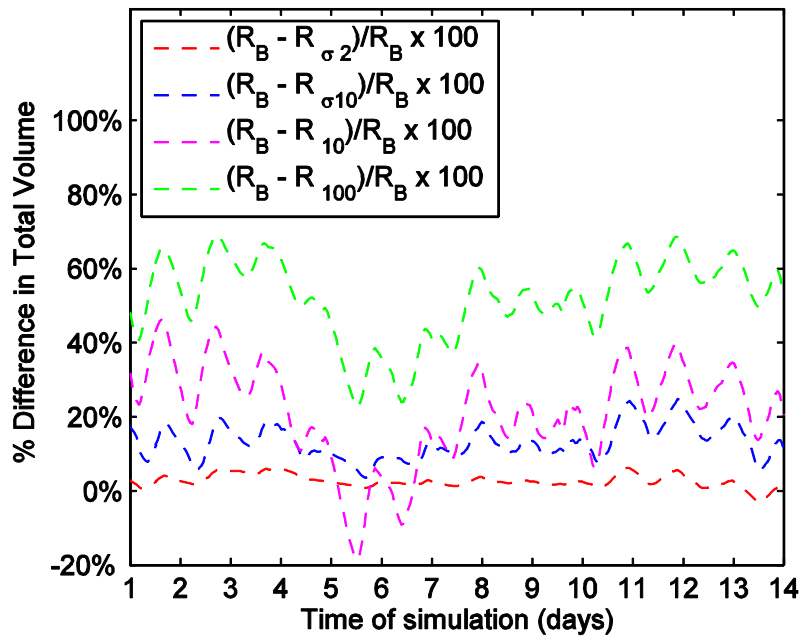
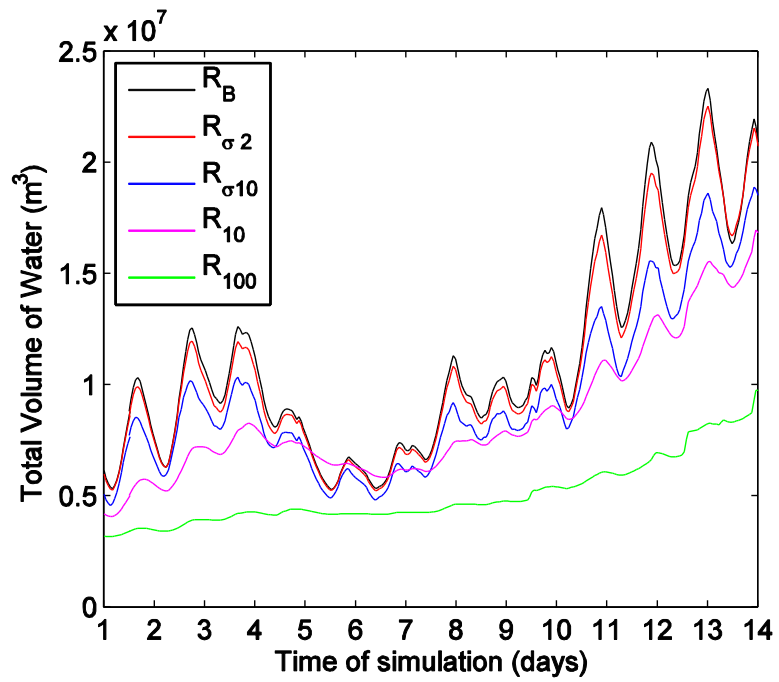


Figure A.17: Effect of surface roughness on total water volume (V_T) for Scenarios 13 through 17 (see Table A.2 for nomenclature)

A.3.7 Model response to freshwater pumping

Scenarios 1-4 are used to evaluate the model's response to freshwater pumping from the Rincon Diversion Pipeline (q.v. Table A.4). The simulations begin from April 14, 2008 using all baseline conditions with the exception of the pumping flow rates. A tracer was used in the model to track the time-space evolution of water that enters the delta from the pipeline. The tracer concentration in any model grid cell reflects the fraction of that grid cell containing pumped water.

In Figure A.10, the total volume of freshwater in the delta is graphed for the pumping scenarios, indicating that the model performs as expected with increases in freshwater volume proportional to the increases in the pump flow. The volume of brackish water, Figure A.19, shows fairly similar proportionality in the first three days; however a sharp reduction in brackish water volume for the low flow (1/3 pump capacity) scenario occurs midway through day 3, followed by a much slower increase in brackish water volume. Further analysis is necessary to understand these phenomena, but initial review of simulations indicates that the lower flow rate is less successful in pushing fresh water out of the Rincon Bayou.

For further insight, Figure A.20 shows the computed pumped water inundated area (A_{pi}) of eq. B.2 for Scenario 3 using a range of cutoff values to define the significant fraction of pumped water in a grid cell. The results show a transition in computed A_{pi} where the cutoff changes from 0.4 and 0.5, indicating that the cutoff may dramatically affect the pumped water inundated area computation. Arguably, either 40% or 50% of the water in a model grid cell being pumped water would seem to be a reasonable definition of significant, but they result in quantitatively different computations. Because the higher cutoff value may understate A_{pi} , we use 0.4 as the cutoff for the analyses below.

Figure A.21 shows the pumped water inundated area for the pumping scenarios. Similar to Figure A.19, these graphs indicate that the relationship between the pumped water area inundated and the pumping rate may not be linear. With 1/3 the flow rate, the inundated area is roughly 10% of the area inundated by the full pump flow rate. In contrast, 2/3 of the pump flow rate provides roughly 80% of the same area. The sharp feature midway through day 3 in the 1/3 flow scenario is similar to that observed in Figure A.19.

Further studies will be necessary to analyze how the inundated area changes with 2 and 3 pumps operating. However, caution must be used in considering with any of these results until the model has been calibrated and validated.

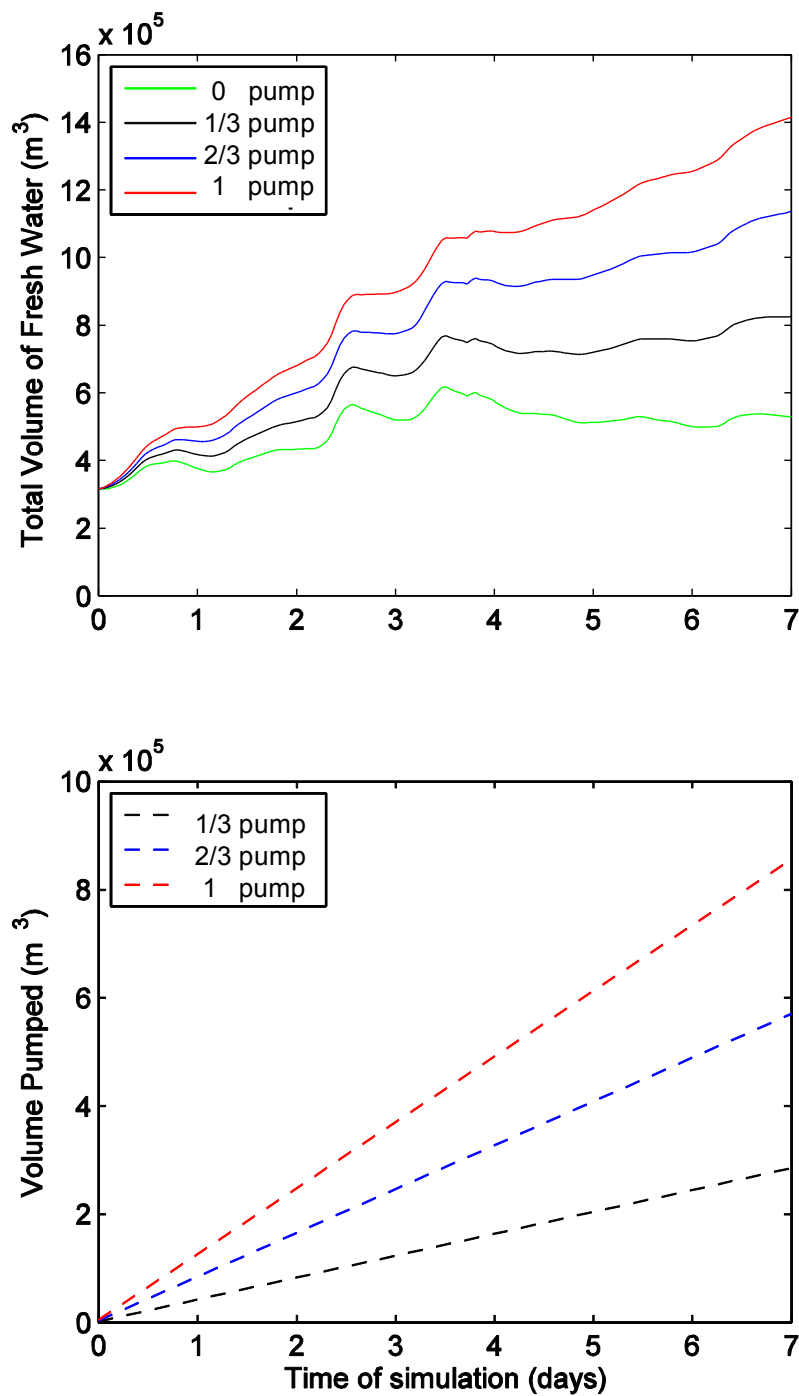


Figure A.18: Fresh water volume (upper frame) and total volume pumped (lower frame) for Scenarios 1 (0 pump), 2 (1/3 pump), 3 (2/3 pump) and 4 (1 pump).

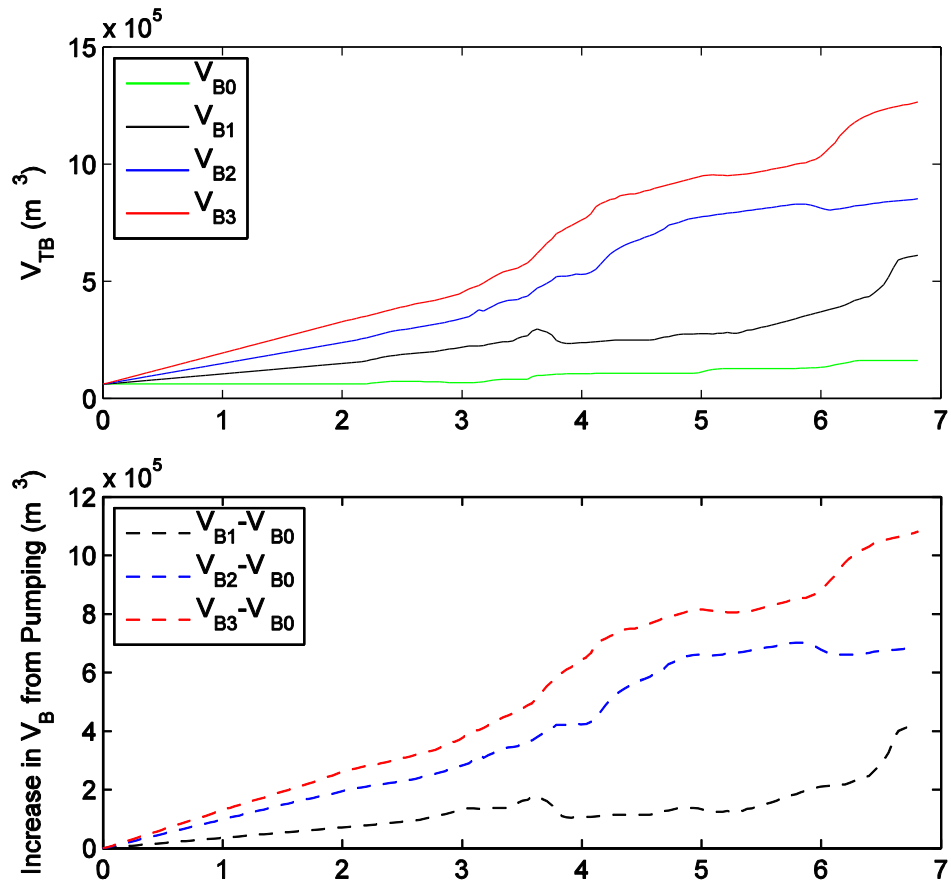


Figure A.19: Brackish water volume (upper frame), difference between brackish water volume in pumping scenarios and baseline (lower frame). B0 = Scenario 1 (0 pump), B1 = Scenario 2 (1/3 pump), B2 = Scenario 3 (2/3 pump) and B3 = Scenario 4 (1 pump).

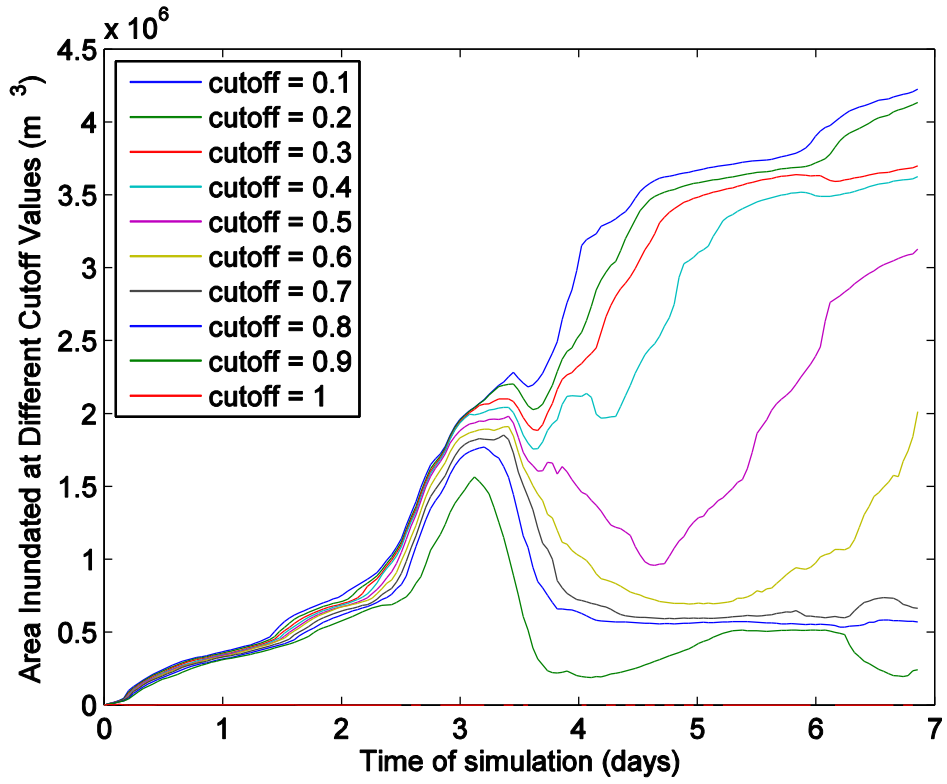


Figure A.20: Pumped water inundated area (A_{pi}) for Scenario 3 over seven days with varying cutoffs for minimum fraction of pumped water in a cell.

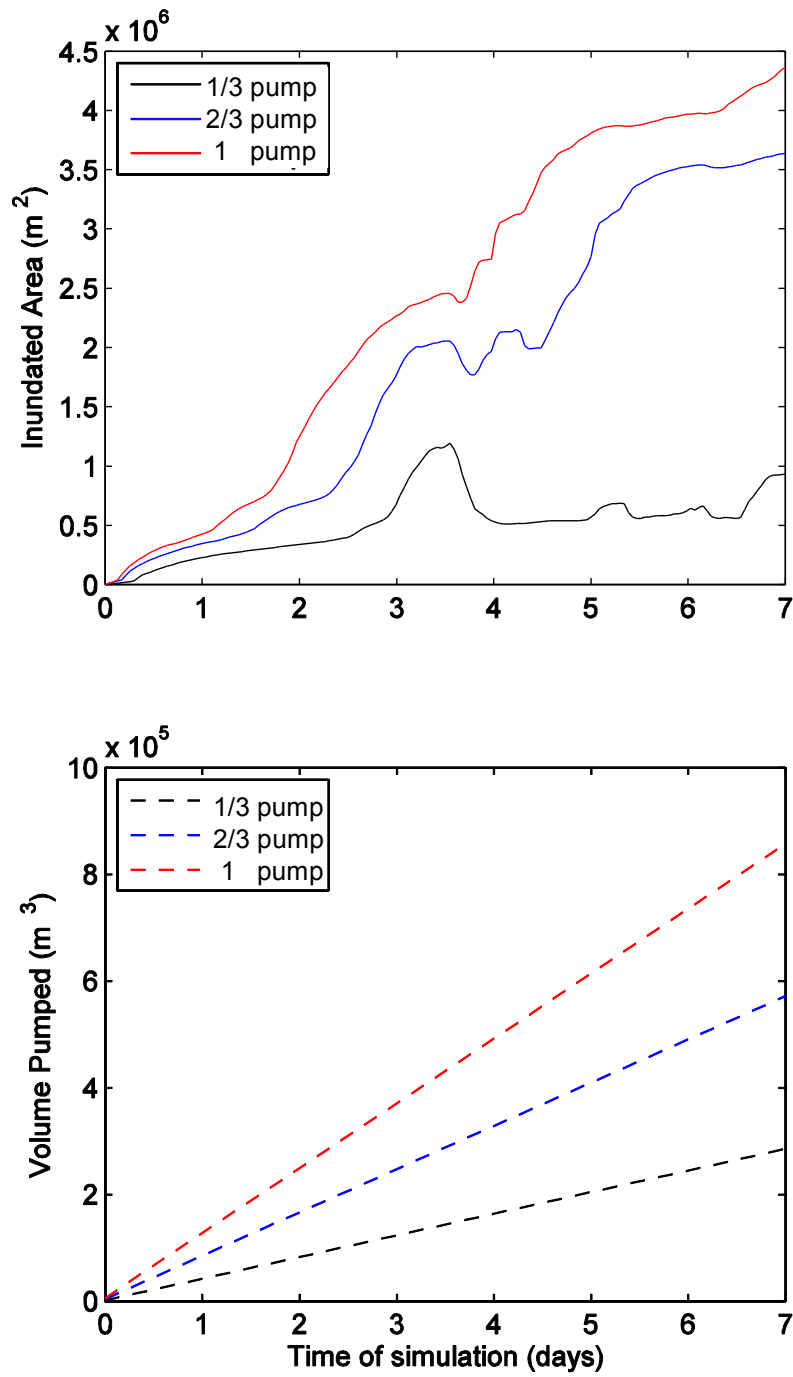


Figure A.21: Pumped water inundated area (upper frame) and total volume pumped (lower frame) for Scenarios 2 (1/3 pump), 3 (2/3 pump) and 4 (1 pump).

A.4 Requirements for Calibration and Validation of NDHM

A.4.1 Overview

The computer code for the Nueces Delta Hydrodynamic Model (NDHM) being developed under CCBEP Nueces Delta Project 1001 was completed on schedule by August 31, 2011. However, the available field data from the existing monitoring systems is inadequate to calibrate and validate the model. There are three principal deficiencies:

1. Insufficient data on salinity and water surface elevation throughout the delta under a variety of flow/tidal/wind conditions,
2. Need for new data regarding flow/velocity conditions through key choke points in the system,
3. Need for new data regarding wind effects over shallow depths.

Deficiency 1 requires emplacement of new Conductivity-Temperature-Depth (CTD) sensors and surveying existing sensors against the NAVD88 vertical datum. Approximately one year of data at 15 minute time intervals is needed with 14 or 15 new sensors. This work would be best conducted by an organization such as the Conrad Blucher Institute at Texas A&M Corpus Christi.

Deficiencies 2 and 3 require short-term field projects that could be conducted by Hodges and graduate students from UT Austin using Vectrino Acoustic Doppler Velocity (ADV) instruments that Hodges has available. These projects would each require 3 or 4 emplacements of equipment for 2 or 3 days each. Detailed proposals for these projects can be developed by Hodges, if requested by USACE or CCBEP. A brief discussion of these deficiencies will be found in section 3 of this report.

The remainder of this report focuses on the sensor network required to provide the necessary salinity and surface water elevation data to calibrate and validate the model.

A.4.2 Sensors for salinity and water surface elevation

Calibrating and validating the NDHM requires measurements of salinity and water surface elevation throughout the delta. Because the delta is a wide network of channels, we need sufficient data to be confident that the transport paths provided by the model are close to the paths in the real system. The timing and magnitude of changes in water surface elevation will enable us adjust the bottom drag coefficients to best approximate the hydrodynamics. The salinity provides a second data set that allows us to examine the effective transport time and mixing.

A.4.3 Sensor requirements

At a minimum all sensors must record conductivity and depth. So that conductivity can be readily converted to salinity and for future use in thermal modeling, it is recommended that CTD (conductivity-temperature-depth) sensors be used at all locations. Each CTD should be deployed, maintained and downloaded routinely for an entire year. The sensors do not require real-time downloading, although this capability might be useful if

the costs for routine data retrieval are too high. All sensors elevations must be surveyed into place with reference to the NAVD88 datum.

A.4.4 Existing sensors

The existing sensors in the delta (Figure A.22) are not referenced to the NAVD88 datum. These sensors were principally installed for tracking salinity and have not been maintained with consistent reference to the vertical datum. As such, they cannot be for calibration/validation until they are surveyed.



Figure A.22. Existing sensor locations requiring NAVD88 reference. (Google Earth)

The existing sensors shown in Figure A.22 provide data along a single path from the Upper Rincon Bayou through to Nueces Bay. Getting these sensors referenced to the NAVD88 datum is necessary, but not sufficient for calibration/validation of the model. To understand why this sensor network is inadequate, we consider what happens if the freshwater inflow from the Rincon Diversion Pipeline is modeled as reaching NuDe1 at the correct time, but is slow in arriving at NuDe2. From the above sensors we cannot determine if the error is caused by the drag coefficients used for flow through the narrow channel east of NuDe1, or in the narrow channel southwest of NuDe2, or in the wind forcing of water into West Lake. Because no sensors are located across the width of the delta, we cannot determine whether the model is correctly representing cross-delta tidal fluxes or wind-driven flows into shallow regions.

A.4.5 Proposed sensor network

Overview

The data set for calibration and validation of salinity and water surface elevation would add at least 14 new sensors locations to the existing 4, in a pattern shown in Figure A.23. This wider network is necessary to obtain an understanding of tidal/salinity propagation through the lower delta and the freshwater fluxes through the Rincon Bayou. The sensor

network is designed so that many sensors serve multiple purposes. A 15th sensor may be necessary for wind forcing in West Lake.

Detailed explanations and justifications of the sensor arrangement are provided in the following sections.



Figure A.23. Overview of proposed sensor network for calibration and validation. CTD01 through CTD14 are new Conductivity-Temperature-Depth sensors. NuDe1, NuDe2, NuDe3 and SALT08 are existing sensors. (Google Earth)

Rincon Bayou sensors

Figure A.24 provides a detailed view of sensors proposed through the Rincon Bayou. From CTD01 through CTD07, these provide data necessary for calibrating the downstream timing of freshwater fluxes from the Rincon Diversion Pipeline and the mixing with salt water. The combinations of NuDe1/CTD005 and CTD06/NuDe2 provide critical information on how the flow moves through two choke points.



Figure A.24. Sensor network for Rincon Bayou. (Google Earth)

Rincon Overflow sensors

Sensors for the Rincon Overflow are shown in Figure A.25. CTD02 provides the input conditions to the overflow, CTD03 provides the conditions just upstream of the outflow, and CTD04 provides the depth in West Lake, which may be influenced both by the overflow and by wind forcing from the Rincon Bayou. If a sensor is required in the main basin of West Lake, then CTD04 may be moved closer to CTD03.



Figure A.25. Sensor Network for Rincon Overflow. (Google Earth)

West Lake wind-forced inundation

Sensors CTD04, 05 and 06 in Figure A.26 provide data on the propagation of water into the West Lake region from the Rincon Bayou through wind forcing. Some further discussion/analysis is required to determine if another sensor is needed in the main basin of West Lake between CTD04 and 05 to better capture wind-forced water movement.



Figure A.26. West Lake sensors to capture wind-forced inundation (Google Earth)

Main channel sensors in lower delta

The main channel from the Rincon Bayou into the Nueces Delta below the railroad requires 5 sensors (Figure A.27) to track the timing of tidal fluxes and mixing with freshwater.

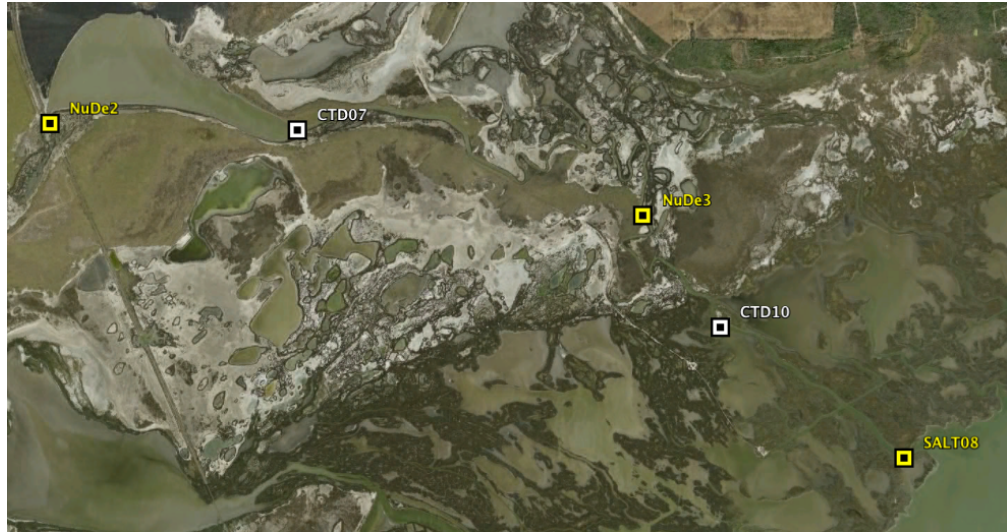


Figure A.27. Sensor network for calibration of freshwater/tidal exchanges in the main channel of the lower delta. (Google Earth)

Offline fluxes north of the main channel

North of the main channel in the lower delta is a region of convoluted narrow channels where tidal water may be stored. The fluxes into and out of this region are of unknown importance and have not been previously studied. Sensor CTD08 (Figure A.28) is included so that in concert with CTD07 and NuDe3 (on the main channel), we can evaluate the ability of the model to move water through this region with tidal and wind fluxes.



Figure A.28. Sensors to evaluate fluxes north of main channel. (Google Earth)

Tidal conditions across lower delta

Existing sensors do not provide any means of evaluating how the fluxes through the main channel are related to tidal intrusion into the marshes of the lower delta. Sensors CTD09, CTD10, CTD11 and CTD14 will provide this information (Figure A.29).



Figure A.29. Tidal forcing through lower delta. (Google Earth)

Fluxes into South Lake

Presently, we have no data on the fluxes into or out of South Lake. CTD12, CTD13, and CTD14 will provide data to calibrate the fluxes through this region (Figure A.30)



Figure A.30. CTD locations for channel leading to South Lake (Google Earth)

A.4.6 Summary

Although the model can be calibrated and validated with the sensors proposed above, there will be two key aspects of the model that will be open to criticism (these are Deficiencies 2 and 3 listed in section A.4.1 and discussed below).

Regarding Deficiency 1 - *velocity data at key choke points*: The model uses a 15 x 15 m grid, so the representation of several key choke points that are narrower than 15 m has been made with the best professional judgment. With the calibration data, we can approximate the flow through these choke points; however, our understanding of how best to model these subgrid-scale features is relatively poor, and the modeled representation is likely to be a key limitation on the model accuracy. That is, the model will be calibrated to capture the correct flux through the choke points at the calibrated conditions, but our confidence in the model's performance outside the calibrated conditions will be limited. Thus, short-term field projects to collect velocity and topographical data at several choke points would be valuable and provide a better mechanistic model of the flow at these key places.

Regarding Deficiency 2 - *wind-forcing of shallow water*: the conditions in the Nueces Delta, with strong wind forcing over water depths less than a foot, have not been studied by any research team. The NDHM started with the wind model used for deeper systems, but this proved to significantly overestimate the wind-driven fluxes. The model used in NDHM provides a means of damping the wind momentum transfer to the water. However, we need a study of the water velocities in West Lake to determine how to correctly parameterize the model.

The Nueces Delta Hydrodynamic Model requires additional field data for calibration and validation before it can be used as a practical engineering and management tool. Collecting a year of data from the sensor network proposed above would provide the minimum necessary to calibrate and validate the model. This data collection is the critical path for moving forward.

A.5 Conclusions from hydrodynamics

A.5.1 Findings

The preliminary model validation was only qualitative; however, results indicate the model approximates the overall observed trends for the available data during the time period tested. In this report, the model's response to changes in wind, rainfall, and roughness on inundated area, total volume of water in the system, and mean depths across the delta were investigated.

Overall, the results indicate the model algorithms controlling the underlying hydrodynamics are working as expected. The model is able to capture tidal propagation from Nueces Bay up through the marsh and freshwater fluxes down the Rincon Bayou. Mixing conditions where salt and fresh water meet show the typical turbulent features expected in a 2D flow. The railroad dike is seen to block water movement except through trestles. The wind model creates upwind flows that push water into the West

Lake area. The rainfall and runoff algorithms can handle heavy rainstorms that create rivulets gathering into streams in the uplands. The model shows nonlinear behaviors in inundation area as the pump flow rate is changed, which is expected if higher flow rates allow water to move further out of the Rincon Bayou.

Specific findings of the present model must be used with caution, and are subject to revision with further studies and analyses. Based on water depth, the model appears to need a week of spin-up time from starting conditions. The model for surface roughness has a significant impact on the timing and amplitude of tidal propagation through the lower marsh; baseline values derived using standard methodology appear to underestimate the topographic roughness effects thereby allowing a greater tidal range in the marsh than observed. Wind forcing appears to create the fluxes into the West Lake region that have been observed (J. Tunnell, pers. comm.), but the relationship between the wind forcing and transport volume cannot presently be validated.

A.5.2 Recommendations for future work

Calibration and validation of the model is incomplete, so further work is essential to improve our understanding of the model's capabilities and limitations. However, the available field data from the existing monitoring systems is inadequate to calibrate and validate the model. There are three principal projects required:

Project 1: Collect new data on salinity and water surface elevation throughout the delta under a variety of flow/tidal/wind conditions,

Project 2: Collect new data required for flow/velocity conditions through key choke points in the system,

Project 3: Collect new data regarding wind effects over shallow depths.

Project 1 requires emplacement of new Conductivity-Temperature-Depth (CTD) sensors and surveying existing sensors against the NAVD88 vertical datum. Approximately one year of data at 15-minute time intervals is needed with 14 or 15 new sensors distributed throughout the delta. Projects 2 and 3 require short-term field studies that could be conducted by using Acoustic Doppler Velocimeter (ADV) instruments. These projects would each require 3 or 4 emplacements of equipment for 2 or 3 days each.

A key focus for future work should be in representing subgrid-scale effects that cannot be captured at the 15 x 15 m grid scale. In particular, there are several choke points narrower than 15 m in the Rincon Bayou that are likely to play a key role in controlling the flow. To calibrate these choke points over a wide range of conditions we need the data from Project 2 above. Baseline calibration can be accomplished using data from Project 1; however, our understanding of how best to model these subgrid-scale features is relatively poor so the modeled representation is likely to be a key limitation on the model accuracy. That is, using data from Project 1, the model would be calibrated to capture the correct flux through the choke points at the calibrated conditions, but our confidence in the model's performance outside the calibrated conditions would be limited. Project 2 collects velocity and topographical data at several choke points,

providing the basis for a better mechanistic model of the flow at these key places. The result would be a model with a wider range of validity and less uncertainty.

The conditions in the Nueces Delta, with strong wind forcing over water depths less than 20 cm, have not been studied by any research team. The NDHM started with the wind model used for deeper systems, but this proved to significantly overestimate the wind-driven fluxes. The model used in NDHM provides a means of damping the wind momentum transfer to the water. However, we need a study of the water velocities in West Lake to determine how to correctly parameterize the model. It appears likely that the wind forcing from the Rincon Bayou into West Lake delivers more water into that system than the Rincon Overflow, so we need a better understanding of the wind-driven fluxes to gain a better understanding of the inundation of this large area.

For simplicity and minimizing computational requirements, the present NDHM excludes the tidal segment of the Nueces River. Future work should add this segment to the model and test the effects of overbanking from the river into the delta.

Future studies should develop more sophisticated approaches to analyzing freshwater inundated area. The channelized nature of the Nueces Delta and distribution of freshwater near the channels affects the vegetation species composition. Two of the principal species in the delta, *Borrichia frutescens* and *Salicornia virginica*, have very different conditions for ideal growth. *B. frutescens* is not hindered by flooding and has a positive growth rate only under low salinity conditions. In contrast, *S. virginica* is unaffected by increased salinity and has inhibited growth from waterlogged soil (Rasser 2009). In the present study, we examined inundated area as a one-dimensional metric, but the model data could be readily analyzed to provide species-specific values. Such an approach might improve our understanding of the impact of different pumping scenarios.

Future work might include developing a management tool for operating the Rincon Diversion Pipeline. This effort might incorporate output from or automatic operation of the hydrodynamic model to determine the most effective pumping scenario associated for existing conditions.

A.6 Literature Cited in Appendix A

- Adams, John S., and Jace Tunnell, (2010). *Rincon Bayou Salinity Monitoring Project..* Technical Report, Coastal Bend Bays & Estuaries Program. Corpus Christi.
- Alan Plummer Associates, Inc. (2007). *City of Corpus Christi Water Supply Project.* Technical Report.
- Alber, Merryl, (2002). "A Conceptual Model of Estuarine Freshwater Inflow Management." *Estuaries* 25:6B:1262-1274.
- Alexander, Heather D., and Kenneth H. Dunton, (2002). "Freshwater Inundation Effects on Emergent Vegetation of a Hypersaline Salt Marsh." *Estuaries*, 25:6B:1426-1425.
- Alexander, Heather D., and Kenneth H. Dunton, (2006). "Treated Wastewater Effluent as an Alternative Freshwater Source in a Hypersaline Salt Marsh: Impacts on Salinity,

- Inorganic Nitrogen, and Emergent Vegetation." *Journal of Coastal Research*, 22:2:377-392.
- Battjes, Jurjen A., (2006). "Developments in coastal engineering research." *Coastal Engineering*, 53:121-132.
- Bisht, Gautam, Virginia Venturini, and Shafiqul Isl. (2005). "Estimation of the net radiation using MODIS (Moderate Resolution Imaging Spectroradiometer) data for clear sky days." *Remote Sensing of Environment*, 97:52-67.
- Bureau of Reclamation. (2000a). *Concluding Report: Rincon Bayou Demonstration Project. Volume I: Executive Summary*. United States Department of the Interior, Bureau of Reclamation, Oklahoma-Texas Area Office, Austin, Texas.
- Bureau of Reclamation, (2000b). *Concluding Report: Rincon Bayou Demonstration Project. Volume II: Findings*. United States Department of the Interior, Bureau of Reclamation, Oklahoma-Texas Area Office, Austin, Texas.
- Casulli, V., and E. Cattani, (1994). "Stability, Accuracy and Efficiency of a Semi-Implicit Method for Three-Dimensional Shallow Water Flow." *Computers & Mathematics with Applications*, 27:4:99-112.
- Casulli, V., and P. Zanolli, (2002). "Semi-Implicit Numerical Modeling of Nonhydrostatic Free-Surface Flows for Environmental Problems." *Mathematical and Computer Modelling*, 36:1131-1149.
- Casulli, Vincenzo, and Ralph T. Cheng, (1992). "Semi-Implicit Finite Difference Methods for Three-Dimensional Shallow Water Flow." *International Journal for Numerical Methods in Fluids*, 15:629-648.
- Charbeneau, Randall J., and Edward R. Holley, (2001). *Backwater Effects of Bridge Piers in Subcritical Flow*. Project Summary Report, Center for Transportation Research, University of Texas at Austin.
- Chen, Changsheng, Hedong Liu, and Robert C. Beardsley, (2003). "An Unstructured Grid, Finite-Volume, Three-Dimensional, Primitive Equations Ocean Model: Application to Coastal Ocean and Estuaries." *Journal of Atmospheric and Oceanic Technology*, 20:159-186.
- Copeland, B.J., (1996). "Effects of Decreased River Flow on Estuarine Ecology." *Water Pollution Control Federation*, 38:11:1831-1839.
- Cunningham, Atlee M., (1999). *Corpus Christi Water Supply Documented History 1852-1997. Second Edition*. Texas A&M University-Corpus Christi,
- Gibeaut, J., (2003). "LiDAR: Mapping a Shoreline by Laser Light." *Geotimes*, 48:11:22-27.
- Heilman, J.L., F.A. Heinsch, D.R. Cobos, and K.J. McInnes, (2000). "Energy Balance of a High Marsh on the Texas Gulf Coast: Effect of Water Availability." *Journal of Geophysical Research*, 105:D17:22371-22377.

- Hodges, Ben R., (2004). "Accuracy Order of Crank–Nicolson Discretization for Hydrostatic Free-Surface Flow." *Journal of Engineering Mechanics-ASCE*, 130:8:904-910.
- Hodges, Ben R., Bernard Laval, and Bridget M. Wadzuk, (2006). "Numerical error assessment and a temporal horizon for internal waves in a hydrostatic model." *Ocean Modelling*, 13:44-64.
- Hodges, Ben R., and Francisco J. Rueda (2008). "Semi-implicit two-level predictor-corrector methods for non-linearly coupled, hydrostatic, barotropic/baroclinic flows." *International Journal of Computational Fluid Dynamics*, 22:9:593-607.
- Hossain, AKMA, Yafei Jia, and Xiabo Chao, (2009). "Estimation of Manning's Roughness Coefficient Distribution for Hydrodynamic Model Using Remotely Sensed Land Cover Features." *2009 17th International Conference on Geoinformatics*, George Mason University. pp. 635-638.
- Irlbeck, M.J., and G.H. Ward, (2000). "Analysis of the historic flow regime of the Nueces River into the upper Nueces Delta, and of the potential restoration value of the Rincon Bayou Demonstration Project." In *Concluding Report: Rincon Bayou Demonstration Project, Appendix C*. (United States Department of the Interior, Bureau of Reclamation),.
- Ji, Z.-G., M.R. Morton, and J.M. Hamrick, (2001). "Wetting and Drying Simulation of Estuarine Processes." *Estuarine, Coastal and Shelf Science*, 53:683-700.
- Montagna, P.A., E.M. Hill, and B. Moulton, (2009). "Role of Science-based and Adaptive Management in Allocating Environmental Flows to the Nueces Estuary, Texas, USA." *WIT Transactions on Ecology and the Environment*, 122:559-570.
- Montagna, Paul A., Alber Merryl, Doering Peter, and Connor S. Michael, (2002). "Freshwater Inflow: Science, Policy, Management." *Estuaries*, 25:6B:1243-1245.
- Montagna, Paul A., Richard D. Kalke, and Christine Ritter, (2002). "Effect of Restored Freshwater Inflow on Macrofauna and Meiofauna in Upper Rincon Bayou, TX, USA." *Estuaries*, 25:6B:1436-1447.
- Nicolau, Brien A., John Jr. W. Tunnell, John S. Adams, and Barbara F. Ruth, (1996). "Long-Term Monitoring of Estuarine Faunal Use in the Nueces Delta Mitigation Project, Corpus Christi, Texas: 1989 Through 1995." *Annual Ecosystem Restoration Conference*. Tampa, Florida.
- Nicolau, Terri, et al. (2002). *Nueces Estuary Advisory Council Recommended Monitoring Plan For Rincon Bayou, Nueces Delta*.
- Ockerman, D.J., (2001). *Water Budget for the Nueces Estuary, Texas, May-October 1998*. Fact Sheet, U.S. Department of the Interior, U.S. Geological Survey.
- Oey, Lie-Yauw, (2006). "An OGCM with movable land-sea boundaries." *Ocean Modelling* 13:176-195.

- Palmer, Terry A., Paul A. Montagna, and Richard D. Kalke, (2002). "Downstream Effects of Restored Freshwater Inflow to Rincon Bayou, Nueces Delta, Texas, USA." *Estuariesc* 25:6B:1448-1456.
- Pulich, Warren, (2006). *Texas Coastal Bend*. USGS.
- Rasser, Michael Kevin, (2009). *The Role of Biotic and Abiotic Processes in the Zonation of Salt Marsh Plants in the Nueces River Delta, Texas*. Dissertation, The University of Texas at Austin.
- Roman, Charles T., Richard W. Garvine, and John W. Portnoy, (1995). "Hydrologic Modeling as a Predictive Basis for Ecological Restoration of Salt Marshes." *Environmental Management* 19:4:559-566.
- Rueda, F.J., E. Sanmiguel-Rojas, and B.R. Hodges, (2007). "Baroclinic stability for a family of two-level semi-implicit numerical methods for the 3D shallow water equations." *International Journal for Numerical Methods in Fluids* 54:3:237-268.
- Ryan, A.J., and B.R. Hodges (2011). *Modeling Hydrodynamic Fluxes in the Nueces River Delta*. CRWR Online Report 11-7, 92 pgs.
- Sellers, William, (1965). *Physical Climatology*. The University of Chicago Press.
- Spillman, C.M., Hamilton, D.P., Hipsey, M.R., Imberger J., (2008). "A spatially resolved model of seasonal variations in phytoplankton and clam (*Tapes philippinarum*) biomass in Barbamarco Lagoon, Italy." *Estuarine Coastal and Shelf Science*, 79:2:187-203.
- Stelling, G.S., H.W.J. Kernkamp, and M.M. Laguzzi, (1998). "Delft Flooding System: A powerful tool for inundation assessment based upon a positive flow simulation." *Hydroinformatics*. 449-456.
- Tolan, J.M., (2007). "El Nino-Southern Oscillation impacts translated to the watershed scale: Estuarine salinity patterns along the Texas Gulf Coast, 1982 to 2004." *Estuarine Coastal and Shelf Science*, 72,:1-2:247-260.
- U.S. Secretary of Commerce (2008). *National Institute of Standards and Technology Chemistry WebBook*.. <http://webbook.nist.gov/chemistry/> (accessed 2011).
- Veilleux, Vicki, (2011). *National Geodetic Survey: Frequently Asked Questions*. January. <http://www.ngs.noaa.gov/faq.shtml>.
- Ward, George H., (1997). *Processes and Trends of Circulation within the Corpus Christi Bay National Estuary Program Study Area*. Corpus Christi: Texas National Resource Conservation Commission.
- Ward, George H., Michael J. Irlbeck, and Paul A. Montagna, (2002). "Experimental River Diversion for Marsh Enhancement." *Estuaries* 25:6B:1416-1425.
- Wunderlich, Walter O. (1972). *Heat and Mass Transfer Between a Water Surface and the Atmosphere*. Laboratory Report No. 14, Tennessee Valley Authority,.
- Xia, Junqiang, Roger A. Falconer, and Binliang Lin, (2010). "Hydrodynamic impact of a tidal barrage in the Severn Estuary, UK." *Renewable Energy*, 35:1455–1468.

- Yang, Zhaoqing, and Tarang Khangaonkar, (2009). "Modeling tidal circulation and stratification in Skagit River estuary using an unstructured grid ocean model." *Ocean Modelling*, 28:34-49.
- Zhang, Yinglong, Antonio M. Baptista, and Edward P. III Myers, (2004). "A cross-scale model for 3D baroclinic circulation in estuary-plume-shelf systems: I. Formulation and skill assessment." *Continental Shelf Research*, 24:2187-2214.
- Zheng, Lianyuan, Changsheng Chen, and Frank Y. Zhang, (2004). "Development of water quality model in the Satilla River Estuary, Georgia." *Ecological Modelling*, 178:457-482.

This page intentionally blank for two-sided printing.

B Appendix: Field Research

B.1 Introduction

This research was conducted on six sampling stations which were established on an estuarine gradient parallel to the Rincon Bayou in the Nueces River Delta (Fig. B.1). High marsh stations 501 and 467 were located above the Rincon overflow channel and between the Nueces overflow channel and Rincon overflow channel, respectively. Middle marsh stations 463 and 451 were positioned approximately 5.7 and 2.5 km from Nueces Bay, respectively. Low marsh stations 450 and 270 were located less than 0.5 and 1.5 km from the Bay, respectively. High marsh stations were located on the freshwater end of the estuarine gradient while low marsh stations close to Nueces Bay were located were located on the seawater end of the estuarine gradient. Middle marsh stations were influenced both by freshwater inflows via the Nueces Overflow Channel and by seawater from Nueces Bay.

The dominant marsh plants in the Nueces River Delta include *Borrichia frutescens*, *Salicornia virginica*, *Batis maritima*, *Spartina spartinae*, *Spartina alterniflora*, *Distichlis spicata*, *Monarthochloe littoralis* and *Lycium carolinianum*. However, *Suaeda linearis* and *Salicornia bigelovii* were observed sporadically. The three most common species, *Borrichia frutescens*, *Salicornia virginica* and *Batis maritima*, account for over 50% of total vegetation cover (Forbes and Dunton 2006; Rasser 2009). *B. frutescens* and *S. virginica* were usually observed growing closer to tidal creeks whereas *B. maritima* was most often found further from tidal creeks. These species often occurred in distinct monospecific zones.

B.2 Porewater Salinity Dynamics

A continuous record of porewater salinity was obtained using remotely deployed conductivity sensors (Model DST CTD, Star-Oddi Ltd., Reykjavik, Iceland). These sensors were buried at a depth of 20 cm below the sediment surface in creekbank and interior marsh areas at two sites (Site 450, Site 463, see Figure B.1). A depth of 20 cm was chosen because this approximates the rooting depth of the two most common emergent vascular plants in the Nueces River Delta, *Borrichia frustescens* and *Salicornia virginica* (Dunton et al., 2001). The accuracy of the conductivity sensors was validated by comparison against porewater samples from sediment cores collected in the field. Porewater was extracted from these cores by centrifugation and measured with a handheld refractometer (Reichert Scientific Instruments, Buffalo, NY).

In order to supplement our continuous monitoring effort, we investigated the relative influence of various freshwater sources on long term records of porewater salinity (Table B.1). Between 2001 and 2010 approximately 220 soil cores measuring 2.5 cm in diameter and 10 cm in length were collected quarterly from 5 sites in the Nueces River Delta (Figure B.1). For this analysis, measurements in creekbank and interior marsh areas were pooled in order to evaluate the general importance of various freshwater sources.

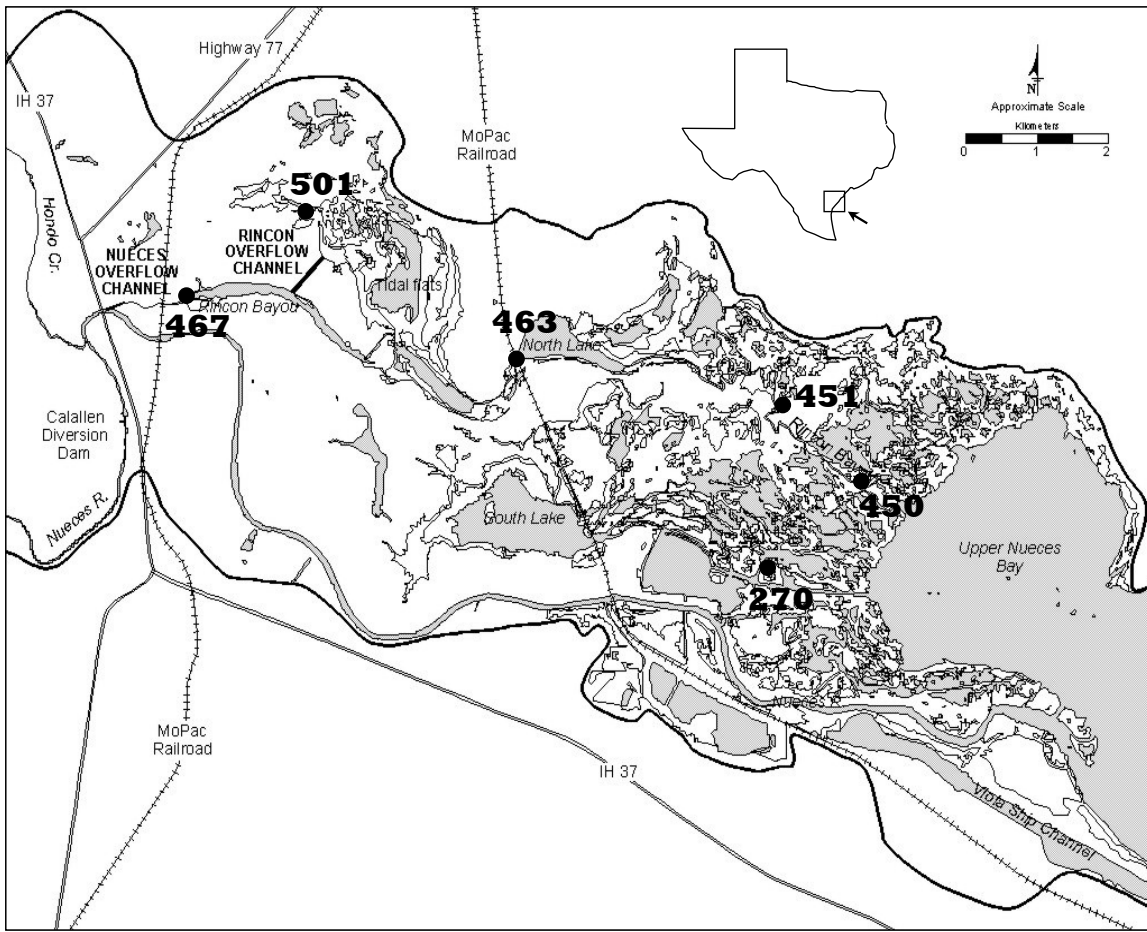


Figure B.1. Location of six sampling stations (501, 467, 463, 451, 450 and 270) in the Nueces River Delta, located in the western Gulf of Mexico, Texas, U.S.A.

Continuous porewater salinity records were compared against multiple environmental variables including precipitation, freshwater inflow, evaporation, tidal creek salinity, and tidal creek water level. Meteorological data including precipitation, wind speed, air temperature, and relative humidity was obtained from the Nueces Delta Weather Station located approximately 10 km from site 450 and 5 km from site 463. Tidal creek salinity information was obtained from stations NUDE2 and Salt08 for stations 463 and 450 respectively (available from the Division of Nearshore Research at Texas A&M – Corpus Christi¹⁴). Both tidal creek salinity stations were located within 300 m of their respective study sites. Tidal creek water level data for site 463 was obtained from station NUDE2 while data for site 450 was obtained from the Nueces Bay tide gauge (available from the National Oceanic and Atmospheric Administration¹⁵). A

¹⁴ <http://lighthouse.tamucc.edu/RinconSalinity>

¹⁵ <http://tidesandcurrents.noaa.gov>

record of freshwater inflow to the Nueces River Delta was compiled from data collected by the Rincon Bayou Channel gauge (available from the U.S. Geological Survey¹⁶).

B.3 Statistical Analysis

We assessed the general importance of various freshwater sources on porewater salinity using a correlation matrix (SigmaPlot software, Version 10.0). For this analysis, porewater salinity and tidal creek salinity data from long term monitoring (2001 – 2010) were reduced to quarterly means. Precipitation and freshwater inflow were aggregated into quarterly sums in order to facilitate comparison with salinity measurements.

The impact of precipitation events on porewater salinity was determined on the basis of inundation. The mean salinity change occurring as a result of precipitation events was evaluated for inundated and exposed sediments. Precipitation events were selected for analysis only if there was a continuous record of porewater salinity for 24 hours prior to the event. The effect of precipitation events on porewater salinity was calculated as the difference between the maximum salinity 24 hours prior to an event and the salinity minimum in following 24 hours. A 24 hour period was chosen because porewater salinities generally returned to their pre-event values by this time.

The influence of each group of precipitation events on porewater salinity (2010–2011) was investigated using a t-test (Systat v.13.0, Systat Software Inc., Richmond, CA, USA). The accuracy of model output with respect to empirically measured porewater salinity measurements was assessed using linear regressions (SigmaPlot software, Version 10.0). Significant differences were determined at $\alpha = 0.05$.

B.4 Plant Parameters

B.4.1 Photosynthesis

Gas exchange measurements ($n = 4$ per assemblage) were performed on uppermost, youngest, and fully expanded leaves using a LI-6400 portable photosynthesis system (LI-COR, Lincoln, NE, USA) with an attached conifer leaf chamber (6400-05).

Measurements were taken from 1000 to 1500, to insure saturating irradiance (usually over 1000 $\mu\text{mol photons m}^{-2} \text{s}^{-1}$). During measurements, relative humidity and air temperature in the chamber was maintained within 5% of ambient values. Carbon dioxide (CO₂) concentrations were kept constant at 400 $\mu\text{mol mol}^{-1}$ using a CO₂ injector. Gas exchange measurements were recorded only when the measurements were steady for at least 90 sec. Measured parameters included net photosynthesis (A_{area}, $\mu\text{mol CO}_2 \text{ m}^{-2} \text{ s}^{-1}$), stomatal conductance (gs, $\text{mol H}_2\text{O m}^{-2} \text{ s}^{-1}$), transpiration (E, $\text{mmol H}_2\text{O m}^{-2} \text{ s}^{-1}$), and intercellular CO₂ concentration (Ci, $\mu\text{mol CO}_2 \text{ mol}^{-1}$).

Intrinsic and instantaneous water use efficiency of leaves was calculated as the ratio of A/gs and A/E, respectively. For leaf dark respiration, the leaf chamber was shaded using a black plastic bag and dark respiration (R_{area}, $\mu\text{mol CO}_2 \text{ m}^{-2} \text{ s}^{-1}$) was recorded

¹⁶ <http://waterdata.usgs.gov/tx/nwis/dv>

when readings stabilized. Light irradiance in the chamber while covered with a black plastic bag was less than $0.1 \mu\text{mol photon m}^{-2} \text{s}^{-1}$. Relative humidity, air temperature, and CO_2 concentration in the chamber were the same when compared to net photosynthesis. The photosynthesis system was calibrated daily before measurements and the chamber was matched every 30 minutes during gas exchange measurements.

Leaves inside the chamber were collected after each measurement, photographed with a digital camera, and subsequently measured using ImageJ computer software (v. 1.44b; National Institutes of Health, Bethesda, Maryland, USA). The surface area ($2\pi rH$) of *B. maritima* and *S. virginianica* was estimated by multiplying $3.14 (\pi)$ by leaf area ($2rH$) as calculated using ImageJ software due to the leaf's cylindrical shape.

The samples collected for leaf area measurements were also used to determine leaf succulence (mg water per cm^{-2} leaf area), and specific leaf area (SLA, $\text{cm}^2 \text{g}^{-1}$). Leaf succulence was calculated as the difference between leaf fresh weight and leaf dry weight divided by leaf area. Dry weight was determined by exposing fresh leaf material to 60°C in a drying oven until achieving a constant weight. The SLA of leaf material was calculated by dividing leaf area by leaf dry mass. Net photosynthesis (Amass, $\mu\text{mol g}^{-1} \text{s}^{-1}$) and dark respiration (Rmass, $\mu\text{mol g}^{-1} \text{s}^{-1}$) of leaf on a per unit mass basis were calculated by multiplying the area-based estimates with the SLA.

B.4.2 Leaf tissue elemental composition

Leaf tissue elemental composition was investigated on a seasonal, annual, and interspecific basis at two sites (270 and 467). A total of 81 leaf samples were prepared and analyzed for tissue carbon and nitrogen content. Of these, xx contained sufficient material for tissue phosphorus analysis. Tissue carbon and nitrogen was determined using a PDZ Europa ANCA-GSL elemental analyzer (Sercon Ltd., Cheshire, UK). Phosphorus content was determined colorimetrically by acid digestion of ashed plant material following the method of Chapman and Pratt (1961).

B.5 Results and Discussion

B.5.1 Porewater Salinity Dynamics

Long term porewater salinity measurements obtained via sediment cores and pooled from both creekbank and interior marsh areas were strongly correlated ($r^2 = 0.83$, $p < 0.05$) with tidal creek salinity. Although precipitation did not appear to be directly linked to long term porewater salinity measurements (Table B.1), continuous monitoring revealed that their influence is highly dependent on water level (Figures B.2, B.3).

This may indicate that coarse temporal sampling (monthly - quarterly) is not sensitive enough to detect the daily influence of precipitation events. Water level measurements showed distinct seasonal differences (Figure B.4C). While high water levels generally occurred during spring and fall, low water levels occurred in winter and summer.

Continuous porewater salinity monitoring revealed that creekbank salinities are highly variable compared to interior marsh areas (Figure B.4A, B.4B). An extended data gap in porewater salinity measurements occurred from November 2010 to March 2011. Prior to this gap, mean porewater salinity in creekbank areas was 23.84 ± 7.68 while porewater salinity in interior marsh areas was 44.20 ± 3.42 . Missing data is attributed to a lack of tidal flooding and near complete drying of the root zone sediments. Gravimetric soil water content measurements ($n = 12$) taken during this period revealed that soils were extremely dry (< 55%). Subsequent laboratory tests ($n=3$) revealed that sensors deployed in soils of less than 42% gravimetric soil water content failed to recover porewater salinity data.

Table B.1: Simple correlation (r) relationships between freshwater sources and salinity parameters. All salinity terms represent quarterly measurements taken between 2001 and 2010 in both creekbank and interior marsh areas. Significant interactions ($\alpha = 0.05$) are denoted by an asterisk.

	Precipitation	Freshwater Inflow	Creekbank Porewater Salinity
Precipitation (mm)	-	-	-
Freshwater Inflow ($m^3 day^{-1}$)	-0.08	-	-
Creekbank			
Porewater	-0.36	-0.14	-
Salinity (‰)			
Tidal creek Salinity (‰)	-0.42*	-0.16	0.91*

Two large freshwater inflow events (July and September 2010) occurred over the course of this study, allowing us to separate the effects of precipitation and freshwater inflow on salinity. Precipitation events appeared to affect the porewater salinity of both creekbank and interior marsh areas whereas the impact of freshwater inflow events was limited to creekbank areas (Figure B.4A-B, B.4D-E). Porewater salinities remained unchanged in 2011 when there was a lack of either precipitation or freshwater inflow events. This suggests that local precipitation causes only minor short term variability (hours to days) in porewater salinity while freshwater inflow events cause critical flushing of sediments that slows or reverses the development of hypersaline marsh areas.

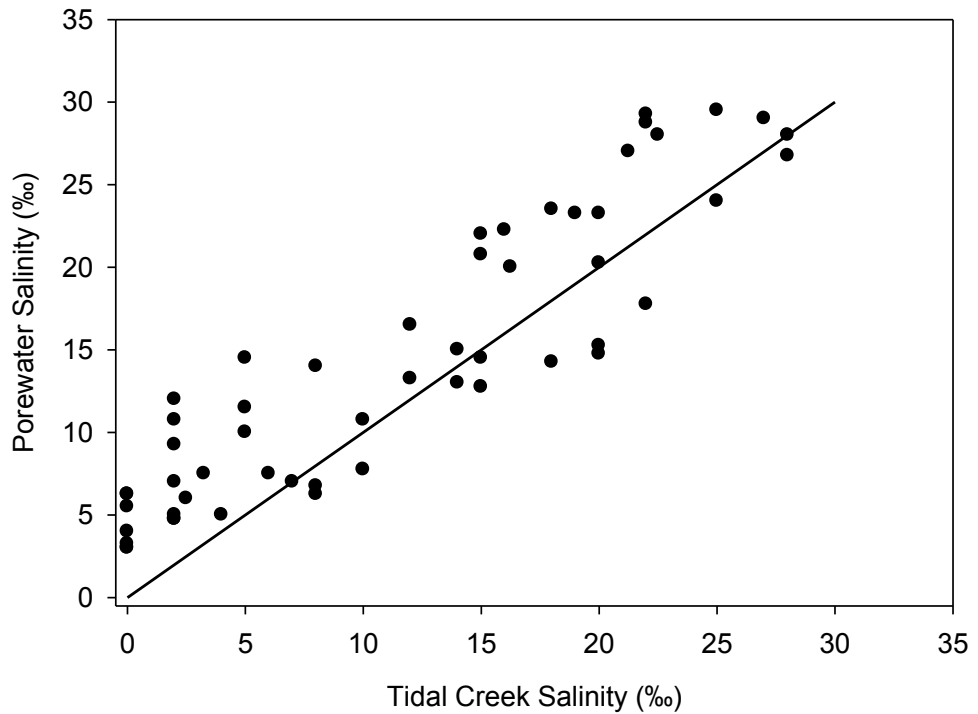


Figure B.2: Continuous measurements of tidal creek salinity, porewater salinity in creekbank areas, and their departure from a one-to-one relationship (solid line).

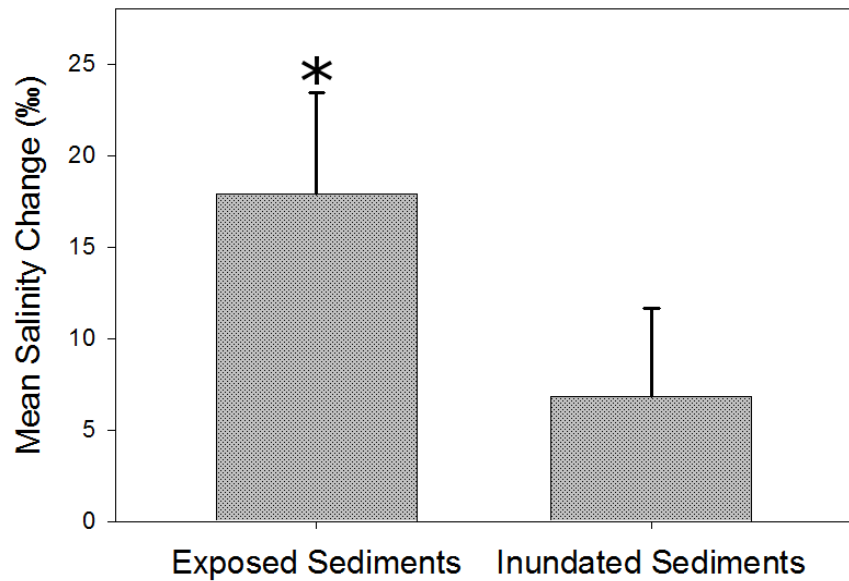


Figure B.3: Porewater salinity change in exposed and inundated sediments as a result of precipitation events. Significant ($\alpha = 0.05$) precipitation effects are denoted by an asterisk.

Differing porewater salinities in creekbank and interior marsh areas may control emergent plant distributions in the Nueces Delta (Forbes and Dunton, 2006; Rasser 2009). For example, *Spartina alterniflora*, which is only found at extremely low elevations adjacent to creekbanks, has a low tolerance for extreme variations in porewater salinity (Touchette et al., 2009). A study by Webb (1983) on Galveston Island, Texas found that porewater salinities exceeding 25‰ resulted in significant reduction in density, height, and standing biomass of *S. alterniflora*. The *S. alterniflora* root zone is generally buffered from extreme variation due to consistent inundation with tidal creek water. The root zone of *Borrichia frutescens*, in contrast, is found on elevated creekbank levees where sediments are irregularly inundated and porewater salinity is highly variable (Figure B.4). Porewater salinity dynamics in interior marsh areas, which are dominated by *Batis maritima*, are generally stable except for small short term variations (Figure B.4). Future studies should assess whether these species have differing physiological responses to variations in porewater salinity occurring at a range of temporal scales.

Another challenge in determining the ecological importance of porewater salinity fluctuations is the difficulty in accounting for fine scale vertical structure (Casey and Lasaga, 1987). This study examined porewater salinity dynamics at a relatively coarse vertical scale (20 cm). One potential disadvantage of this approach is that fine scale vertical patterns in porewater salinity are not resolved. However, our results remain useful as a first approximation of the plant community's exposure to fluctuations in porewater salinity. Unfortunately, the extent to which differences in rooting depth control plant species' distributions in the Nueces Delta is unknown (Rasser, 2009). It is likely that species with a shallow root zone such as *B. maritima* respond more strongly to small precipitation events where porewater flushing is limited to the top several centimeters of sediment while species with a deep root zone may only benefit from the large magnitude flushing events that accompany tidal creek inundation. Alternatively, species with a deep root zone may be adapted for survival at high elevations such as atop creekbank levees where deep penetrating roots are necessary to tap deeper groundwater (Bonin and Zedler, 2008). Under this scenario, increases in drought frequency would likely lead to a decrease in the abundance of deep rooted species in favor of shallow rooted stress-tolerant species (Forbes and Dunton, 2006). Future studies, resolving this fine scale structure, have the potential to predict the trajectory of future plant community assemblages as functions of climate, rooting depth, and physiological tolerance to fluctuations in porewater salinity.

The relative effects of various freshwater sources on the porewater salinity of salt marsh sediments is likely to vary among estuarine systems according to local and regional hydrography/meteorology. We conclude that, in the Nueces Delta, freshwater inflow events provide critical moderation and flushing of sediment porewaters. The importance of these events is especially apparent during drought years when the absence of freshwater inflow leads to hypersalinity and extreme soil moisture deficit (Forbes and Dunton, 2006). A substantial portion of this study encompassed a severe drought period beginning in May, 2011 that intensified following the conclusion of monitoring in July,

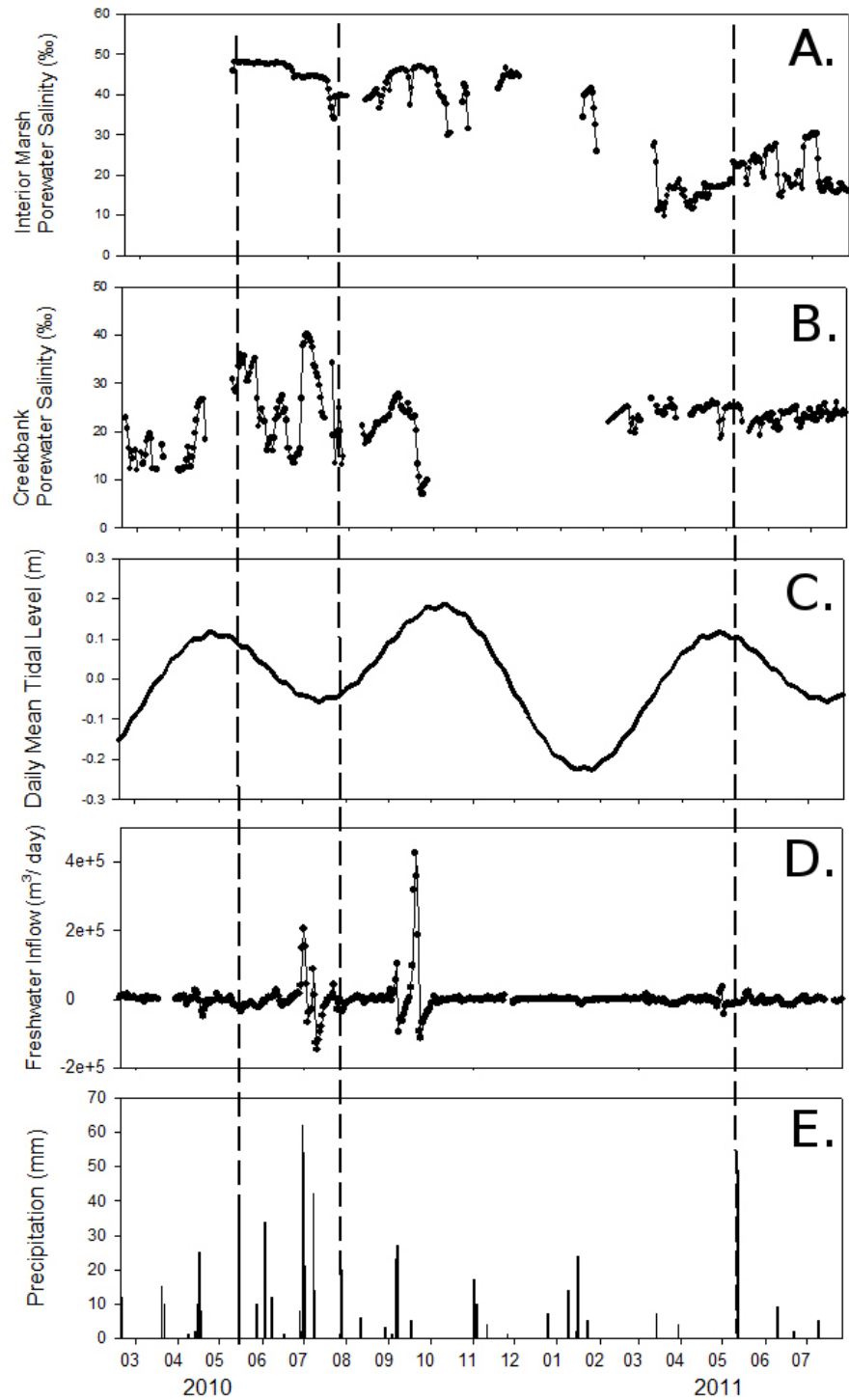


Figure B.4: Times series of porewater salinity at site 450 (A and B), mean water level in Nueces Bay (C), freshwater inflow to the Rincon Bayou (D), and precipitation (E). Local precipitation data was recorded at the Nueces Delta weather station (NUDEWX). Freshwater inflow (discharge) data was taken at the USGS Rincon Bayou gage station (#08211503). Gaps in the porewater salinity data occurred as a result of low soil moisture conditions. Dashed lines highlight precipitation events not accompanied by a freshwater inflow event.

2011. Palmer Drought Severity Index values at the conclusion of monitoring (< -2.75) indicated that South Texas was in an exceptional drought (see National Climate Data Center¹⁷).

Further declines in freshwater inflow due to a combination of municipal water withdrawals and global climate change are likely to reduce the frequency of low porewater salinity periods that are critical for maintenance of emergent plant communities. Similar studies incorporating continuous monitoring of porewater salinity are needed in order to estimate the potential negative impact of municipal water withdrawals from upstream water sources as well as the potential for river diversions and other mitigation efforts to offset negative anthropogenic impacts.

B.5.2 Gas exchange measurements

The seasonal patterns of net photosynthesis varied with species. Net photosynthesis of *B. frutescens* highly varied with season and showed bimodal peaks (fall and spring), whereas net photosynthesis of both *S. virginica* and *B. maritima* was constant with season (Fig. B.5A, B, C, D and E). At each station, *B. frutescens* had higher net photosynthesis than *S. virginica* and *B. maritima*. Average net photosynthesis in *B. frutescens* ranged from 5.8 $\mu\text{mol CO}_2 \text{ m}^{-2} \text{ s}^{-1}$ at station 463 to 10.6 $\mu\text{mol CO}_2 \text{ m}^{-2} \text{ s}^{-1}$ at station 467. Average net photosynthesis of *S. virginica* and *B. maritima* was 3.9 and 3.0 $\mu\text{mol CO}_2 \text{ m}^{-2} \text{ s}^{-1}$, respectively. Seasonal patterns of stomatal conductance were similar to that of net photosynthesis (Fig. B.5F, G, H, I and J). Average stomatal conductance of *B. frutescens* (0.106 mol $\text{H}_2\text{O m}^{-2} \text{ s}^{-1}$) was 2.5 – 3.2 times higher than that of *S. virginica* (0.043 mol $\text{H}_2\text{O m}^{-2} \text{ s}^{-1}$) and *B. maritima* (0.033 mol $\text{H}_2\text{O m}^{-2} \text{ s}^{-1}$). Transpiration exhibited strongly seasonal patterns, but different patterns from net photosynthesis and stomatal conductance (Fig. B.5K, L, M, N and O). Transpiration of all three species increased during spring and summer and decreased during fall and winter. *B. frutescens* had the highest transpiration (3.6 mmol $\text{H}_2\text{O m}^{-2} \text{ s}^{-1}$), while the lowest transpiration were found for *B. maritima*, with 1.4 $\mu\text{mol CO}_2 \text{ m}^{-2} \text{ s}^{-1}$; *S. virginica* exhibited intermediate values (1.8 $\mu\text{mol CO}_2 \text{ m}^{-2} \text{ s}^{-1}$). Leaf vapor pressure deficit showed a similar seasonal trend to transpiration (Fig. B.5P, Q, R, S and T). Average leaf vapor pressure deficit of *B. frutescens*, *S. virginica* and *B. maritima* was 3.6, 3.8 and 4.0 kPa, respectively.

Intrinsic water use efficiency (WUE_i) varied with season, but this was dependent on species and station (Fig. B.6A, B, C, D and E). At stations 463, 451 and 450, *S. virginica* showed the highest rates compared to both *B. frutescens* and *B. maritima*. However, average intrinsic water use efficiency in *B. maritima* at both 467 and 270 was slightly higher than that in *S. virginica* and *B. frutescens*. Instantaneous water use efficiency (WUE_T) exhibited a clear seasonal trend, increasing during fall and winter and decreasing during summer and spring (Fig. B.6F, G, H, I and J). This pattern indicates that instantaneous water use efficiency was dependent on fluctuations in transpiration rather than net photosynthesis. As the result, there was no consistent peak in instantaneous water use efficiency coincident with the spring peak in net photosynthesis. Apparent leaf carboxylation efficiency varied with species (Fig. B.6K, L, M, N and O). While apparent

¹⁷ <http://www.ncdc.noaa.gov/sotc/drought/2011/7>

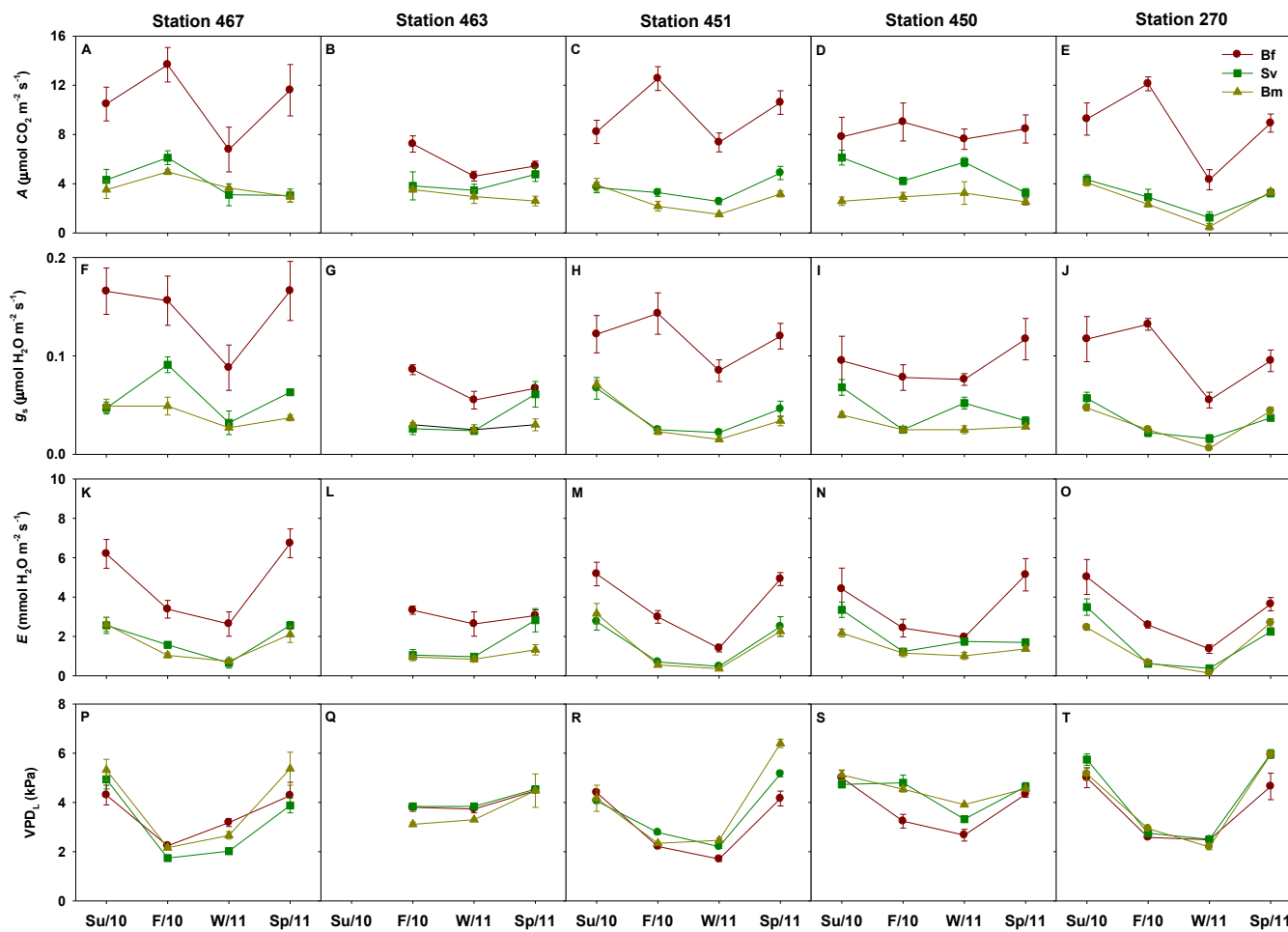


Figure B.5. Seasonal variations (Su/10 – summer 2010; F/10 – fall 2010; W/11 – winter 2011; Sp/11 – spring 2011) in net photosynthesis A (A, B, C, D and E), stomatal conductance g_s (F, G, H, I and J), transpiration E (K, L, M, N and O), and leaf vapor pressure deficit VPD_L (P, Q, R, S and T) of *Borrichia frutescens* (Bf), *Salicornia virginica* (Sv) and *Batis maritima* (Bm) at five stations (467, 463, 451, 450 and 270). Any data did not collect at station 463 during summer 2010. Data are means \pm SE (n=4-12).

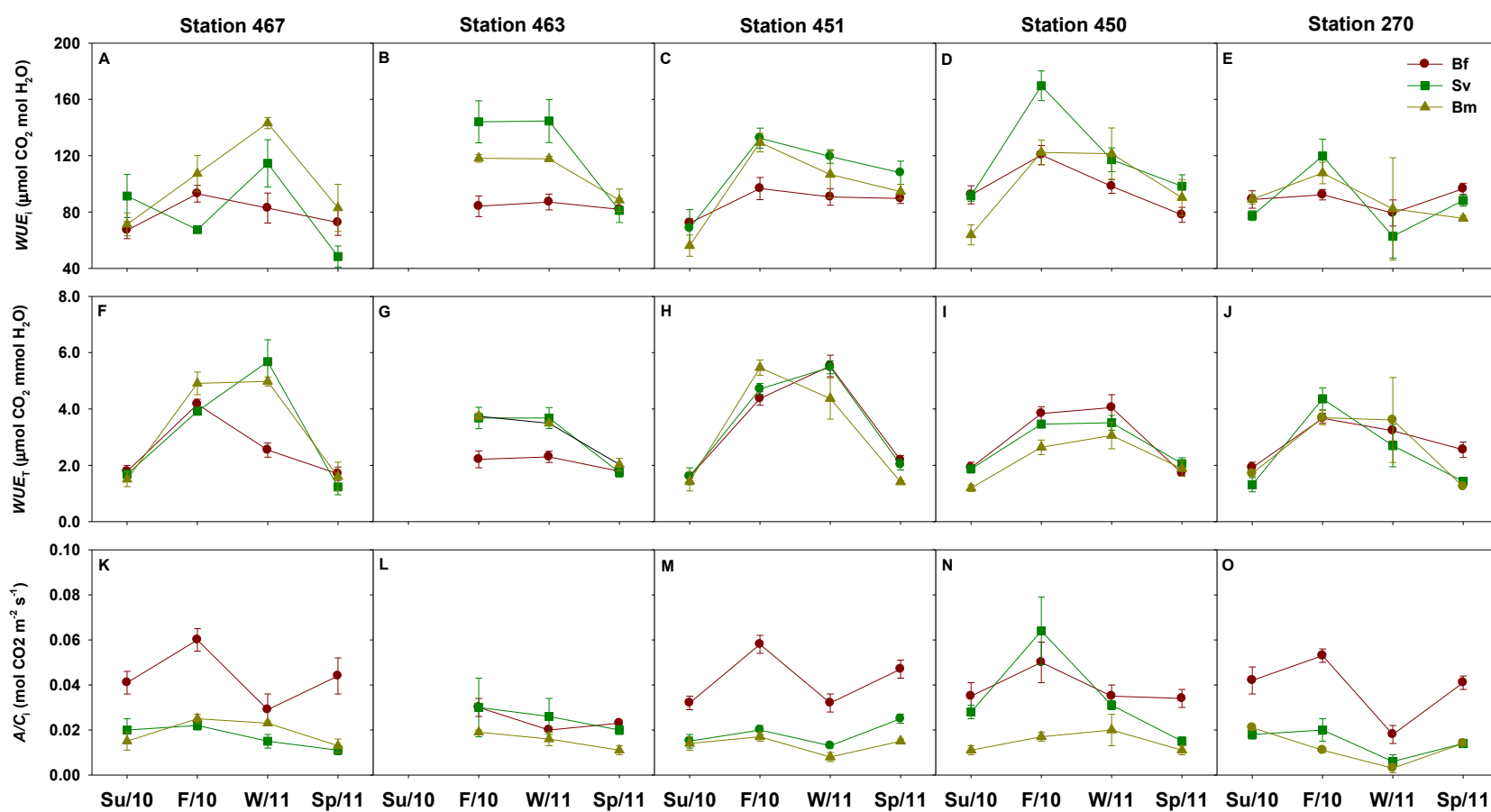


Figure B.6. Seasonal variations (Su/10 – summer 2010; F/10 – fall 2010; W/11 – winter 2011; Sp/11 – spring 2011) in intrinsic water use efficiency WUE_i (A, B, C, D and E), instantaneous water use efficiency WUE_T (F, G, H, I and J), and apparent leaf carboxylation efficiency A/C_i (K, L, M, N and O) of *Borreria frutescens* (Bf), *Salicornia virginica* (Sv) and *Batis maritima* (Bm) at five stations (467, 463, 451, 450 and 270). Any data did not collect at station 463 during summer 2010. Data are means \pm SE (n=4-12).

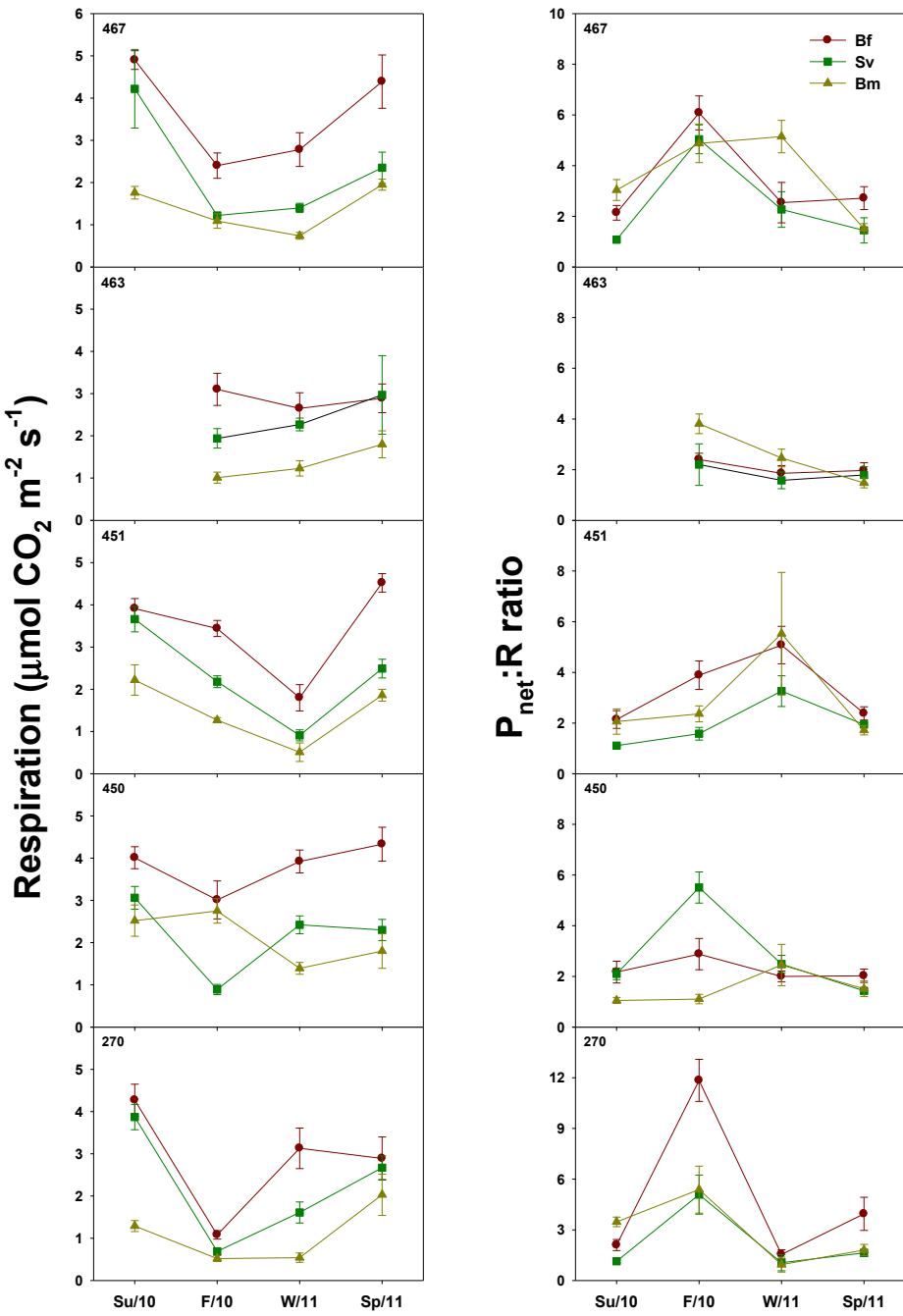


Figure B.7. Seasonal variations (Su/10 – summer 2010; F/10 – fall 2010; W/11 – winter 2011; Sp/11 – spring 2011) in leaf dark respiration (A, B, C, D and E) and net photosynthesis:respiration ($P_{\text{net}}:\text{R}$) ratio (F, G, H, I and J) of *Borrichia frutescens* (Bf), *Salicornia virginica* (Sv) and *Batis maritima* (Bm) at five stations (467, 463, 451, 450 and 270). Any data did not collect at station 463 during summer 2010. Data are means \pm SE (n=4-12).

leaf carboxylation efficiency of *B. frutescens* highly varied seasonally, apparent leaf carboxylation efficiency of both *S. virginica* and *B. maritima* was relatively constant over the experimental period with the exception of *S. virginica* at station 450. Average apparent leaf carboxylation efficiency was highest in *B. frutescens* and lowest in *B. maritima*.

Leaf dark respiration showed clear seasonal variations, increasing during spring and summer and decreasing during fall and winter (Fig. B.7). As with net photosynthesis, *B. frutescens* showed the highest leaf dark respiration ($3.3 \mu\text{mol CO}_2 \text{ m}^{-2} \text{ s}^{-1}$), different from that of both *S. virginica* ($2.3 \mu\text{mol CO}_2 \text{ m}^{-2} \text{ s}^{-1}$) and *B. maritima* ($1.5 \mu\text{mol CO}_2 \text{ m}^{-2} \text{ s}^{-1}$). The ratio of net photosynthesis to respiration ($P_{\text{net}}:R$) also exhibited seasonal trends (Fig. B.7). The ratio of all three species was highest during fall and winter and lowest during summer and spring. The ratio of *B. frutescens* ranged from 1.5 and 11.8. Average ratio of *S. virginica* and *B. maritima* was 2.3 and 2.7, respectively.

B.5.3 Leaf characteristics

Specific leaf area showed clear seasonal trend; it was dependent on station and species (Table B.2). Specific leaf area of all three species at 467 exhibited seasonal trends. Additionally, only *B. maritima* at 450 showed a clear seasonal variation. However, seasonal trends in any species were not observed at other stations (463, 450 and 270). Specific leaf area was highest in *B. maritima* and lowest in *B. frutescens* at all stations. Average specific leaf area of *B. maritima* ranged between 153 at station 467 and $175 \text{ cm}^2 \text{ g}^{-1}$ at station 270, with an average of $158 \text{ cm}^2 \text{ g}^{-1}$. Average specific leaf area in *S. virginica* and *B. frutescens* was 125 and $62 \text{ cm}^2 \text{ g}^{-1}$, respectively. In contrast to specific leaf area, leaf succulence of three species at all stations showed clear seasonal variations (Table B.2). Leaf succulence was highest during fall and winter, and lowest during summer and spring. Average leaf succulence in *B. frutescens* was 1.4–2.0 times higher than that in both *B. maritima* and *S. virginica*, ranging between 56 mg cm^{-2} at station 467 and 77 mg cm^{-2} at station 450 (Table B.2).

B.5.4 Plant biomass

Significant relationships between above- and below-ground biomass and percent cover were observed in all three species (Fig. B.8). According to the results of regression, above-ground biomass per percent cover was higher than or similar to below-ground biomass per percent cover in *B. frutescens* (Fig. B.8A, D and G). Also, *S. virginica* showed highest above-ground biomass per percent cover compared to below-ground biomass per percent cover (Fig. B.8F and I). However, *B. maritima* was dependent on station. At 467 and 463, above-ground biomass per percent cover was slightly higher than or was similar to below-ground biomass per percent cover (Fig. B.8B and E). At 450, above-ground biomass per percent cover, however, was much higher than below-ground biomass per percent cover (Fig. B.8H). This result may be explained due to soil moisture at each station. Soil moisture may affect the growth and morphology of below-ground tissues. Thus, below-ground biomass was not high because plant may easily access water at higher soil moisture.

Table B.2. Comparisons of specific leaf area ($\text{cm}^2 \text{ g}^{-1}$) and leaf succulence (mg cm^{-2}) of three species (*Borrichia frutescens*, *Salicornia virginica* and *Batis maritima*) at five stations in the Nueces River from summer 2010 to spring 2011. Data are means \pm SE (n=4-12). N/A = not available.

<i>Borrichia frutescens</i>				<i>Salicornia virginica</i>				<i>Batis maritima</i>				
Summer 2010	Fall 2010	Winter 2011	Spring 2011	Summer 2010	Fall 2010	Winter 2011	Spring 2011	Summer 2010	Fall 2010	Winter 2011	Spring 2011	
Specific leaf area												
467	75.6 \pm 2.8	62.7 \pm 3.1	59.0 \pm 2.1	81.8 \pm 2.7	125.8 \pm 5.3	101.5 \pm 5.3	111.9 \pm 3.6	130.0 \pm 2.4	188.9 \pm 10.0	150.7 \pm 5.3	136.8 \pm 6.3	193.1 \pm 13.6
463	N/A	69.5 \pm 14.1	57.0 \pm 3.1	57.3 \pm 2.5	N/A	129.7 \pm 3.0	131.5 \pm 4.7	93.4 \pm 2.4	N/A	131.8 \pm 16.3	164.5 \pm 4.1	147.7 \pm 11.6
451	57.5 \pm 2.8	61.8 \pm 3.2	60.3 \pm 3.1	64.4 \pm 2.7	136.6 \pm 10.1	130.6 \pm 13.2	140.2 \pm 11.3	99.8 \pm 3.3	150.5 \pm 11.4	159.0 \pm 3.5	125.2 \pm 5.7	128.9 \pm 10.1
450	51.7 \pm 1.3	60.9 \pm 3.4	60.7 \pm 2.6	47.1 \pm 1.1	124.9 \pm 5.4	142.3 \pm 7.8	143.4 \pm 5.1	114.3 \pm 4.5	215.1 \pm 11.3	179.2 \pm 12.3	141.2 \pm 10.6	166.1 \pm 2.5
270	62.3 \pm 3.0	58.5 \pm 3.2	90.4 \pm 4.7	64.8 \pm 1.6	124.8 \pm 5.8	142.1 \pm 10.1	136.3 \pm 5.0	127.6 \pm 3.3	171.0 \pm 12.0	170.8 \pm 7.7	168.6 \pm 13.9	190.7 \pm 14.4
Leaf succulence												
467	42.3 \pm 3.4	66.7 \pm 3.2	72.1 \pm 3.9	41.9 \pm 3.7	23.6 \pm 2.8	44.8 \pm 1.4	46.4 \pm 2.6	31.3 \pm 1.3	34.4 \pm 3.0	49.8 \pm 3.6	53.4 \pm 4.1	40.9 \pm 2.7
463	N/A	62.2 \pm 6.7	106.5 \pm 6.9	39.7 \pm 3.1	N/A	37.2 \pm 2.2	44.0 \pm 2.3	25.3 \pm 2.4	N/A	43.2 \pm 4.2	43.8 \pm 3.0	27.7 \pm 3.1
451	53.7 \pm 1.7	76.3 \pm 2.9	97.3 \pm 3.9	58.7 \pm 7.5	25.3 \pm 1.7	37.5 \pm 4.3	45.1 \pm 2.2	33.3 \pm 2.4	38.4 \pm 5.1	36.8 \pm 0.5	54.1 \pm 3.0	39.9 \pm 1.5
450	N/A	98.4 \pm 5.4	72.0 \pm 4.6	61.7 \pm 1.8	N/A	43.1 \pm 1.7	41.9 \pm 0.8	36.5 \pm 1.3	N/A	45.4 \pm 2.7	49.2 \pm 2.3	29.7 \pm 1.9
270	45.1 \pm 1.6	83.7 \pm 6.0	70.9 \pm 4.8	58.1 \pm 4.7	23.6 \pm 1.2	37.5 \pm 1.4	40.3 \pm 1.6	27.4 \pm 0.6	37.4 \pm 2.7	32.7 \pm 2.2	47.5 \pm 7.2	37.3 \pm 0.5

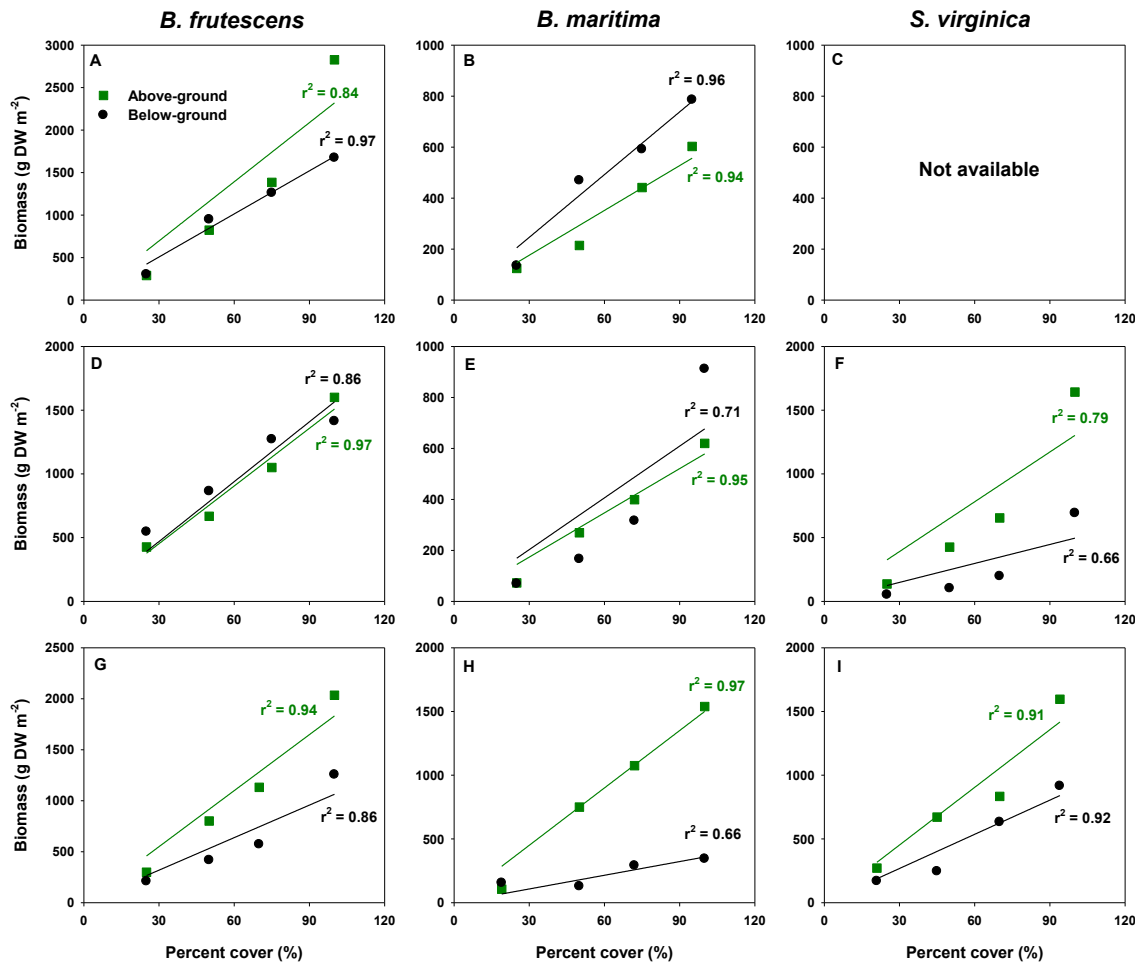


Figure B.8. Relationships between above- (green color) and below-ground biomass (black color) and percent cover in three dominant species at three stations during summer 2011 (467: A, B and C; 463: D, E and F; 450: G, H and I). Missing data in C was due to a lack of *S. virginica* population at 467. All regressions were significant at the 0.05 level.

B.5.5 Soil respiration

Soil respiration was almost constant values throughout the experimental period with the exception of summer 2010 canopy measurements, both within plant canopies and in bare areas (Fig B.9). Soil respiration within plant canopies was much higher than that in bare area. Maximum respiration within plant canopy was $4.5 \mu\text{mol CO}_2 \text{ m}^{-2} \text{ s}^{-1}$ during the summer sampling period with an average of $3.1 \mu\text{mol CO}_2 \text{ m}^{-2} \text{ s}^{-1}$ (Fig. B.9A) Soil respiration rates in bare areas were less than $1 \mu\text{mol CO}_2 \text{ m}^{-2} \text{ s}^{-1}$ over the entire study period (Fig. B.9A). Soil respiration was strongly correlated with litter/root biomass (Fig. B.9B). This result shows that soil respiration was significantly affected by litter/root biomass, explaining 39% of variation in soil respiration.

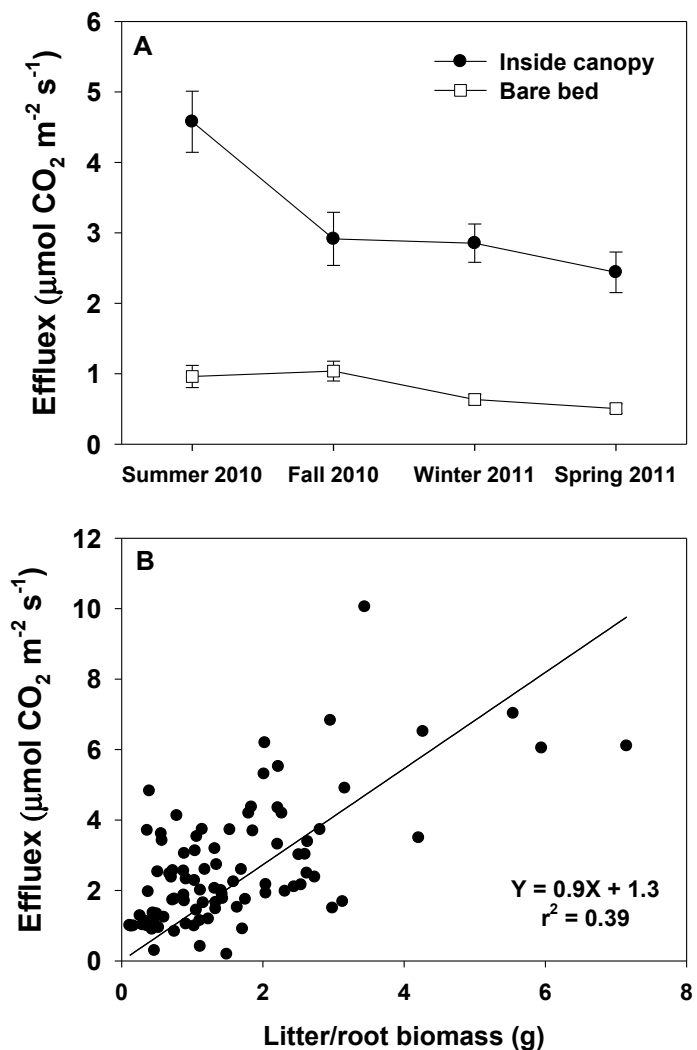


Figure B.9. Seasonal patterns of soil respiration (A) within plant canopy and in bare area and the relationship between soil respiration and litter/root biomass (B) in the Nueces River Delta from August 2010 to April 2011. Values are expressed as mean \pm SE.

B.6 Literature Cited in Appendix B

- Bonin, C. L., and J. B. Zedler. 2008. Plant traits and plasticity help explain abundance ranks in a California salt marsh. *Estuaries and Coasts* 31:682-693.
- Casey, W.H. and A.C. Lasaga, 1987. Modeling solute transport and sulfate reduction in marsh sediments. *Geochimica et Cosmochimica Acta* 51:1109-1120.
- Chapman, H.D. and P.F. Pratt. 1961. *Methods of analysis for soils, plants and waters*. Univ. of California, Division of Agricultural Sciences, Berkeley.
- Dunton K., B. Hardegree, T.E. Whitledge. 2001. Response of estuarine marsh vegetation to interannual variations in precipitation. *Estuaries* 24: 851–861.
- Forbes, M.G., Dunton, K.H., 2006. Response of a subtropical estuarine marsh to local climatic change in the southwestern Gulf of Mexico. *Estuaries and Coasts* 29, 1242-1254
- Rasser, M.K. 2009. *The role of biotic and abiotic processes in the zonation of salt marsh plants in the Nueces River Delta*, Texas. Ph.D. Thesis, The University of Texas at Austin. Austin, USA.
- Touchette B.W., G.A. Smith, K.L. Rhodes, and M. Poole. 2009. Tolerance and avoidance: two contrasting physiological responses to salt stress in mature marsh halophytes *Juncus roemerianus* Scheele and *Spartina alterniflora* Loisel. *Journal of Experimental Marine Biology and Ecology* 380: 106-112.
- Webb, J.W. 1983. Soil water salinity variations and their effects on *Spartina alterniflora*. *Contributions in Marine Science* 26: 1-13.

This page intentionally blank for two-sided printing.

C Appendix: Ecological Modeling

C.1 Introduction

C.1.1 Overview

Coastal marshes are important ecosystems that provide many benefits to human health and well-being including: protecting the inland areas from storm surge, storing water, removing nutrients that flow in from watersheds, and providing nursery habitat for key commercial and recreational fisheries. Yet, marshes are under extreme pressure from development and 50% of the marshes nationwide have disappeared since the founding of the United States.

The Texas coast is flat, hot, and windy; which makes coastal marshes very susceptible to effects of climate change and water resource development. Climate change can have three effects: sea-level rise, water cycle alterations, and temperature alterations. The main effects will be to drown marshes during rising water levels or dry them out as evapotranspiration rates increase during droughts. Water resource development has decreased water delivery to marshes in the Nueces Delta by 45% over the last 40 years, which has led to marsh degradation (Ward et al. 2002).

There is a need to understand the dynamics and the interactive roles of climate and water cycle changes in order to predict changes in salt marshes in the future. This information is critical for resource management (Montagna et al. 2002a). However, few tools exist to forecast effects of human activities on marsh function. Results and models of the ongoing research could be extended to coastal estuaries in other regions of the world.

C.1.2 Marshlands

The main goal of this project is to develop a forecasting system to allow us to determine effects of human activities on marsh structure and function, in particular vegetation. One of the problems facing us in the Nueces Delta is to determine how much water to divert back into the marsh to increase water levels in order to restore the vegetated wetlands. To solve this problem, the goal of this project is to create good and workable mathematical models for marsh ecosystems for the wetlands at the Nueces River mouth (Figure C.1). Then such mathematical models could



Figure C.1. Nueces Marsh surrounding the Nueces River entering Nueces Bay. Photo by Paul Montagna July 1997 during high flow conditions.

be modified as needed and applied to marshes in other regions of the country that are susceptible to the negative ecological and environmental impact from construction and water resource development.

C.1.3 Connectivity in the Nueces Estuary

Rincon Bayou is located at the junction between Nueces Bay and the Nueces River. This junction is integral in making the connection of nutrient-laden freshwater in the Nueces River with the salt water of Nueces Bay. Under current conditions, where inflow is approximately 1% of historic levels, freshwater inflow from the Nueces River does not reach Nueces Bay often (Irlbeck and Ward 2000). Tidal flooding of saltwater from Nueces Bay enters Rincon Bayou, which is concentrated by evaporation and a reverse estuary forms. A reverse estuary is where salinity increases as you move upstream rather than decreasing, as would occur in a normal estuary. The salinity gradient between the Nueces River and Nueces Bay reverts to a normal pattern (i.e. salinity increases downstream) periodically after large natural inflow events from the Nueces River (Irlbeck and Ward 2000) or when pumping of freshwater into Rincon Bayou occurs (Barajas 2011; Tunnell and Lloyd 2011; Hill *et al.* 2012). A return to a normal pattern of salinity in Rincon Bayou is evidence of lateral mixing within the Nueces Estuary, which has positive effects on the connectivity of aquatic fauna.

Connectivity, with respect to fishes and invertebrates, implies ‘the enhanced storage of genetic and energetic pools due to variable migration and dispersal patterns across habitats and ecosystems’ (Secor and Rooker 2005). Connectivity within estuaries and between estuaries and marine areas is especially important for mobile marine fauna that utilize different habitats along a salinity gradient in different parts of their life cycles, or utilize tides or other flow as mechanisms for larval dispersal (Riera *et al.* 2000; Gillanders *et al.* 2003; Vasconcelos *et al.* 2010). Techniques such as comparing carbon and nitrogen isotopes of tissues with those of potential food sources (Riera *et al.* 1996; Herzka 2005) and comparing elemental signatures in otoliths of fish found in similar and different habitats (Gillanders 2005) confirm that connectivity within estuaries, and between estuaries and marine waters is important in the life cycles of some mobile aquatic species.

Several aquatic invertebrate and fish species gain connectivity with Rincon Bayou, especially when freshwater inflows are favorable enough to create a positive salinity gradient (Barajas 2011; Kalke 2012). Juvenile brown shrimp (*Farfantepenaeus aztecus*) enter Rincon Bayou in late winter (February March) and usually peak in abundance in April, before migrating back downstream in May and June as sub-adults (Hill and Nicolau 2007; Kalke 2012). The main sources of food for brown shrimp are *Spartina alterniflora* and *S. spartinae* detritus and benthic diatoms and organic matter inputs carried by river flow contribute greatly to the brown shrimp diet while in Rincon Bayou (Riera *et al.* 2000).

White shrimp (*Litopenaeus setiferus*) also utilize Rincon Bayou in juvenile stages of their lives. White shrimp enter Rincon Bayou in late spring and leave at the start of winter. Both brown and white shrimp forage in the top 2 cm of the sediment, and are known to prey on infauna, such as polychaete worms, in addition to having other food

sources (Hunter and Feller 1987; Beseres and Feller 2007). Infauna biomass and diversity are strongly correlated with temporal changes in salinity in Rincon Bayou (Montagna *et al.* 2002b), which in turn are directly related to freshwater inflows and tidal flushing.

Various other invertebrate and fish species (red drum [*Sciaenops ocellatus*], black drum [*Pogonias cromis*] menhaden [*Brevoortia patronus*] and croaker [*Micropogonias undulatus*], blue crab [*Callinectes sapidus*]) are ecologically connected to Rincon Bayou, however the link to freshwater inflow is less direct. Red and black drum feed on shrimp and other invertebrates, and can get temporarily isolated in shallow pools in Rincon Bayou if the flow into Rincon Bayou decreases to the extent that the water is not deep enough to easily swim. High blue crab abundances often coincide with low salinities in Rincon Bayou, however this is not always consistent (Hill and Nicolau 2007).

The flow required for ecological connectivity in Rincon Bayou does not occur often enough from existing freshwater flooding events because of the high extraction of water for municipal and agricultural uses. The artificial pumping of water from the Nueces River into Rincon Bayou at more frequent intervals (nine times from May 2009 to August 2012) has decreased salinities in mid-Rincon Bayou (station NUDE02) and therefore shows the potential to increase ecological connectivity in the area. However, the effects of the inflows on salinity are much shorter than natural flooding events and the flows are largely restricted to existing channels. Overbanking of the existing channels both dilutes salts in the surface sediments of surrounding areas, making it more suitable for marsh plants to grow, and washes detritus into the channels, which provides food for brown shrimp. It is inconclusive that there is enough flow from these pumping events to increase the amount of connectivity for species that inhabit Rincon Bayou for part of their life cycles. However, it is assumed that an increase in pumped and ‘natural’ freshwater inflows would increase the amount of food available and accessibility into and out of Rincon Bayou, thereby increasing the habitat available and connectivity in the system for mobile aquatic species.

C.1.4 Marsh Plant Zonation

Salt marshes are characterized by physical gradients including pore water salinity, frequency of inundation, both from freshwater pulses and tidal variation, and nutrient availability. Zonation of plants in the marsh is defined by these gradients (Chapman 1974; Adam 1990; Raffaelli and Hawkins 1996). The high and low areas of the marsh are the extreme points in the physical gradients and are characterized by distinct plant assemblages. The low marsh is characterized by higher tidal energy and is more frequently inundated by tidal flow. Salinities in the low marsh are usually dominated by bay salinities. The high marsh is rarely inundated by bay water and prolonged exposure to dry conditions leads to higher salinities. The mid-marsh, in semi-arid climates, contains plants from both the high and low marsh assemblages (Zedler *et al.* 1999).

The general patterns of zonation have a strong influence on how plants in the Nueces Marsh respond to elevation (Rasser 2009). The cover of plants and physical characteristics of the Nueces Marsh was identified in a geographic information system and elevation was taken from a lidar digital elevation model (Figure C.2). The plants

Borrichia frutescens and *Salicornia virginica* dominate cover at the lowest elevations around 50 cm above mean sea level. *Spartina alterniflora* dominates cover at higher elevations between 120 -200 cm (Figure C.3).

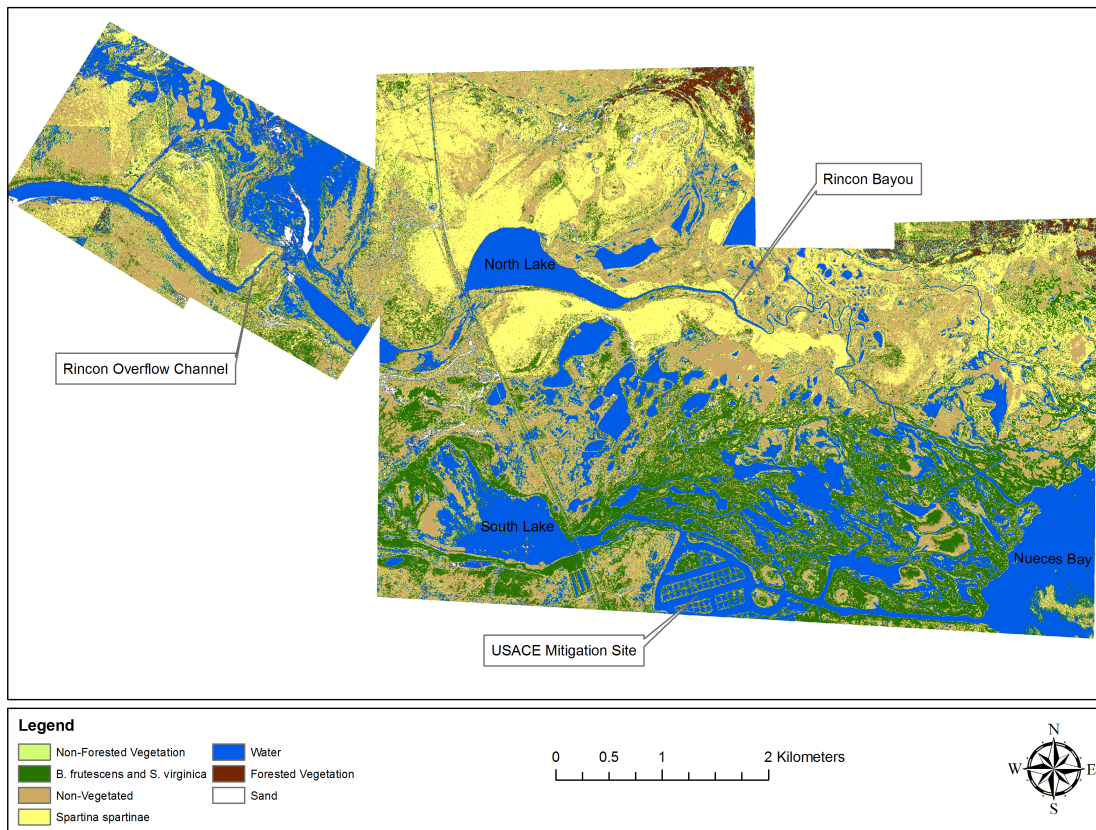


Figure C.2. Classified image of the Nueces Marsh based on classification of digital aerial imagery acquired 1 November 2005 (Rasser 2009).

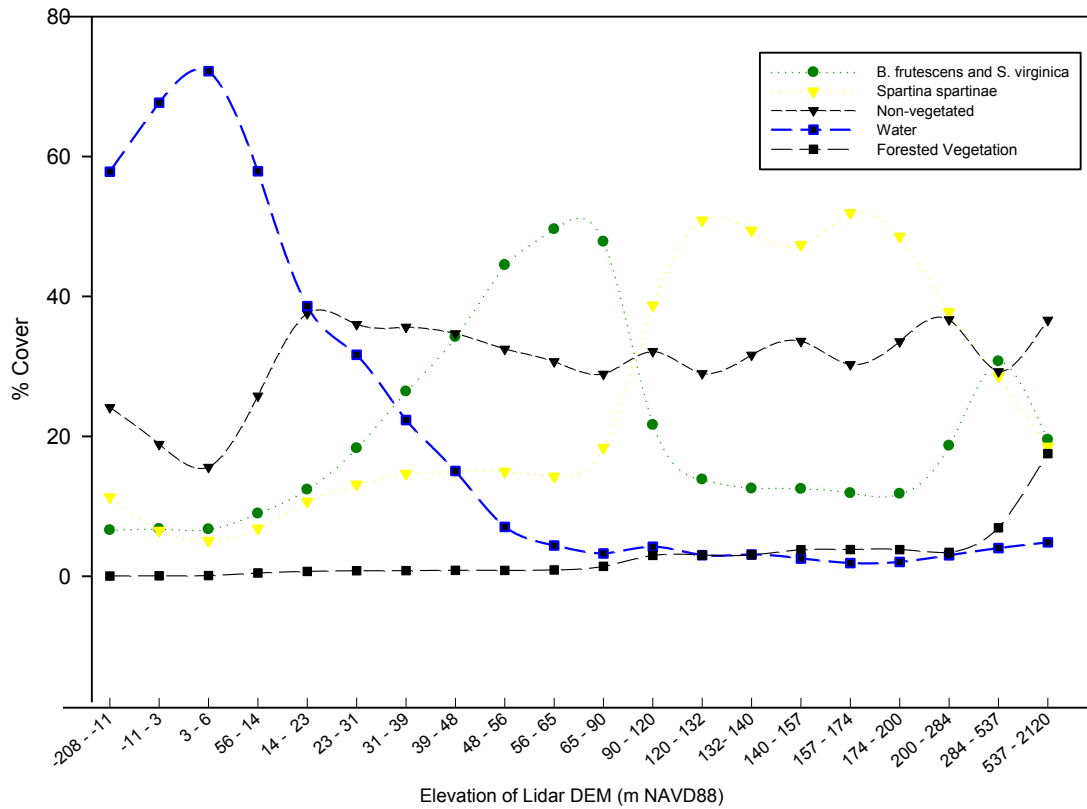


Figure C.3. Percent cover of classes from Figure 2 within the Nueces Marsh as a function elevation (Rasser 2009).

C.2 Objectives

The motivation of the current study is to determine how changes in freshwater inflow patterns might be used to restore the Nueces Marsh. The marsh has been degraded because of reductions of freshwater inflow following construction of the Choke Canyon Reservoir in 1983 (Ward et al. 2002, Montagna et al. 2009a, Montagna et al. 2009b). So, it is important to determine what effect an increase or decrease of freshwater inflow would have on salt marsh plant growth and development. Growth and development here is defined in units of percent cover of salt marsh surface. The approach is to develop a model for growth of plant cover.

In the model developed for this project, the definition of marsh regions is based on elevation. For this report, water areas are designated by areas of elevation less than 0.0 m. The low marsh is all points between 0.0 m to 1.0 m, the mid marsh from 1.0 m to 2.0 m and the high marsh anything above 2.0 m. While three elevation ranges were used in this study, the number of ranges and the size of the elevation bins can be varied in the model. Elevation was used for grouping plant species in this study. Other grouping schemes could have been used, such as distance from water edge, or salinity tolerance.

C.3 Methods

C.3.1 Field data

Field studies have been ongoing in the Nueces Marsh since 1994 (Ward et al. 2002, Montagna et al. 2002b, Alexander and Dunton 2002), so there is a large amount of spatial and temporal data. The original purpose of the data collection was to determine the freshwater inflow needs of the marsh in the context of marsh restoration. Recent projects have focused on synthesizing the data (Montagna et al. 2009b).

The vegetation data set includes plant species, elevation distributions, percent cover, growth rates, and biomass (Rasser 2009, Alexander and Dunton 2002). This data set is available at www.ccbay.tamu.edu (Montagna et al. 2012). The physical data set includes water flows and levels obtained from flow USGS flow gauges and a digital elevation model (DEM) obtained from James Gibeaut of the Harte Research Institute. Largely this data is acquired from cells, that is, specific locations on the surface (space) at specific moments in time.

The data set is ideal for creating a forecast system on how the marsh might change with changes in climate or water resource development. This forecast system is the new research direction that this project will enable.

C.3.2 Functional Grouping and Growth Rates of Marsh Plants

The model developed for this project can be tailored to represent individual species or groups of species based on any group definition. Following a previous study in the Nueces Delta, plants were divided functionally into two groupings: 1) clonal stress tolerant (CST) plants, and 2) clonal dominants (CD) (Forbes and Dunton 2006). Clonal stress tolerant plants are small, slow-growing plants including *Batis maritima*, *Distichlis spicata*, *Monanthcloe littoralis*, and *Salicornia virginica*. The clonal dominant plants are taller, faster-growing species, which include *Borrichia frutescens* and *Spartina alterniflora* (Grime 1979; Boutin and Keddy 1993). Facultative annuals, which do not spread clonally, were not included in this study, but with suitable growth rate estimates, could be easily included.

Growth rates for the two functional groupings for use in the model were determined from long-term observations of the marsh plant cover over three distinct climatological periods characterized by the average number of freshwater flooding events in a year during the period from 1996 to 2006 (Figure C.4) (Forbes and Dunton 2006). Growth rates were estimated from linear trends (Forbes and Dunton 2006) in each of the three marsh zones (

Table C.1).

The graph denoting the number of events passing the flooding threshold shows events where the Nueces River discharge was ≥ 14.2 cubic meters per second for two or more days (Figure C.4). This rate was determined to be the rate that will cause flow into the delta. (Bureau of Reclamation (BOR) 2000). This rate was revised down from 59.5 cm when the Nueces Overflow Channel was built.

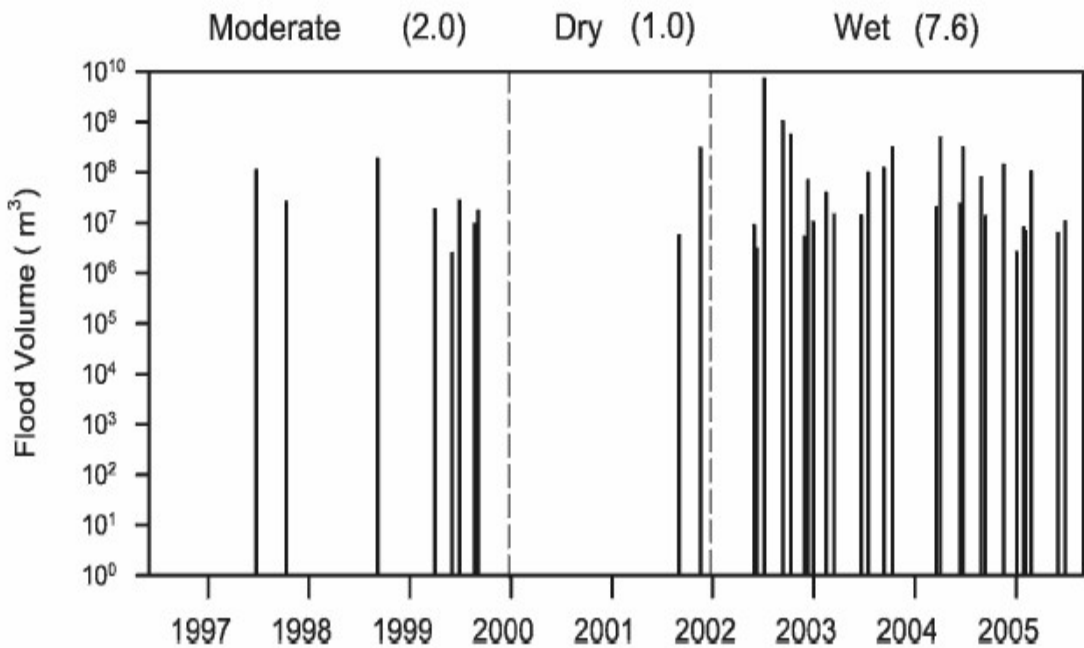


Figure C.4. Nueces River flood volumes where mean daily discharge exceeded flood threshold for two or more days. Annual flood frequencies within each climate period are shown in parentheses. From (Forbes and Dunton 2006).

Table C.1 - Growth rates for drought, moderate and wet periods for clonal dominants (CD) and clonal stress tolerant plants (CST) for the low, mid, and high marsh zones. Rates are percent change in coverage per year

Climate	Group	Marsh Zone		
		High	Mid	Low
Drought	CD	-0.24	-0.18	-0.36
	CST	-0.83	0.01	-0.25
Moderate	CD	0.01	0.01	-0.10
	CST	0.01	-0.07	1.40
Wet	CD	1.75	-0.50	1.40
	CST	-0.20	1.86	1.29

C.3.3 Modeling Changes in Marsh Plant Coverage

The change over time in the population \mathbf{X} for species s (X_s), for a particular area that has a carrying capacity of \mathbf{C} is modeled with:

$$\frac{\partial X_s}{\partial t} = r_s X_s * \left(1 - \sum_s^N \frac{X_s}{C_s} \right) + \varepsilon_s \nabla^2 \left(\frac{X_s}{C_s} \right)$$

Where N is the number of species, r is the growth rate, and ε is the diffusion rate. In our system, we model the Marsh as a regular grid of areas, with the highest resolution being 1 square meter areas, since that is the resolution of our elevation map and the plant coverage observations. In theory, ∂t should be very small, but we use 1 day as noticeable changes in plant coverage take many days, and the observations are 90 days apart. The above equation models individuals, but here we use it to model clonal expansion, so we consider instead percent of area covered by a species. We therefore set C_s to 100, which allows X_s to represent the percentage of area covered. The diffusion rate, ε_s , controls the rate of expansion between grid cells and diffusion happens when there are differences (pressure) in populations between neighboring cells. If the percent coverage gets above 100, then the model forces the change to go negative. This is why ∂t , needs to be small, so that you don't get the populations to go above 100 by very much.

In reality, the growth rate of a species, r_s , changes over time and is affected by many factors. Our implementation allows r_s to be a function that can vary over whatever we want: t , grid location, species, salinity, weather, precipitation, water flow, etc. For the results presented here, masks are used to specify which group a grid belongs to: high marsh, mid marsh, or low marsh. Instead of using just elevation, the masks can also be created interactively and any number of groups can be used. To determine the second derivative, $\nabla^2 \left(\frac{X_s}{C_s} \right)$, we use 2nd order central difference in each grid direction (i and j).

The Nueces Marsh covers an area roughly 14 km × 10 km (Figure C.5). At 1 meter resolution, which creates a map that has 10,018 rows and 14,451 columns yielding a total of 144,770,118 cells. Elevation data is used to determine the land-water-marsh group, where water is 0 m and below, low marsh is 0-1 m, mid marsh is 1-2 m, and high marsh is 2 m and above. Using this scheme, 7,093,931 of the cells are labeled as water and 99,676,278 cells are labeled as marsh land (30,849,641 cells as low marsh, 22,160,762 cells as mid marsh, and 46,665,875 cells as high marsh). The remaining 37,999,909 cells are outside the marsh area. The grid is aligned with longitude and latitude lines, but the Nueces Marsh is not, giving rise to the extra cells.

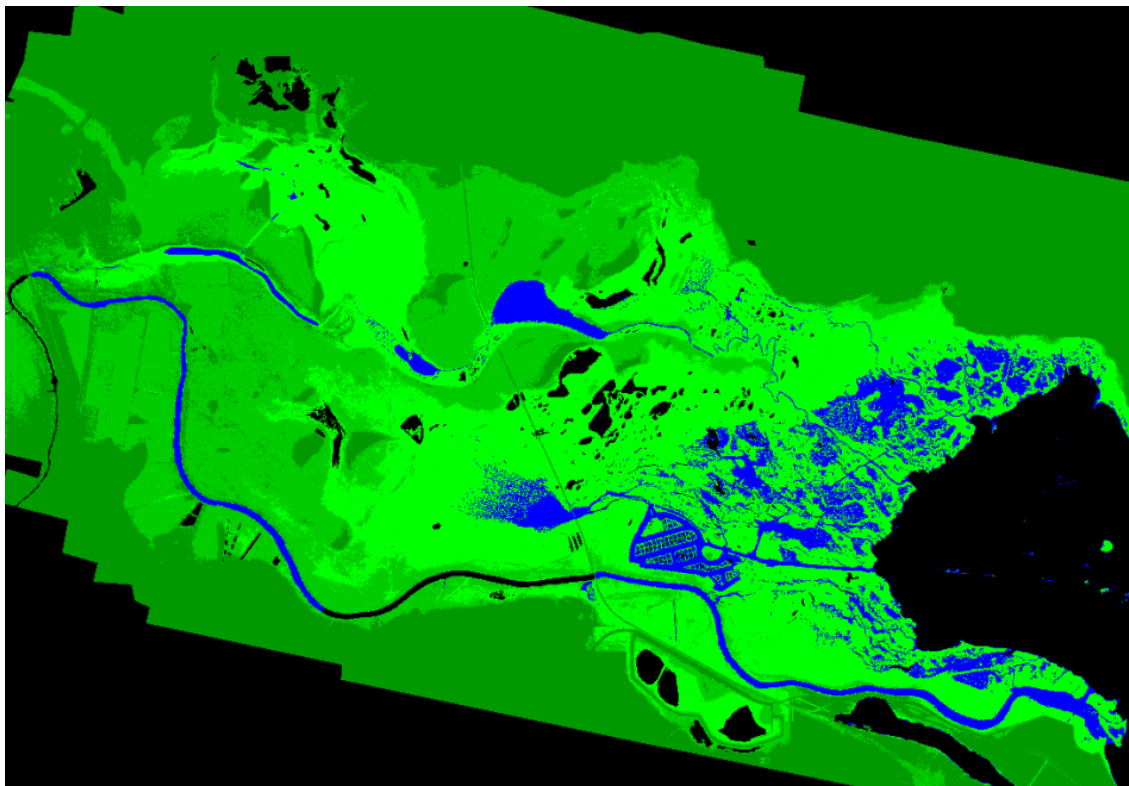


Figure C.5. Nueces Marsh areas: blue = water, light green = lower marsh, medium green = middle marsh, dark green = high marsh, black – non marsh areas (mainly Nueces Bay).

C.4 Results

C.4.1 Model Behavior

The model behavior for two different species groups X-species and Y-species was investigated in a rectangle area that is 3x4 unit squares of marshland with arbitrary initial conditions and arbitrary carrying capacity for each area and species. The dynamics of the populations of species X (Figure 6A) and species Y (Figure 6B) exhibit those of a so-called weakly coupled system of parabolic partial differential (difference) equations with Dirichlet boundary conditions (Bandle and Levine 1989).

It has been proven that such systems have a unique solution that is asymptotically stable if diffusion coefficients and other parameters of the system are satisfied with some conditions (Leiva and Sequera 2003, Ramsey and Schager 2002). The system can be extended to the 5 to 7 species of marshland vegetation that exist in the Nueces system by simply creating a system of 5 to 7 weakly connected differential equations with given boundary conditions. The simulations demonstrate that populations of two species have asymptotic stability and that diversity of species is preserved at all areas of marshlands under consideration in these models (Figure 6). Therefore, for two species: the system of partial differential equations with $N=2$, nonzero, and smooth carrying capacities functions $L_i(x,y)$, $i=1,2$ has unique asymptotically stable solution.

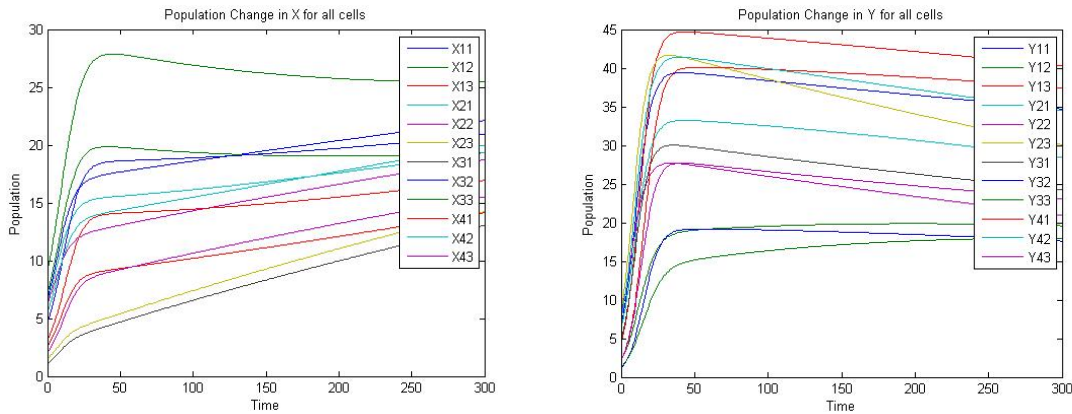


Figure C.6. Population change in 12 cells from a 3 x 4 spatial matrix. A) Species X and B) Species Y.

Model Results

The model predicts mostly reductions in plant cover for various initial plant coverage conditions (Figure C.7). In both drought and moderate conditions (as defined in Table 1), the model as currently configured predicts a decline in plant coverage. Marsh plant coverage increase in area only during the wet conditions when there is space available (Figure C.7). If the initial conditions are that there is already 100% coverage (as it is on the far left) then there is no room for plants to grow and fill more space. It is not until there is at least about 20% space vacant that plants will grow and fill the remaining space.

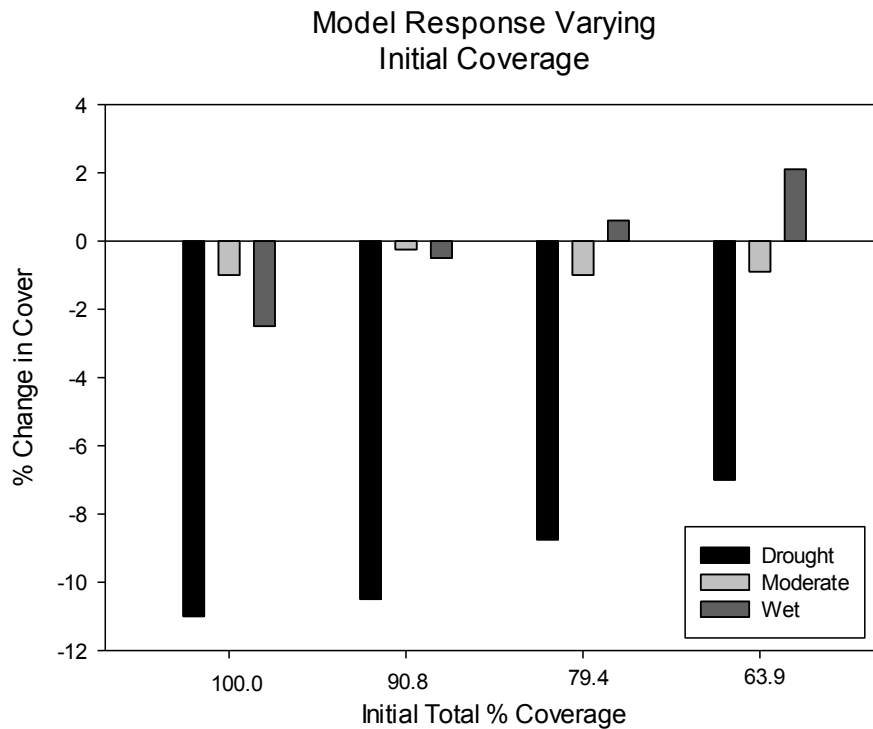


Figure C.7. Change in percent coverage based on various initial coverage conditions. Run duration was 3-months, and climate defined in Table 1.

The modeling experiment was run for a 10-year period nine times: three climate periods times three initial coverage conditions (Figure C.8). The three climate conditions were dry, moderate, and wet as defined in Table 1. The three initial starting plant coverage conditions were 2%, 50%, and 100% (Figure C.8, solid lines, thick lines, and dotted lines respectively). It was assumed that the initial conditions contained equal amounts of each functional group, thus two species starting at 25% cover (the thick lines) have a total coverage of 50%. The marsh plants consistently approach a steady state of maximum coverage during wet periods for all starting conditions. Coverage decreases during moderate conditions and more dramatically during drought conditions.

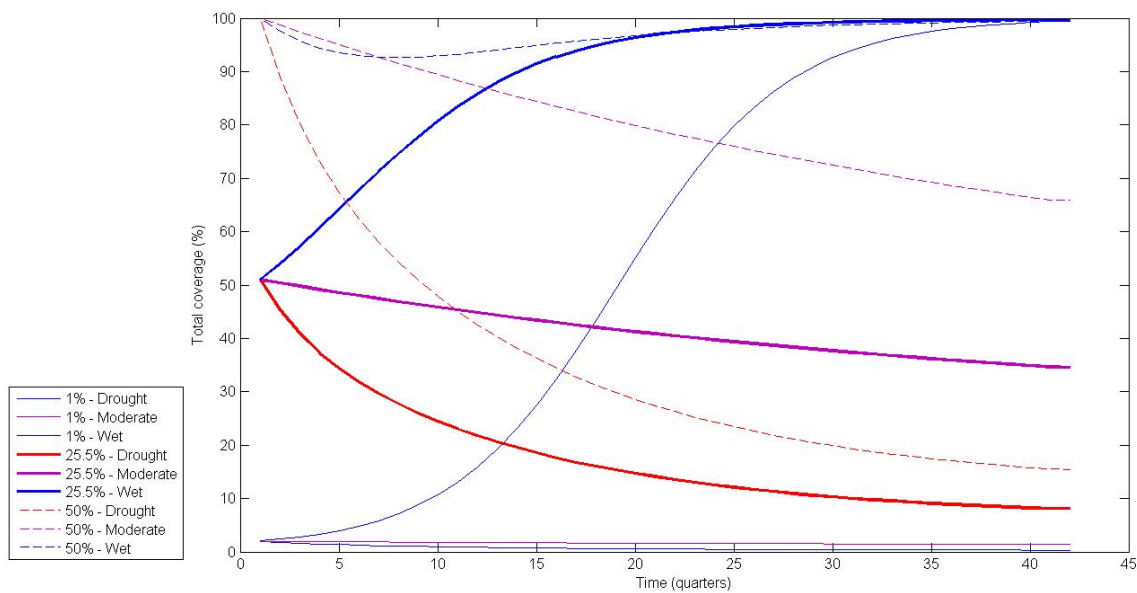


Figure C.8. Modeled marsh coverage over 10-year run starting at 2%, 50%, and 100% initial coverage.

The simulation of plant cover change over the entire Nueces Marsh was run at 10 m resolution using the two functional groups: clonal stress tolerant (CST) plants and clonal dominant (CD) plants. There was about a 1% difference in outcome between the 10 m and the 100 m resolution, and between 0.1% and 1% difference when running the model at the highest resolution of 1 m. The simulation was run for a 10-year period with daily time steps and on a high-end laptop the simulations took about 5 seconds to run at 100 m resolution, 15 minutes at 10 m resolution, and about a full day at 1 m resolution. Because of the small differences in changes at the different resolutions, but significant time savings at 10 m, the simulations at run at 10 m resolution for reporting here (Figures 9 - 11). The simulations were run for three climate regimes: wet, moderate, and dry as defined in Figure C.4 and Table C.1.

In the simulation, the clonal dominant (CD) plant group is denoted in red and the clonal stress tolerant (CST) plant group is denoted in green. Pure red or green denotes

100% coverage of that functional grouping while shades of yellow/orange/brown denote a mix of members from each functions grouping (Figure 9).

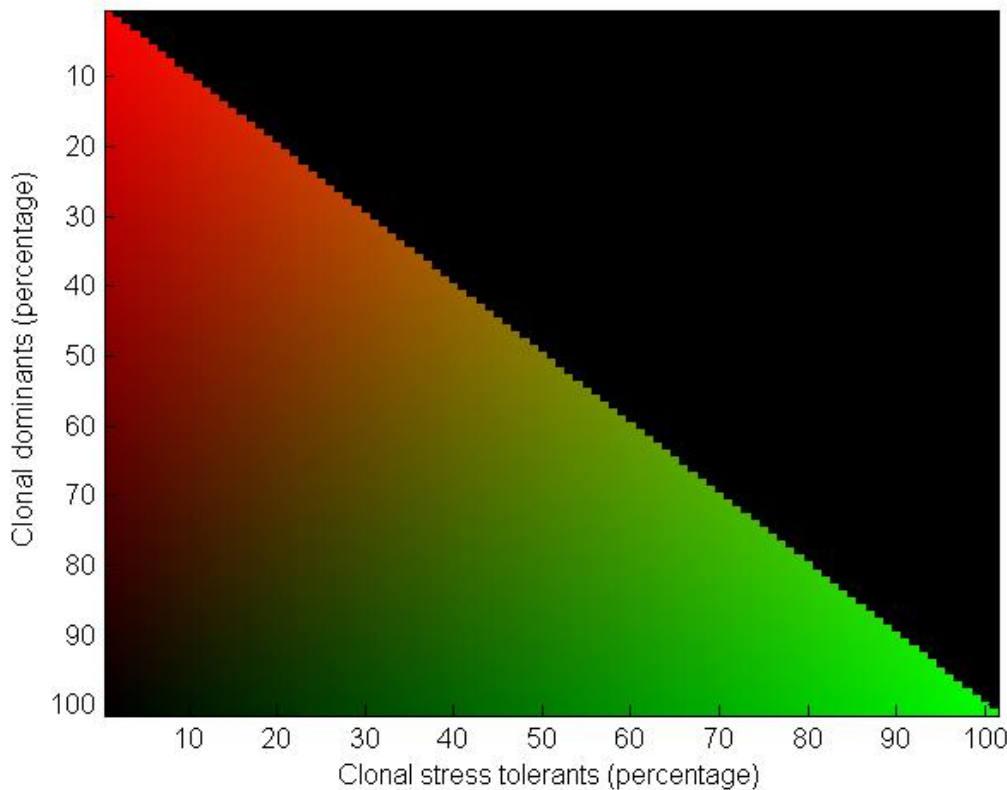


Figure 9. Color scale for simulations in Figures 10-12 where 100% cover of clonal dominant species is red, and 100% of clonal stress tolerant species is green.

The relative spatial coverage of the two functional groups was different under different climate regimes (Figures C.10 – C.12 and Table C.2). There is more coverage of CD after 10 years of wet conditions (Figure C.10) than moderate climate conditions (Figure 11), but virtually no CD during dry conditions (Figure C.12). While there is little diversity during dry conditions, moderate climate conditions yield mixtures of the two plant community groups, thus higher plant diversity. Under dry conditions the area of bare marsh without vegetation is quite large because marsh vegetation coverage decreases by 84.1% (Table C.2)

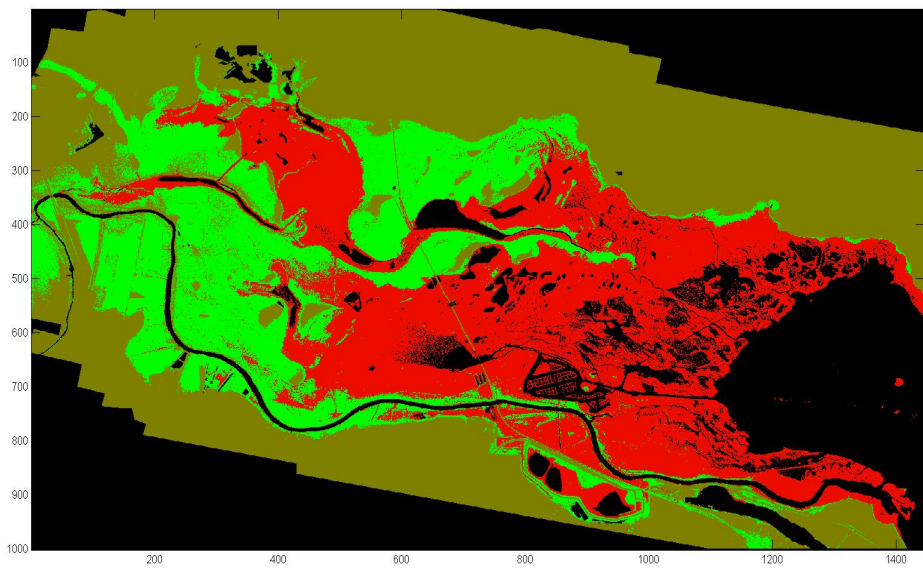


Figure 10. Modeled marsh coverage over 10-year run during wet conditions for two species. Clonal dominant (CD) species is red, and clonal stress tolerant (CST) species is green. At full red, that species is at 100% coverage, cells with both species will be combinations of red and green colors (yellow when equal). See Figure 9 for color scale.

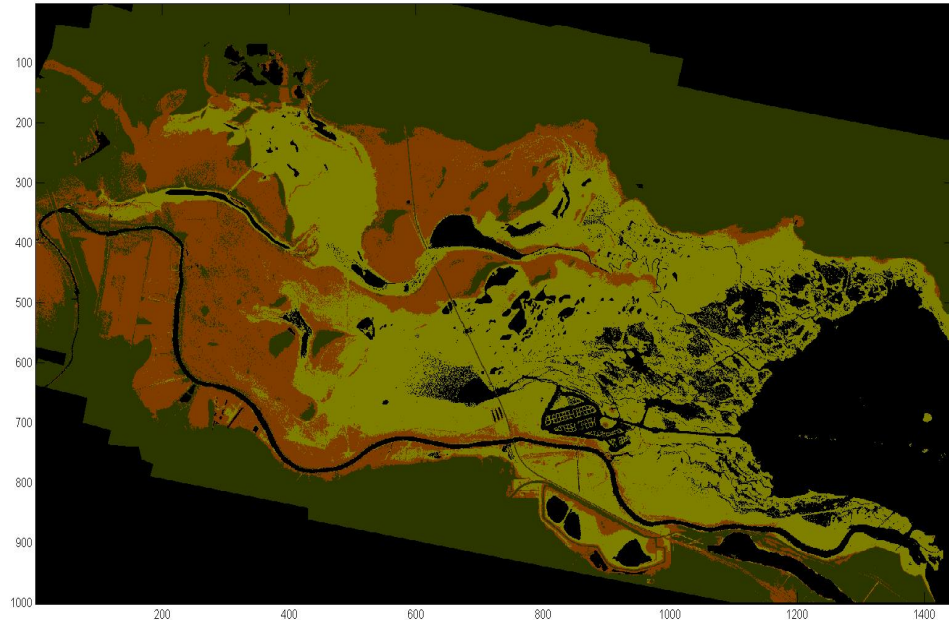


Figure 11. Modeled marsh coverage over 10-year run during moderate conditions for two species. CD species is red, and CST species is green. At full red, that species is at 100% coverage. Yellow is thus a mix of the two species. See Figure 9 for color scale.

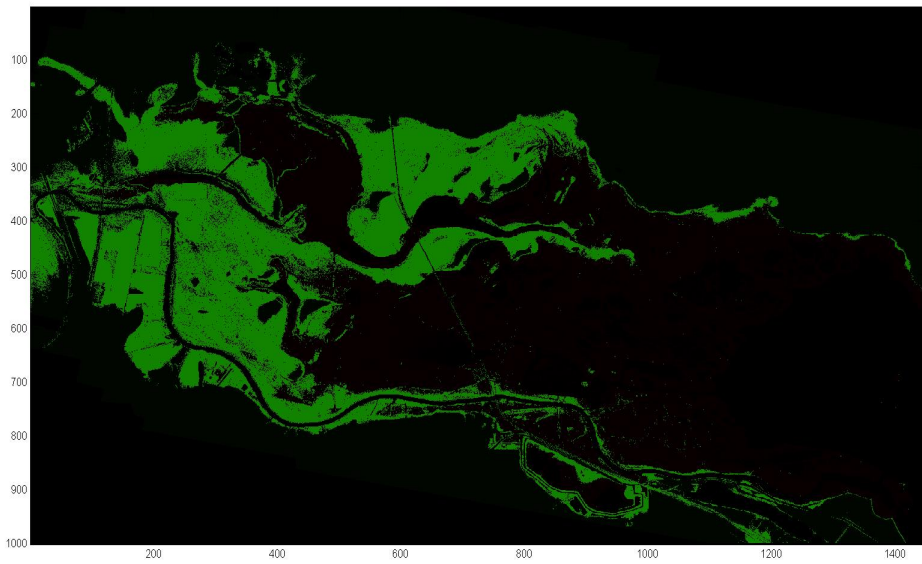


Figure C.12. Modeled marsh coverage over 10-year run during dry conditions for two species. CD species is red, and CST species is green. At full green, CST species is at 100% coverage. See Figure 9 for color scale.

Table C.2. Cover and percent change in marsh areas under three climate regime simulations.

Climate Period	Area	Cover		Change	
		%	km ²	km ²	%
Wet	Total Marsh	100%	99.1	-0.4	-0.4
	Low Marsh	31%	30.3	-0.4	-1.4
	Mid Marsh	22%	22.1	0	-0.1
	High Marsh	47%	46.7	0	0
Moderate	Total Marsh	100%	65.7	-33.8	-33.9
	Low Marsh	47%	30.9	0.1	0.4
	Mid Marsh	25%	16.6	-5.5	-25.0
	High Marsh	28%	18.3	-28.4	-60.9
Dry	Total Marsh	100%	15.5	-84.1	-84.4
	Low Marsh	6%	1.0	-29.9	-96.8
	Mid Marsh	83%	12.9	-9.1	-41.3
	High Marsh	10%	1.6	-45.1	-96.7

C.5 Discussion

Fresh water flow from the Nueces River through Rincon Bayou into the Nueces Marsh is important for two reasons: 1) it creates connectivity between the marsh and Nueces Bay that is critical for growth and development of estuarine dependent animal species, and 2) it promotes growth of marsh plants that require fresh water for growth. These two functions (connectivity and marsh growth) are also synergistic because marshes provide the critical habitat that the estuarine dependent species require. For example, detrital remnants of clonal dominant species *Spartina alterniflora* and *S. spartinae* are an important part of the diet of brown shrimp (*Farfantepenaeus aztecus*), which migrate into and out of the marsh (Riera et al. 2000). Extended wet periods (ten years) allow a greater spatial coverage of clonal dominant species than during moderate or drought conditions (Figures 9, 10, and 11), therefore increasing potential conductivity of brown shrimp. Thus every gallon of fresh water that enters the marsh provides multiple environmental benefits. However, there must be sufficient water flow to flush the marsh from the point where the Nueces River enters Rincon Bayou and Rincon Bayou exits to Nueces Bay (Palmer et al. 2002).

To provide for marsh growth and development, the flow must also be sufficient to overbank the berms along the marsh edge and fill the marsh with fresh water. The results from the current modeling study appear to indicate that there are rarely sufficient flows to promote full connectivity along the complete axis of Rincon Bayou, nor provide for overbanking. This is because only during the wettest periods do we see growth in marsh areal coverage (Figure 6).

One would expect the marsh coverage to expand when there is a transition from dry to wet conditions. But under the current definition of moderate climate (Figure 4, Table 1), there is still not enough water entering the marsh to increase plant coverage in the short term. This condition could become worse as climate change is likely to affect coastal south Texas with higher temperatures in the summer, less frequent rainfall, and longer periods of dry conditions between wetter periods (Twilley et al. 2001).

The model shows decreases in coverage during wet conditions under some initial starting conditions (Figure 7). This could be because some plants, particularly in the lower marsh decrease coverage during wet conditions when salinity declines. Additionally, since the growth rates used for this model are aggregate rates for functional groupings, different species can dominate the growth rate in a grouping depending differences in zonation and climate. These differences within a functional grouping are not reflected in the model. In essence, a decline in one species could be offset by an increase in another within a functional group leading the aggregate rate being near zero.

One would expect that during moderate or wet conditions, the marsh vegetation coverage would expand. However, cannot happen if the marsh is in healthy conditions such as near 100% cover (Figure 7). If the plants have already filled the area, then the growth rates are very small because cover cannot exceed 100%. There are also decreases in coverage during wet conditions under some starting conditions. This is likely because some plants, particularly in the lower marsh decrease coverage during wet conditions

when salinity declines. While the model allows for diffusion from one grid to another, this does not account for competition or the propensity for some plants such as pioneer species to move more aggressively into bare areas.

Further, marsh coverage approaches equilibrium in the long-term only during wet periods (Figure 8). The temporal simulation also shows that several years, depending upon the model's initial conditions, are required for the marsh to return to full coverage. This seems to contradict shorter-duration empirical measurements (Forbes and Dunton 2006). The current modeled growth rates are based on long-term observations of plant cover. However, actual growth rates are influenced by shorter-term events like inundation and the following recovery. During these times, the growth rates could be different due to the lack of competition and other species-specific factors.

Improvements can be made to the existing marsh development model. The diffusion equations employed in the current study allow for dispersal of plants from one grid to another, however it does not account for competition between plants or the ability of some plants (such as pioneering species) to colonize bare areas rapidly. Adding competition and distinguishing between pioneer and climax species could improve model performance.

Improvements to the model performance may be possible by modeling individual species instead of functional groupings. This would make it possible to see species growth or decline irrespective of functional grouping. Another possible improvement could be to create growth rate functions based on other physical aspects such as finer resolution of elevation and distance from the tidal creek or bay.

C.6 Implications

Now that we have a spatial-temporal model that describes vegetation growth in Nueces Marsh, it is apparent that growth in areal extent of the marsh largely depends on water flow and elevation, which in turn depends on the quantity of fresh water in marshes and also drives salinity of marsh waters. This fresh water has two sources: flows down the Nueces River from precipitation in the watershed or pass-through releases from Lake Corpus Christi. The next logical step is to determine whether it is possible to control releases of fresh water in such a way that it produces the most desirable quantity and quality of restoration of marshes. Here we have to deal with the modeling system governed by the partial differential equations, and a stochastic factor, namely, precipitation and storm events. This is essentially a problem of optimal control where we have to define the objectives of the control problem. Here is a short but incomplete list of a few possible objective restoration goals:

- To minimize time of restoration of vegetation cover
- To maximize the area of vegetation cover or habitat
- To promote a species or functional group to enhance ecosystem services
- To conserve fresh water
- To minimize the cost of restoration

- Any combination of all of the above

If we are to deal with the cost problem and/or with multiple restoration goals then we would need to use experts to evaluate importance of goals and objectives, and compare the cost of water for human consumption and for environmental needs.

C.7 Literature Cited in Appendix C

- Adam, P. 1990. *Salt Marsh Ecology*. Cambridge, U.K.: Cambridge University Press.
- Alexander, H.D., and K.H. Dunton. 2002. Freshwater inundation effects on emergent vegetation of a hypersaline salt marsh. *Estuaries* 25: 1424-1435.
- Anderson, J.R., and K. Deng. 1995. Global existence for nonlinear diffusion equations. *J. Math. Anal. Appl.* 196: 479-501.
- Bandle, C., and H.A. Levine. 1989. On the existence and nonexistence of global solutions of reaction-diffusion equations in sectorial domains. *Trans. Amer. Math. Soc.* 316: 595-622.
- Barajas, M.J. 2011. Effects of Enhancing Freshwater Inflow on Macrofaunal Communities in a Marsh, Texas A&M University - Corpus Christi Corpus Christi, TX.
- Bureau of Reclamation (BOR). 2000. Concluding Report: Rincon Bayou Demonstration Project Volume II: Findings. Austin, Texas: United States Department of the Interior, Bureau of Reclamation.
- Beseres, J.J., and R.J. Feller. 2007. Importance of predation by white shrimp *Litopenaeus setiferus* on estuarine subtidal macrobenthos. *Journal of Experimental Marine Biology and Ecology* 344: 193-205.
- Boutin, C., and P.A. Keddy. 1993. A functional classification of wetland plants. *Journal of Vegetation Science* 4: 591-560.
- Chapman, V.J. 1974. *Salt Marshes and Salt Deserts of the World*. Lehre, Germany.
- Forbes, M.G., and K.H. Dunton. 2006. Response of a subtropical estuarine marsh to local climatic change in the southwestern Gulf of Mexico. *Estuaries and Coasts* 29: 1242-1254.
- Gillanders, B.M., K.W. Able, J.A. Brown, D.B. Eggleston, and P.F. Sheridan. 2003. Evidence of connectivity between juvenile and adult habitats for mobile marine fauna: an important component of nurseries. *Marine Ecology Progress Series* 247: 281-295.
- Gillanders, B.M. 2005. Using elemental chemistry of fish otoliths to determine connectivity between estuarine and coastal habitats. *Estuarine, Coastal and Shelf Science* 64: 47-57.
- Grime, J.P. 1979. Evidence for the existence of three primary strategies in plants and its relevance to ecological and evolutionary theory. *The American Naturalist* 111: 1169 - 1178.

- Herzka, S.Z. 2005. Assessing connectivity of estuarine fishes based on stable isotope ratio analysis. *Estuarine, Coastal and Shelf Science* 64: 8 - 69.
- Hill, E.M., and B.A. Nicolau. 2007. Rincon Bayou diversion project, FY 2006 Annual Report October 2005 - September 2006. In CBBEP Publication 81, Project Number 1202, 60. Corpus Christi, TX: Center for Coastal Studies, Texas A&M University - Corpus Christi.
- Hill, E.M., J.W. Tunnell, and L. Lloyd. 2012. Spatial Effects of Rincon Bayou Pipeline Freshwater Inflows on Salinity in the Lower Nueces Delta, Texas. *CBBEP Publication 81, Project Number 1202*: 30.
- Hunter, J., and R.J. Feller. 1987. Immunological dietary analysis of 2 penaeid shrimp species from a South Carolina tidal creek. *Journal of Experimental Marine Biology and Ecology* 107: 61-70.
- Irlbeck, M.J., and G.H. Ward. 2000. Analysis of the historic flow regime of the Nueces River into the upper Nueces Delta, and of the potential restoration value of the Rincon Bayou Demonstration Project, Volume II, Appendix B. In Bureau of Reclamation, Concluding Report: Rincon Bayou Demonstration Project. Austin, TX: U.S. Department of the Interior, Bureau of Reclamation.
- Kalke, R. 2012. *pers. comm.*
- Leiva, H., and I. Sequera. 2003. Existence and stability of bounded solutions for a system of parabolic equations. *J. Math. Anal. Appl.* 279.
- Montagna, P.A., M. Alber, P. Doering, and M.S. Connor. 2002a. Freshwater inflow: Science, policy, management. *Estuaries* 25: 1243-1245.
- Montagna, P.A., R.D. Kalke, and C. Ritter. 2002b. Effect of restored freshwater inflow on macrofauna and meiofauna in upper Rincon Bayou, Texas, USA. *Estuaries* 25: 1436-1447.
- Montagna, P.A., E.M. Hill, and B. Moulton. 2009a. Role of science-based and adaptive management in allocating environmental flows to the Nueces Estuary, Texas, USA. In *Ecosystems and Sustainable Development VII*, ed. C.A. Brebbia and E. Tiezzi, 559-570. Southampton, UK: WIT Press.
- Montagna, P.A., T. Palmer, M. Gil, E. Hill, B. Nicolau, and K. Dunton. 2009b. Response of the Nueces Estuarine Marsh System to Freshwater Inflow: An Integrative Data Synthesis of Baseline Conditions for Faunal Communities. Report submitted to the Coastal Bend Bays & Estuaries Program for project # 08-21, 27: Texas A&M University - Corpus Christi, Harte Research Institute for Gulf of Mexico Studies.
- Montagna, P.A., K. Nelson, and A. Uppaluri. 2012. Water and Sediment Quality Status and Trends in the Coastal Bend Area - Phase 1: Data Archiving and Publishing, Publication CBBEP - 77, Project Number - 1105. Corpus Christi, TX: Harte Research Institute for Gulf of Mexico Studies.
- Palmer, T.A., P.A. Montagna, and R.D. Kalke. 2002. Downstream effects of restored freshwater inflow to Rincon Bayou, Nueces Delta, Texas, USA. *Estuaries* 25: 1448-1456.

- Raffaelli, D., and S. Hawkins. 1996. *Intertidal Ecology*. London: Chapman and Hall.
- Ramsey, F.L., and D.W. Shchafer. 2002. *The Statistical Sleuth: A Course in Methods of Data Analysis*. Belmont, CA: Duxbury-Thomson Learning.
- Rasser, M.K. 2009. The Role of Biotic and Abiotic Processes in the Zonation of Salt Marsh Plants in the Nueces River Delta, Texas. Ph.D., University of Texas Austin.
- Riera, P., P. Richard, A. Grémare, and G. Blanchard. 1996. Food source of intertidal nematodes of the Bay of Marennes-Oléron (France), as determined by dual stable isotope analysis. *Marine Ecology Progress Series* 142: 303-309.
- Riera, P., P.A. Montagna, R.D. Kalke, and P. Richard. 2000. Utilization of estuarine organic matter during growth and migration by juvenile brown shrimp *Penaeus aztecus* in a South Texas estuary. *Marine Ecology-Progress Series* 199: 205-216.
- Secor, H., and J.R. Rooker. 2005. Connectivity in the life histories of fishes that use estuaries. *Estuarine, Coastal and Shelf Science* 64: 1-3.
- Tunnell, J.W., and L. Lloyd. 2011. Effects of Rincon Bayou Pipeline Inflows on Salinity Structure Within the Nueces Delta, Texas. In CBBEP Publication 76, Project Number 1106.
- Twilley, R., E.J. Barron, H.L. Gholz, M.A. Harwell, R.L. Miller, D.J. Reed, J.B. Rose, E.H. Siemann, R.G. Wetzel, and R.J. Zimmerman. 2001. The Report: Confronting Climate Change in the Gulf Coast Region: Prospects for Sustaining Our Ecological Heritage. Washington, D.C.
- Vasconcelos, R.P., P. Reis-Santos, A. Maia, V. Fonseca, S. Franca, N. Wouters, M.J. Costa, and H.N. Cabral. 2010. Nursery use patterns of commercially important marine fish species in estuarine systems along the Portuguese coast. *Estuarine and Coastal Shelf Science* 86: 613-624.
- Ward, G.H., Jr., M.J. Irlbeck, and P.A. Montagna. 2002. Experimental river diversion for marsh enhancement. *Estuaries* 25: 1416-1425.
- Zedler, J.B., J.C. Callaway, J.S. Desmond, G. Vivian-Smith, G.D. Williams, G. Sullivan, A.E. Brewster, and B.K. Bradshaw. 1999. California salt marsh vegetation: An improved model of spatial pattern. *Ecosystems* 2: 19-25.